SANS (USH1G) in USH-Proteinnetzwerken von Photorezeptorzellen der Vertebratenretina

Dissertation
zur Erlangung des Grades
„Doktor der Naturwissenschaften“

am Fachbereich Biologie
der Johannes Gutenberg-Universität Mainz

von Tina Märker
geb. in Traben-Trarbach

Mainz, Oktober 2007

So eine Arbeit wird eigentlich nie fertig,
man muss sie für fertig erklären,
wenn man nach Zeit und Umständen
das möglichste getan hat.

Johann Wolfgang von Goethe

Anmerkungen

Die vorliegende Arbeit ist kumulativ gestaltet und besteht im Kern aus den beiden Hauptpublikationen Overlack *et al.*, 2007 (Publikation I) und Maerker *et al.*, 2007 (Publikation II). Anzumerken ist, dass die Publikation I, bei der ich zusammen mit Nora Overlack gleichberechtigte Erstautorin bin, sich gerade im Druck bei Vision Research befindet und die Publikation II seit September 2007 bei Human Molecular Genetics als elektronische Version vorliegt. Die Ergebnisse der Publikationen I und II sind im Wesentlichen im Abschnitt „Zusammenfassung der Ergebnisse“ dargestellt. Über die beiden Hauptpublikationen hinausgehende Resultate sind im Abschnitt „Weiterführende Analysen“ aufgeführt. Alle weiteren Publikationen, zu denen im Rahmen dieser Arbeit ein Beitrag geleistet werden konnte, sind mit einem Stern (*) versehen. Eine detaillierte Übersicht der geleisteten Beiträge zu jeder einzelnen Publikation ist im Anhang dargestellt.

Veröffentlichungen und Kongressbeiträge

Teile der vorliegenden Dissertation wurden auf internationalen Kongressen vorgestellt und in folgenden Zeitschriften veröffentlicht:

Publikationen

Maerker T, van Wijk E, Overlack N, Kersten FFJ, McGee J, Goldmann T, Sehn E, Roepman R, Walsh EJ, Kremer H, Wolfrum U (2007) A novel Usher protein network at the periciliary reloading point between molecular transport machineries in vertebrate photoreceptor cells. *Hum Mol Genet.*, Epub ahead of print

Overlack N**, Maerker T**, Latz M, Nagel-Wolfrum K, Wolfrum U (2007) SANS (USH1G) expression in developing and mature mammalian retina. *Vision Res*., in press, Epub ahead of print

Arts HH, Doherty D, van Beersum SEC, Parisi M, Letteboer SJF, Gorden NT, Peters TA, **Maerker T**, Voesenek K, Kartono A, Ozyurek H, Farin FM, Kroes HY, Wolfrum U, Brunner HG, Cremers FPM, Glass IA, Knoers NVAM, and Roepman R (2007) Mutations in the gene encoding the basal body protein KIAA1005, a novel nephrocystin-4 interactor, cause Joubert syndrome. Nat Genet. 2007 Jul;39(7):882-8. Epub 2007 Jun 10.

Gosens I, van Wijk E, Kersten F, Krieger E, van der Zwaag B, **Maerker T**, Letteboer SJF, Dusseljee S, Peters T, Spierenburg HA, Punte IM, Wolfrum U, Cremers FPM, Kremer H, and Roepman R (2007) MPP1 links the Usher protein network and the Crumbs protein complex in the retina. Hum Mol Genet. 2007 Jun 21; 8 (Epub ahead of print)

Kremer H, van Wijk E, **Maerker T**, Wolfrum U, Roepman R (2006) Usher syndrome: Molecular links of pathogenesis, proteins and pathways. Hum. Mol. Genet. 15 Spec No 2:R262-R270

Reiners J, Nagel-Wolfrum K, Juergens K, **Maerker T**, Wolfrum U (2006) Molecular basis of human Usher syndrome: deciphering the meshes of the Usher protein network provides insights into the pathomechanisms of the Usher disease. Exp. Eye Res. 83:97-119

Van Wijk E, van der Zwaag B, Peters T, Zimmermann U, te Brinke H, Kersten FF, **Maerker T**, Aller E, Hoefsloot LH, Cremers CW, Cremers FP, Wolfrum U, Knipper M, Roepman R, Kremer H (2006) The DFNB31 gene product whirlin connects to the Usher protein network in the cochlea and retina by direct association with USH2A and VLGR1. Hum. Mol. Genet. 15:751-765

Reiners J, van Wijk E, **Maerker T**, Zimmermann U, Juergens K, Te Brinke H, Overlack N, Roepman R, Knipper M, Kremer H, Wolfrum U (2005) Scaffold protein harmonin (USH1C) provides molecular links between Usher syndrome type 1 and type 2. Hum. Mol. Genet. 14:3933-3943

Reiners J, **Maerker T**, Juergens K, Reidel B, Wolfrum U (2005) Photoreceptor expression of the Usher syndrome type 1 protein protocadherin 15 (USH1F) and its interaction with the scaffold protein harmonin (USH1C). Mol. Vis. 11:347-355

Kongressbeiträge

Maerker T, Overlack N, van Wijk E, Roepman R, Kremer H, Reiners J, Wolfrum U (2007) Synaptic localization of a protein network related to the human Usher syndrome in the mammalian retina. European Retina Meeting (ERM), Frankfurt

Maerker T, Overlack N, van Wijk E, Goldmann T, Kremer H, Wolfrum U (2007) The periciliary Usher syndrome protein network in vertebrate photoreceptor cells. 100th Annual Meeting of the German society of zoology (DZG), p121 – N41

Maerker T, Overlack N, van Wijk E, Goldmann T, Roepman R, Kremer H, Wolfrum U (2007) The periciliary Usher syndrome protein network and its role for the molecular targeting to the connecting cilium in mammalian photoreceptor cells. FASEB summer research conferences “The biology of Cilia and Flagella”, Vermont

Wolfrum U, Overlack N, van Wijk E, Reidel B, Goldmann T, Roepman R, Kremer H, **Maerker T** (2007) The molecular arrangement of an Usher syndrome protein network at the photoreceptor cilium and its role in the intersegmental transport in photoreceptors. Arvo Annual Meeting 2007 – The aging eye p3066/B422

Maerker T, Overlack N, van Wijk E, Reidel B, Goldmann T, Roepman R, Kremer H, Wolfrum U (2007) The molecular arrangement of an Usher syndrome protein network at the photoreceptor cilium and its role in the intersegmental transport in photoreceptors. 3rd Pro Retina Research-Colloquium Potsdam, Retinal Degeneration: Genes -Progression - Therapy, p46

Overlack N, **Maerker T**, van Wijk E, Reidel B, Goldmann T, Roepman R, Kremer H, Wolfrum U (2007) Retinal expression and integration of the USH1G protein SANS in the USH protein interactom. 7th Meeting of the German Neurosience Society/ 31th Goettingen Neurobiology Conference pTS4-15A

Maerker T, Overlack N, van Wijk E, Reidel B, Goldmann T, Roepman R, Kremer H, Wolfrum U (2007) SANS (USH1G) and whirlin (USH2D) – putative molecular organizers of an Usher syndrome protein network at the ciliary apparatus. 30th Annual Meeting of the German society of cell biology (DGZ), Frankfurt p52

Maerker T, Overlack N, van Wijk E, Reidel B, Goldmann T, Roepman R, Kremer H, Wolfrum U (2006) The molecular organization of an Usher syndrome protein network at the ciliary apparatus and its function in molecular trafficking in photoreceptor cells. IAK 6th Annual Meeting of the Interdisciplinary Science Network Molecular & Cellular Neurobiology, Mainz p15

Maerker T, Overlack N, van Wijk E, Reidel B, Goldmann T, Roepman R, Kremer H, Wolfrum U (2006) SANS (USH1G) – a scaffold protein in the Usher interactome of photoreceptor cells. Usher syndrome and related disorders symposium, Omaha, p45

Van Wijk E, Kersten F, Peters T, **Maerker T**, Wolfrum U, te Brinke H, van der Zwaag B, Knipper M, Cremers F, Roepman R, Kremer H (2006) Whirlin ist the second multi-PDZ scaffold protein that associates with USH1 and USH2 proteins in the cochlea and retina. Usher syndrome and related disorders symposium, Omaha, p67

Maerker T, Overlack N, van Wijk E, Reidel B, Roepman R, Kremer H, Wolfrum U (2006) SANS (USH1G) – a scaffold protein in the Usher interactome of photoreceptor cells. ISOCB, Cambridge, P56 (IS6094)

Maerker T, Overlack N, van Wijk E, Reidel B, Roepman R, Kremer H, Wolfrum U (2006) SANS (USH1G) – a scaffold protein in the Usher interactome of photoreceptor cells. Pro Retina Research-Colloquium, Illuminating Molecular Complexities of the Retina, Potsdam p68/69

Maerker T, Reiners J, van Wijk E, Zimmermann U, Juergens K, Harf J, te Brinke H, Overlack N, Roepman R, Knipper M, Kremer H, Wolfrum U (2005) Usher syndrome type I and II are molecularly linked via the scaffold protein harmonin (USH1C). IAK 5th Annual Meeting of the Interdisciplinary Science Network Molecular & Cellular Neurobiology, Mainz p9

Juergens K, Reiners J, van Wijk E, **Maerker T**, Zimmermann U, Roepman R, Knipper M, Kremer H, Wolfrum U (2005) Harmonin provides the molecular link between Usher syndrome 1 and 2. Occular Cell and Molecular Biology Conference, Sarasota (Florida), p54

Maerker T, Reiners J, Juergens K, Overlack N, Goldmann T, Wolfrum U (2005) The scaffold protein harmonin (USH1C) also integrates Usher syndrome 2 proteins into synaptic Usher protein complexes in retinal photoreceptor cells. Pro-Retina Research Colloqium, Potsdam, p55

Reiners J, **Maerker T**, Juergens K, Reidel B, Harf J, Wolfrum U (2005) Molecular analysis of Usher syndrome 1 and 2 proteins in retinal photoreceptor cells. Pro-Retina Research Colloqium, Potsdam, p21

Reiners J, Harf J, **Maerker T**, Juergens K, Wolfrum U (2005) Expression and localization of the scaffold protein harmonin and its interaction partners at synapses. 6th Meeting of the German Neuroscience Society/ 30th Goettingen Neurobiology Conference p156 B

Maerker T, Reiners J, Juergens K, Overlack N, Goldmann T, Wolfrum U (2005) The scaffold protein harmonin (USH1C) also integrates Usher syndrome 2 proteins into synaptic Usher protein complexes in retinal photoreceptor cells. 6th Meeting of the German Neuroscience Society/ 30th Goettingen Neurobiology Conference p160 B

Inhaltsverzeichnis

Tabellenverzeichnis

Abbildungsverzeichnis

1. Einleitung

Um die Ursache einer Krankheit aufzuklären und wirksame therapeutische Strategien zu entwickeln ist Grundlagenforschung unabdingbar. Die vorliegende Arbeit befasst sich mit der Erforschung des Usher Syndroms (USH), der häufigsten Form erblicher Taub-Blindheit beim Menschen. Im Rahmen der vorgelegten Dissertation wurde insbesondere die Rolle der USH-Proteine SANS („Scaffold protein containing Ankyrin repeats and SAM domain"), (USH1G), USH2A Isoform b (USH2A), VLGR1b („Very Large G-protein coupled Receptor 1b") (USH2C) und Whirlin (USH2D) in der Retina untersucht.

1.1. Das Usher Syndrom

Das Usher Syndrom ist eine autosomal rezessive Erbkrankheit des Menschen, die durch das kombinierte Auftreten von Taub-Blindheit charakterisiert ist. Bisher konnten zwölf Genloci für das USH identifiziert werden. Aufgrund der klinischen Merkmale wurde eine Unterteilung des Usher Syndroms in drei Typen vorgenommen (USH1- 3; Tab.1.) (Davenport und Omenn, 1977). Die schwerwiegendste Form des Usher Syndroms ist Typ 1 (USH1) (Petit, 2001; Kremer *et al.*, 2006*; Reiners *et al.*, 2006*), die durch Taubheit von Geburt an, konstante Störungen des Gleichgewichtssinns und den meist vorpubertären Beginn der Dystrophie der Retina, der so genannten *Retinitis pigmentosa* (RP) charakterisiert ist. USH Typ 2 (USH2) tritt am häufigsten auf. USH2 Patienten haben zwar einen normal ausgeprägten Gleichgewichtssinn, sind aber meist schwerhörig mit einhergehender post-pubertärer Degeneration der Retina (Reisser *et al.*, 2002). USH Typ 3 (USH3) ist durch das spätere Einsetzen von sowohl Taubheit als auch *Retinitis pigmentosa* in der zweiten Lebensdekade charakterisiert (Petit, 2001).

Klinischer Typ	Gehörbeeinträchtigung	Störungen des Gleichgewichtsinnes	Retinitis Pigmentosa
USH1	taub	kongenital	prä-pubertär
USH2	mittelmäßig – schwer	-	post-pubertär
USH3	progressiv	variabel	variabel

Tabelle 1. Charakterisierung der klinischen Typen des Usher Syndroms (USH). Darüber hinaus gibt es erste Hinweise auf Störungen im olfaktorischen System und Gehirnatrophien bei USH1- und USH2-Patienten (modifiziert nach Pennings, 2006).

Die drei beschriebenen Haupttypen lassen sich wiederum in genetisch heterogene Subtypen (USH1B-G, USH2A-D, USH3A und B) untergliedern (Tab. 2.). Bislang konnten neun der zwölf bekannten Gen-Loci der Subtypen auch das betroffene Gen bzw. Genprodukt zugeordnet werden (Weil *et al.*, 1995; Eudy *et al.*, 1998; Bitner-Glindizcz *et al.*, 2000; Verpy *et al.*, 2000; Bolz *et al.*, 2001; Bork *et al.*, 2001; Burgess *et al.*, 2001; Joensuu *et al.*, 2001; Petit, 2001; Adato *et al.*, 2002; Ahmed *et al.*, 2003; Bok *et al.* 2003; Weil *et al.*, 2003; Weston *et al.*, 2004; Ebermann *et al.*, 2007) (Tab. 2.).

USH Typ	Genlocus	Gen	Protein	Funktion	Mausmodell
1 B	11q13.5	MYO7A	Myosin VIIA	Molekularer Motor	*shaker-1*
1 C	11q15.1	USH1C	Harmonin	Gerüstprotein	*deaf circler*
1 D	10q21-q22	CDH23	Cadherin 23	Zell-Zelladhäsion	*waltzer*
1 E	21q21	n.b.	n.b.	n.b.	n.b.
1 F	10q11.2-q21	PCDH15	Protocadherin 15	Zell-Zelladhäsion	*ames waltzer*
1 G	17q24-25	USH1G	SANS	Gerüstprotein	*jackson shaker*
2 A	1q41	USH2A	Usherin, USH2A Isoform b	extrazelluläres Matrixprotein Zell-Zelladhäsion	*USH2A k.o.*
2 B	3p23- 24.2	SLC4A7	NBC3	Ionenkanal, USH-Kandidat	n.b.
2 C	5q14.3-21-3	VLGR1	VLGR1b	7-Transmembran G-Protein gekoppelter Rezeptor	*frings Vlgr1/del7TM*
2 D	9q32	DFNB31	Whirlin	Gerüstprotein	*whirler*
3 A	3q21-25	USH3A	Clarin-1	Transmembranprotein	*clarin-1 k.o.*
3 B	20q	n.b.	n.b.	n.b.	n.b.

Tabelle 2. Gliederung des Usher-Syndroms (USH) (Stand: Oktober 2007). Den bislang bekannten USH-Subtypen sind Genlocus, identifiziertes Gen, Protein, Funktion und Mausmodell zugeordnet. Referenzen: USH1B (Weil *et al.*, 1995; Astuto *et al.*, 2000), USH1C (Bitner-Glindizcz *et al.*, 2000; Verpy *et al.*, 2000), USH1D (Bolz *et al.*, 2001; Bork *et al.*, 2001), USH1E (Chaib *et al.*, 1997), USH1F (Ahmed *et al.*, 2001; Alagramam *et al.*, 2001), USH1G (Kikkawa *et al.*, 2003; Weil *et al.*, 2003), USH2A (Eudy *et al.*, 1998; Bhattacharya *et al.*, 2002; van Wijk *et al.*, 2004), USH1C (Burgess *et al.*, 2001; Weston *et al.*, 2004; Yagi *et al.*, 2005), USH1D (Ebermann *et al.*, 2007), USH3A (Joensuu *et al.*, 2001; Adato *et al.*, 2002), SANS („Scaffold protein containing Ankyrin repeats and SAM domain“), VLGR1 („Very Large G-protein coupled Receptor 1“), n.b. = nicht bekannt.

1.2. Einführung in die USH-Genprodukte

Die tabellarische Übersicht der USH-Genprodukte in Tabelle 2 sowie das Schema aller USH-Proteine in Abbildung 1 macht deutlich, dass die bislang identifizierten USH-Proteine funktionell unterschiedlichen Proteinfamilien zuzuordnen sind (Kremer *et al.*, 2006*; Reiners *et al.*, 2006*). USH1B kodiert für das Aktin-assoziierte Motorprotein Myosin VIIa, wohingegen Harmonin (USH1C), SANS (USH1G) und Whirlin (USH2D) „Scaffold"-Proteine (Gerüstproteine) repräsentieren. Generell sind „Scaffold"-Proteine in der Lage, funktionell ungleiche Proteine wie Zell-Zelladhäsionsproteine, Cytoskelettelemente sowie Rezeptoren und Ionenkanäle zu rekrutieren und in Netzwerke zu integrieren (Garner *et al.*, 2000; Caruana, 2002; Bilder *et al.*, 2003; Roh und Margolis, 2003; Aartsen *et al.*, 2006; Kneussel und Loebrich, 2007). Die USH-Proteine Cadherin 23 (CDH23) (USH1D) und Protocadherin 15 (PCDH15) (USH1F) sind der Familie der Zell-Zelladhäsionsmoleküle zuzuordnen. USH2A und USH2C kodieren für die Transmembranproteine USH2A Isoform b und VLGR1b. Das Vier-Transmembran-Domänen Protein Clarin-1 (USH3A) ist bisher das einzige identifizierte USH3 Protein.

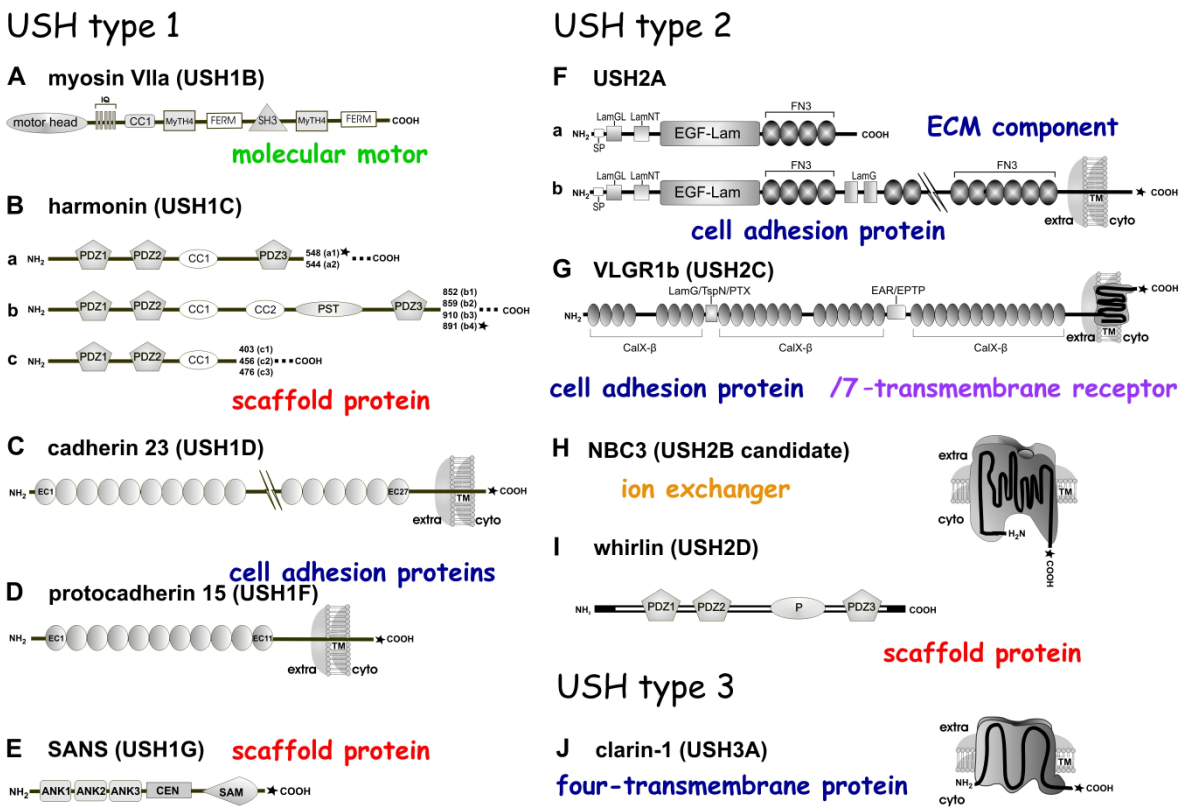

Abb. 1. Schema aller bisher identifizierten USH1-, USH2- und USH3-Proteine. (**A**) Das Motorprotein Myosin VIIa (USH1B) besteht aus einer Kopfregion, die den eigentlichen Motor darstellt, einer Halsregion mit fünf Isoleucin-Glutamin (IQ) „repeats" und einer Schwanzregion. Die Schwanzregion setzt sich aus einer "coil-coiled" (CC1) Domäne, zwei MyTH4 („Myosin Tail Homology 4") - FERM (4.1, „Four-point-one, Ezrin, Radixin, Moesin") „repeats", die durch eine SH3 („Src Homology-3") Domäne voneinander getrennt sind, zusammen. (**B**) Die Isoformen des Gerüstproteins Harmonin (USH1C) können in drei Klassen unterteilt werden (a-c). Allen Isoformen sind zwei PDZ (PSD95, Discs large, ZO-1) Domänen sowie eine „coiled-coil" (CC1) Domäne gemein. Die Harmonin Isoformen, die der Klasse a zugeordnet werden können besitzen eine zusätzliche PDZ (PDZ3) Domäne. Die längsten Isoformen der Klasse b beinhalten neben einer dritten PDZ (PDZ3) Domäne auch eine zweite „coiled-coil" (CC2) Domäne und eine Prolin, Serin, Threonin (PST)-reiche Region. Harmonin a1und b4 besitzen zudem ein C-terminales PDZ-Bindemotiv der Klasse I (PBM I). (**C**) Cadherin 23 (USH1D) besteht aus 27 extrazellulären „repeats" (EC1-EC27), einer Transmembrandomäne (TM) und einer kurzen cytoplasmatischen Domäne mit einem PBM I. (**D**) Protocadherin 15 (USH1F) ist durch elf Ektodomänen (EC1-EC11), einer TM und einem C-terminalen PBM I definiert. (**E**) Das zweite USH-Gerüstprotein SANS („Scaffold protein containing Ankyrin repeats and SAM domain", USH1G) besteht aus drei N-terminalen Ankyrin „repeats" (ANK1-ANK3), einer zentralen Region (CEN), einer SAM („Sterile Alpha Motif") Domäne und einem PBM I am C-Terminus. (**F**) Die extrazelluläre Domäne der USH2A Isoform b (USH2A) beinhaltet eine Laminin G-ähnliche Domäne (LamGL), eine N-terminale Laminin Domäne (LamNT), 10 Laminin-EGF Einheiten (EGF-Lam) sowie 32 Fibronectin Typ III (FN3) repeats (4+28), die durch zwei Laminin-G Domänen (LamG) unterbrochen sind. C-terminal befindet sich neben einer TM ein PBM der Klasse I. (**G**) Charakteristisch für VLGR1b („Very Large G-protein coupled Receptor 1b", USH2C) ist dessen große extrazelluläre Domäne, die aus einer Domäne homolog zu Laminin-G-Thrombospondin Pentraxin (LamGTspPtx), aus sieben EAR/EPTP („Epilepsy-Associated Repeats/Epitempin") „repeats" sowie aus 35 Kalzium-Bindedomänen (CalX-β) besteht. C-terminal befindet sich eine 7-TM sowie eine intrazelluläres PBM I. (**H**) Das TM-Protein NBC3 (USH2B Kandidat) besitzt 12 TM-Regionen und ein C-terminales PBM I. (**I**) Das „Scaffold"-Protein Whirlin (USH2D) besteht aus 3 PDZ-Domänen sowie einer Prolinreichen-Region (P). (**J**) Clarin-1 (USH3A) ist ein 4-TM- Domänenprotein mit einem potentiellen C-terminalen PBMI. Sterne repräsentieren PBM Is, extra = extrazellulär, cyto = Cytoplasma, ECM = extrazelluläres Matrixprotein (modifiziert nach Reiners *et al.*, 2006*)**.**

1.3. Das USH-Interaktom

Die Übersicht aller USH-Proteine in Abbildung 1 macht deutlich, dass obwohl alle USH-Proteine sehr unterschiedlichen Proteinfamilien, wie beispielsweise molekularen Motoren, Zell-Zelladhäsionsmolekülen oder Gerüstproteinen zuzuordnen sind, deren Defekte aber in einen gemeinsamen Pathomechanismus resultieren. Diese Tatsache impliziert eine gemeinsame Assoziation aller USH-Proteine innerhalb eines Proteinnetzwerkes. Kolokalisationsanalysen und Interaktionsexperimente vorangegangener Arbeiten haben gezeigt, dass das „Scaffold"-Protein Harmonin (USH1C) für die Organisation aller USH1- und USH2-Proteine in einem Multiproteinnetzwerk verantwortlich ist (Boeda *et al.*, 2002; Siemens *et al.*, 2002; Reiners *et al.*, 2003; Weil *et al.*, 2003; Adato *et al.*, 2005a; Reiners *et al.*, 2005a*; Reiners *et al.*, 2005b*; Kremer *et al.*, 2006***;** Reiners *et al.*, 2006*). Der Begriff USH-Interaktom umfasst die Protein-Interaktionen aller USH-Proteinnetzwerke. Die Existenz eines durch Harmonin organisierten USH-Proteinnetzwerkes konnte sowohl in Photorezeptorzellen als auch in Haarsinneszellen aufgezeigt werden (Abb. 2.)

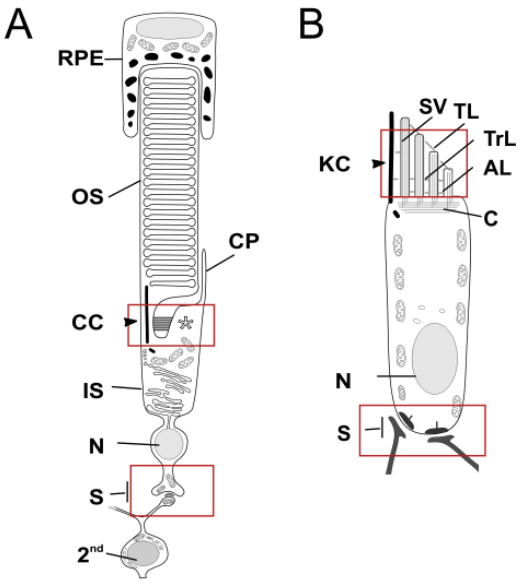

Abb. 2. Schemata der von USH betroffenen sensorischen Sinneszellen in Retina und Cochlea. (**A**) Schema einer Stäbchen Photorezeptorzelle. Die Ausläufer des Retinalen Pigmentepithels (RPE) umgeben die Enden der lichtsensitiven Außensegmente (OS). Die OS sind durch das Verbindungscilium (CC, Pfeilkopf) mit dem biosynthetisch aktiven Innensegment (IS) verbunden. Das CC wird basal kragenförmig vom apikalen IS umschlossen (Stern). Ausläufer des apikalen IS - „calycal processes" (CP) - ziehen lateral am OS hoch. Die Zellkerne der Photorezeptorzellen (N) sind in der äußeren nukleären Schicht lokalisiert. Die Synapsen der Photorezeptorzellen und nachgeschalteten Bipolar- und Horizontalzellen (2^{nd}) sind in der äußeren plexiformen Schicht (S) der Retina lokalisiert. (**B**) Schema einer Haarsinneszelle. Apikal sind Aktin-reiche Stereovilli (SV) lokalisiert, die die Mechanotransduktion vermitteln. Verankert sind alle SV in der Kutikularplatte (C). Lateral zum längsten SV ist das Kinocilium (KC) lokalisiert (Pfeilkopf). Benachbarte SV sowie SV und das KC sind durch apikale „Tip links" (TL), „transient links" (TrL) sowie basal lokalisierte „ankle links" (AL) miteinander verbunden. Rote Kästchen deuten die Lokalisation der durch Harmonin vermittelten USH-Proteinnetzwerke an den Synapsen von Photorezeptorzellen und Haarsinneszellen (S) an (modifiziert nach Reiners *et al.*, 2006*).

In Stereovilli von Haarsinneszellen wird eine Beteiligung des USH-Proteinnetzwerkes an der Entwicklung von Stereovilli sowie an Signaltransduktionsmechanismen diskutiert (Boeda *et al.*, 2002; Adato *et al.*, 2005a; Kazmierczak *et al.*, 2007; Michalski *et al.*, 2007). Darüber hinaus wurden diese Proteinkomplexe an den Synapsen von Haarsinneszellen detektiert, wo sie eine Funktion in der Aufrechterhaltung der Synapsenintegrität erfüllen könnten (Kremer *et al.,* 2006*; Reiners *et al.,* 2006*). In der Retina wurde ein Protein-„Cluster" bestehend aus allen USH1- und USH2-Proteinen an Photorezeptorzellsynapsen beschrieben (Reiners *et al.,* 2005b*; Reiners *et al.*, 2006*; Abb. 3.). Dem Gerüstprotein Harmonin wird bislang die Rolle der Organisation aller USH1- und USH2-Moleküle innerhalb eines USH-Proteinnetzwerkes in Photorezeptorzellsynapsen zugeordnet (Reiners *et al.*, 2005a*; Reiners *et al.,* 2005b*; Reiners *et al.*, 2006*). Als Funktion dieses USH-Proteinnetzwerkes wird zurzeit die Erhaltung der Synapsenintegrität vermutet (Reiners *et al.*, 2005b*; Kremer *et al.*, 2006*; Reiners *et al.*, 2006*).

Neben der Kolokalisation aller USH1- und USH2-Proteine an Photorezeptorzell-synapsen konnten mehrere USH-Proteine auch im Bereich des Verbindungsciliums lokalisiert werden (Abb. 3.). Diese Resultate warfen die Frage nach der Existenz eines weiteren USH-Proteinnetzwerkes in der ciliären Region auf. Da das Gerüstprotein Harmonin nicht im Bereich des Verbindungsciliums detektiert werden konnte, lag es nahe, dass ein alternatives USH-„Scaffold"-Protein die Organisation eines ciliären USH-Proteinnetzwerkes vermitteln könnte (Reiners *et al.*, 2003; Reiners *et al.*, 2006*; Dissertation Publikation II). Viel versprechende Kandidaten zur Formation eines ciliären USH-Proteinnetzwerkes stellten die USH-Gerüstproteine SANS und Whirlin dar (Abb. 3.). Die Bearbeitung dieser Fragestellung erfolgte durch eigene Arbeiten mit Hauptfokus auf dem USH1G-Protein SANS, wohingegen unsere Kooperationspartner aus Nijmegen ihren Augenmerk auf das zweite Gerüstprotein Whirlin richteten. Die Charakterisierung dieses ciliären USH-Proteinnetzwerkes ist von besonderem Interesse, da dem Verbindungscilium in Photorezeptorzellen eine besondere Bedeutung zukommt. Die funktionelle Relevanz von Verbindungscilien wird bei der Betrachtung deren Positionierung in Photorezeptorzellen deutlich. Das Verbindungscilium ist die einzige zelluläre Brücke zwischen dem lichtsensitiven Außensegment und dem biosynthetisch aktiven Innensegment. Alle im Außensegment lokalisierten Proteine, wie beispielsweise die an der Signaltransduktionskaskade beteiligten Proteine Opsin und Transducin, werden im Innensegment translatiert und müssen den schmalen Weg über das Verbindungscilium nehmen, um an ihren Wirkungsort im Außensegment zu gelangen. Somit

stellen alle Proteine mit ciliärer Lokalisation aussichtsreiche Kandidaten dar, die in die Strukturerhaltung des Verbindungsciliums sowie in ciliäre Transportmechanismen involviert sein könnten (Roepman und Wolfrum, 2007).

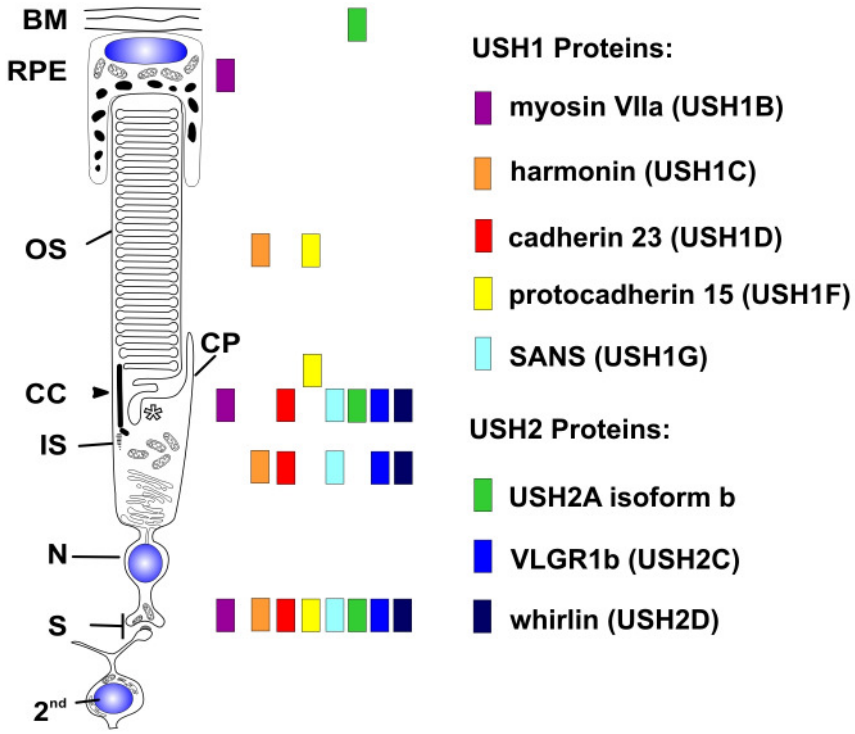

Abb. 3. Lokalisation der USH1- und USH2-Proteine in Photorezeptorzellen der Maus. Schematische Zusammenfassung der Lokalisation aller USH1- und USH2-Proteine in unterschiedlichen subzellulären Kompartimenten der Photorezeptorzelle, repräsentiert durch einen Farbkode in der Legende. Besonders deutlich wird die Kolokalisation aller USH1- und USH2-Proteine in einem „Cluster" an Photorezeptorzellsynapsen. Mit Ausnahme von Harmonin und Protocadherin 15 sind alle USH1- und USH2-Proteine auch im Verbindungscilium (CC) von Photorezeptorzellen lokalisiert (Pfeilkopf). Der Stern markiert den Bereich des apikalen Innensegments. BM = Bruch'sche Membran, RPE = Retinales Pigmentepithel, OS = Außensegment, IS = Innensegment, CP = „calycal process", N = Zellkern einer Photorezeptorzelle, S = Photorezeptorzellsynapse, 2^{nd} = Zellkern einer Bipolar- / Horizontalzelle.

1.4. Die Organisation des Transportes in Photorezeptorzellen

Transportvorgänge in Photorezeptorzellen sind essentiell, um die im biosynthetisch aktiven Innensegment translatierten Proteine an ihrem Wirkungsort im Außensegment zu platzieren (Williams, 2002). Transportvesikel werden im trans-Golginetzwerk im Innensegment gebildet und an Mikrotubuli entlang zur Membran des apikalen Innensegments transportiert (Tai *et al.*, 1999; Deretic, 2006). Tctex-1, eine leichten Kette des Mikrotubuli-assoziierten Motorproteins Dynein, konnte durch direkte Interaktion mit dem C-Terminus von Rhodopsin eine direkte Beteiligung am Transport von Rhodopsin-Vesikeln im Innensegment von Photorezeptorzellen

nachgewiesen werden (Tai *et al.*, 1999). An der Membran des apikalen Innensegments in Säugern bzw. der entsprechenden Struktur in Amphibien, dem so genannten „periciliary ridge complex“, fusionieren Cargovesikel mit der Plasmamembran und inkorporieren ihre Fracht (Sung und Tai, 2000; Papermaster, 2002; Deretic *et al.*, 2004; Deretic, 2006; Liu et al., 2007). Für den Weitertransport von Proteinen innerhalb des Verbindungsciliums zum Außensegment von Photorezeptorzellen werden derzeit zwei unterschiedliche Mechanismen diskutiert (Williams, 2002; Roepman und Wolfrum, 2007). Zum Einen könnte der ciliäre Transport durch das Aktin-assoziierte Motorprotein Myosin VIIa (USH1B) vermittelt werden (Liu *et al.,* 1997; Wolfrum und Schmitt, 2000). Zum Anderen ist der Transport von Proteinen innerhalb des Verbindungsciliums durch das Zusammenspiel von intraflagellaren Transportkomplexen mit Mikrotubuli-assoziierten Motorproteinen möglich (Marszalek *et al.,* 2000; Rosenbaum und Witman, 2002; Davenport *et al.*, 2007). Bisher konnte die Kinesin II Untereinheit Kif3a für den anterograden Transport sowie cytoplasmatisches Dynein 1b als essentielle Untereinheit für den retrograden Transport identifiziert werden (Kozminski *et al.*, 1995; Cole *et al.*, 1998; Pazour *et al.*, 1999; Porter *et al.*, 1999; Rosenbaum, 2002). Unter Verwendung einer selektiven Kif3a „knock-out“ Maus wurde eine Misslokalisation und Akkumulation von Opsin im Innensegment dokumentiert (Marszalek *et al.*, 2000). Analysen mit Myosin VIIa defizienten Mäusen (*shaker-1*) zeigten ebenso eine abnorme Verteilung von Opsin im Verbindungscilium von Photorezeptorzellen (Liu *et al.*, 1999). Diese Resultate lassen eine gleichberechtigte Beteiligung beider Motorproteine, Myosin VIIa und Kinesin II, am Transport von Opsin und weiteren Proteinen zu (Williams, 2002). Es gilt allerdings zu klären, ob beide molekulare Motoren gleichzeitig oder im Wechsel agieren (Williams, 2002). Der Austausch von Cargovesikeln zwischen zwei Transportsystemen wurde bereits für die Motorproteine Myosin V und Kinesin II beschrieben (Tabb *et al.*, 1998). Für den Wechsel von Transportvesikeln zwischen zwei molekularen Motoren sind verschiedene Szenarien denkbar. Einerseits könnte ein Motor die Fracht des anderen Motors sein, wie es bereits für intraflagellaren Transport diskutiert wurde (Rosenbaum und Witman, 2002). Andererseits könnten Mikrotubuli- und Aktin-Motoren zur Übergabe der Transportvesikel direkt miteinander interagieren (Brown, 1999; Huang *et al.*, 1999; Beningo *et al.*, 2000; Tuxworth und Titus, 2000; Cao *et al.*, 2004; Ali *et al.*, 2007).

1.5. Zielsetzung der Arbeit

Vorausgegangene Arbeiten haben gezeigt, dass das Gerüstprotein Harmonin (USH1C) die Integration aller USH1- und USH2-Proteine innerhalb eines Mulitproteinnetzwerkes vermittelt (Boeda *et al.*, 2002; Siemens *et al.*, 2002; Reiners *et al.*, 2003; Weil *et al.*, 2003; Adato *et al.*, 2005a; Reiners *et al.*, 2005a*; Reiners *et al.*, 2005b*; Kremer *et al.*, 2006*; Reiners *et al.*, 2006*). Abgesehen von der Kolokalisation aller USH1- und USH2-Moleküle an Synapsen von Photorezeptorzellen konnte eine Vielzahl von USH-Proteinen auch im Bereich des Verbindungsciliums detektiert werden (Abb. 3.). Da Harmonin nicht im Verbindungscilium lokalisiert ist, kann das USH1C-Protein als Organisator eines ciliären USH-Proteinkomplexes ausgeschlossen werden (Reiners *et al.*, 2003). Als aussichtsreiche Kandidaten für die potentielle Organisation eines USH-Proteinnetzwerkes im Bereich des Verbindungsciliums rückten die USH-„Scaffold"-Proteine SANS und Whirlin in den Fokus unserer Analysen. Bedingt durch die Interaktion von SANS und Whirlin zu zahlreichen ciliären USH-Proteinen, sind beide Gerüstproteine zur Organisation eines USH-Protein-netzwerkes im Bereich des Verbindungsciliums von Photorezeptorzellen prädestiniert (Adato *et al.*, 2005a; van Wijk *et al.*, 2006*; Abb. 3.).

In der vorliegenden Dissertation soll das „Scaffold"-Protein SANS als potentielles Organisationsmolekül eines ciliären USH-Proteinnetzwerkes in Verbindungscilien von Photorezeptorzellen überprüft werden. Dies soll durch folgende Zielsetzungen erreicht werden:

a) Analyse der Expression und (sub-) zellulären Lokalisation von SANS
b) Identifikation und Validierung neuer Interaktionspartner von SANS mittels Hefe-2-Hybrid Analysen
c) Identifikation der molekularen Komponenten eines ciliären-periciliären USH-Proteinnetzwerkes

zu a) Analyse der Expression und (sub-) zellulären Lokalisation von SANS

Zu Beginn der vorliegenden Arbeit waren bereits einige Daten zur Expression von SANS auf RNA-Niveau vorhanden. Es existierte allerdings kein Antikörper gegen SANS um Analysen auf Proteinebene durchzuführen. Zunächst war demzufolge die Generierung und Charakterisierung spezifischer Antikörper gegen SANS ein wichtiges Ziel dieser Arbeit. Im Anschluss daran sollten Expressionsanalysen von SANS auf Protein-Niveau durchgeführt

werden sowie die (sub-) zelluläre Lokalisation von SANS ermittelt werden. Zur Charakterisierung der zellulären Funktion eines Proteins ist die Kenntnis der (sub-) zellulären Lokalisation von besonderer Relevanz. Deshalb ist die Anwendung hochauflösender fluoreszenz- und elektronenmikroskopischer Untersuchungen unabdingbar. Eine wesentliche Zielsetzung der vorliegenden Arbeit stellte die Etablierung der Methode der „pre-embedding" Elektronenmikroskopie zur Durchführung von subzellulären Lokalisations-analysen dar. Als primäre Untersuchungsobjekte standen die Retinae der Maus und des Frosches (*Xenopus laevis*) im Vordergrund.

zu b) Identifikation und Validierung neuer Interaktionspartner von SANS mittels Hefe-2-Hybrid Analysen

Die Wechselwirkung mit anderen Proteinen vermag die Funktion eines Proteins zu charakterisieren. Zu Beginn der vorliegenden Arbeit waren nur wenige Interaktionspartner von SANS bekannt. Daher war es von besonderem Interesse weitere Bindepartner von SANS zu identifizieren, um dessen zelluläre Funktion aufzuklären. Hierzu sollte eine neue, von unseren Kooperationspartnern in Nijmegen modifizierte „mating" Hefe-2-Hybrid Technik in unserem Labor etabliert werden. Diese Technik zeichnet sich durch eine hohe Sensitivität zur Identifikation schwacher Proteinwechselwirkungen sowie der Reduktion falsch positiver Klone gegenüber konventionellen Methoden aus. Um ein möglichst breites Spektrum von potentiellen Bindepartnern von SANS zu identifizieren, sollten Hefe-2-Hybrid Analysen mit der zentralen Domäne (CEN) bzw. dem C-Terminus von SANS als Köder („bait") und einer bovinen Retina cDNA-Bank (HybiZap library) als Beute („prey") durchgeführt werden.

Um die Wechselwirkung von SANS mit neu identifizierten Interaktionspartnern auf bestimmte Kompartimente der Photorezeptorzelle eingrenzen zu können, sollte die (sub-) zelluläre Lokalisation neuer Bindepartner in der Retina ermittelt werden. Darüber hinaus war es ein Ziel, die identifizierte Interaktion mittels verschiedener Interaktionsassays, wie GST (Glutathion-S-Transferase) pull-downs, Koimmunpräzipitationen und Kolokalisationsstudien in Zelkultur und Mausretina zu validieren.

c) Identifikation der molekularen Komponenten eines ciliären-periciliären USH-Proteinnetzwerkes

Immunfluoreszenzanalysen konnten die Kolokalisation der USH-Proteine SANS, Whirlin, USH2A Isoform b und VLGR1b im Bereich des Verbindungsciliums in Photorezeptorzellen

aufzeigen (Reiners *et al.*, 2006*, van Wijk *et al.*, 2006*). Darüber hinaus wurden SANS und die USH2-Transmembranproteine USH2A Isoform b und VLGR1b als direkte Interaktionspartner von Whirlin identifiziert (Adato *et al.*, 2005b; van Wijk *et al.*, 2006*). Diese Resultate stellten die Weichen einer gemeinsamen Beteiligung von SANS, Whirlin, USH2A Isoform b und VLGR1b an der Organisation eines potentiellen ciliären-periciliären USH-Proteinnetzwerkes. Ein weiteres Hauptziel der vorliegenden Arbeit war die elektronenmikroskopische Analyse der subzellulären Lokalisation dieser vier USH-Proteine im Bereich des Verbindungsciliums von Photorezeptorzellen. Es wurden vergleichende Untersuchungen in den Modellorganismen Maus und Frosch durchgeführt, um Rückschlüsse auf die Funktion eines durch die Gerüstproteine SANS und Whirlin vermittelten potentiellen USH-Proteinnetzwerkes ziehen zu können.

2. Publikationen

I Overlack, N., Maerker, T., Latz, M., Nagel-Wolfrum, K., Wolfrum, U. (2007) SANS (USH1G) expression in developing and mature mammalian retina. *Vision Res*., in press., Epub ahead of print

II Maerker, T., van Wijk, E., Overlack, N., Kersten, F. F. J., McGee, J., Goldmann, T., Sehn, E., Roepman, R., Walsh, E.J., Kremer, H., Wolfrum, U. (2007) A novel Usher protein network at the periciliary reloading point between molecular transport machineries in vertebrate photoreceptor cells. *Hum Mol Genet.*, Epub ahead of print

I Overlack, N., Maerker, T., Latz, M., Nagel-Wolfrum, K., Wolfrum, U. (2007) SANS (USH1G) expression in developing and mature mammalian retina. *Vision Res*., in press., Epub ahead of print

Available online at www.sciencedirect.com
ScienceDirect
Vision Research xxx (2007) xxx–xxx
Vision Research
www.elsevier.com/locate/visres

SANS (USH1G) expression in developing and mature mammalian retina

Nora Overlack [1], Tina Maerker [1], Martin Latz, Kerstin Nagel-Wolfrum, Uwe Wolfrum *

Department of Cell and Matrix Biology, Institute of Zoology, Johannes Gutenberg-University of Mainz, Germany

Received 17 July 2007; received in revised form 16 August 2007

Abstract

The human Usher syndrome (USH) is the most common form of combined deaf-blindness. Usher type I (USH1), the most severe form, is characterized by profound congenital deafness, constant vestibular dysfunction and prepubertal-onset of retinitis pigmentosa. Five corresponding genes of the six USH1 genes have been cloned so far. The USH1G gene encodes the SANS (scaffold protein containing ankyrin repeats and SAM domain) protein which consists of protein motifs known to mediate protein–protein interactions. Recent studies indicated SANS function as a scaffold protein in the protein interactome related to USH.

Here, we generated specific antibodies for SANS protein expression analyses. Our study revealed SANS protein expression in NIH3T3 fibroblasts, murine tissues containing ciliated cells and in mature and developing mammalian retinas. In mature retinas, SANS was localized in inner and outer plexiform retinal layers, and in the photoreceptor cell layer. Subcellular fractionations, tangential cryosections and immunocytochemistry revealed SANS in synaptic terminals, cell–cell adhesions of the outer limiting membrane and ciliary apparati of photoreceptor cells. Analyses of postnatal developmental stages of murine retinas demonstrated SANS localization in differentiating ciliary apparati and in fully developed cilia, synapses, and cell–cell adhesions of photoreceptor cells.

Present data provide evidence that SANS functions as a scaffold protein in USH protein networks during ciliogenesis, at the mature ciliary apparatus, the ribbon synapse and the cell–cell adhesion of mammalian photoreceptor cells. Defects of SANS may cause dysfunction of the entire network leading to retinal degeneration, the ocular symptom characteristic for USH patients.

Keywords: Usher syndrome; Photoreceptor cells; Connecting cilium; Synapse; Ciliogenesis; Retinal development

1. Introduction

The human Usher syndrome (USH) is the most frequent cause of combined hereditary deaf-blindness. USH is genetically heterogeneous with at least 12 chromosomal loci involved (Ebermann et al., 2007; Reiners, Nagel-Wolfrum, Jurgens, Marker, & Wolfrum, 2006). Depending on the degree of clinical symptoms, USH can be divided into three types USH1, USH2, and USH3 (Ahmed, Riazuddin, Riazuddin, & Wilcox, 2003; Davenport & Omenn, 1977; Petit, 2001). USH1 represents the most severe form, characterized by profound congenital deafness, constant vestibular dysfunction and prepubertal-onset of retinitis pigmentosa (RP) (Kremer, van Wijk, Märker, Wolfrum, & Roepman, 2006; Reiners et al., 2006).

The gene products of the nine identified USH genes are assigned to various protein classes and families as recently reviewed in Reiners et al. (2006) and Kremer et al. (2006): USH1B encodes for the molecular motor myosin VIIa. Harmonin (USH1C), SANS (scaffold protein containing ankyrin repeats and SAM domain, USH1G) and whirlin, more recently identified as USH2D (Ebermann et al., 2007) belong to the group of scaffold proteins. Cadherin 23 (USH1D) and protocadherin 15 (USH1F) represent cell–cell adhesion proteins, whereas USH2A and USH2C

* Corresponding author. Address: Johannes Gutenberg-Universität, Institut für Zoologie, D-55099 Mainz, Germany. Fax: +49 6131 39 23815.
E-mail address: wolfrum@uni-mainz.de (U. Wolfrum).
[1] These authors contributed equally to this work.

0042-6989/$ - see front matter © 2007 Elsevier Ltd. All rights reserved.
doi:10.1016/j.visres.2007.08.021

encode for the large transmembrane proteins, the USH2A isoform b and the very large G protein coupled receptor 1b (VLGR1b). The four-transmembrane-domain protein clarin-1 (USH3A) is so far the only identified member of USH3.

Previous analyses elucidated the assembly of all USH1 and USH2 proteins into an USH protein network mediated by the USH1C gene product—the scaffold protein harmonin (Adato et al., 2005; Boeda et al., 2002; Reiners, Marker, Jurgens, Reidel, & Wolfrum, 2005; Reiners et al., 2003, Reiners, van Wijk, et al., 2005; Siemens et al., 2002; Weil et al., 2003). Since all proteins of the network were found at the synapse of photoreceptor cells, a role of this network in maintaining synaptic integrity was proposed (Reiners, van Wijk, et al., 2005). In inner ear hair cells the USH protein network is involved in the development of stereocilia and in signal transduction (Adato et al., 2005; Boeda et al., 2002; Kremer et al., 2006). Lately, the scaffold protein SANS came into focus of interest to mediate further protein complexes (Adato et al., 2005). Most recent work identified SANS as an organizer of a harmonin independent USH protein network at the ciliary apparatus of vertebrate photoreceptor cells (Maerker et al., 2007).

The USH1G gene product SANS is composed of different domains (Fig. 1a) capable of mediating protein-protein interactions (Nourry, Grant, & Borg, 2003; Sedgwick & Smerdon, 1999; Stapleton, Balan, Pawson, & Sicheri, 1999; Weil et al., 2003). Three N-terminal ankyrin repeats are followed by a central domain, a SAM (sterile alpha motif) domain and a class I PBM (PDZ-binding motif) at the C-terminus. The central domain is interacting with both MyTH4 (myosin tail homology 4) and FERM (4.1, ezrin, radixin, moesin) domains of myosin VIIa and mediates SANS homodimerization. The SAM domain interacts with harmonin PDZ1 and PDZ3 (Adato et al., 2005), whereas the C-terminus of SANS containing the SAM domain and the PBM class I interact with whirlin PDZ1 and PDZ2 (van Wijk et al., 2006) (Fig. 1b).

So far, the SANS protein expression and its function was predominantly studied in inner ear hair cells. Analyses in SANS deficient *jackson shaker* mice revealed disorganized stereocilia bundles in the hair cells of the cochlea (Kikkawa et al., 2003). Further studies elucidated SANS localization in the apical part and the synapses of outer and inner hair cells as well as in the basal body of outer hair cells (Adato et al., 2005). Due to the latter localization pattern SANS was proposed as an important component for proper development of hair cells. Since the SANS protein expression was still elusive, the present study was performed to analyze the localization of SANS during retinal development and its subcellular distribution in mature retina.

Here, we show that SANS is not only expressed in the cochlea, but also in other tissues containing ciliated cells, as the retina, the brain, the lung, the testis, and the olfactory epithelium. Immunohistochemistry of adult murine retina indicated SANS localization in the inner plexiform layer and outer plexiform layer, as well as in the photoreceptor cell layer. The subcellular expression of SANS was further analyzed by different independent methods revealing SANS expression at the ciliary complex and at the synapse of photoreceptor cells. During postnatal development of the retina SANS was localized in basal bodies and maturating cilia of photoreceptor cells. Present data provide evidence that the SANS protein functions as an integral component of USH protein networks in diverse compartments of photoreceptor cells.

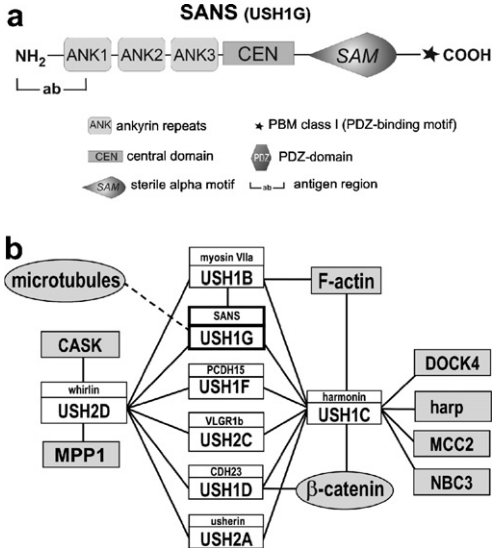

Fig. 1. Domain structure of the USH1G protein SANS and simplified scheme of the protein interactome related to human Usher syndrome. (a) SANS (Scaffold protein containing ankyrin repeats and SAM domain) consists of three N-terminal ankyrin repeats (ANK1-3), a central domain (CEN) and a C-terminal SAM (sterile alpha motif) domain. The last three amino acids comprise a PBM class I (PDZ-binding motif I) indicated by an asterisk. The region chosen for antibody generation is accentuated. (b) Scheme of a simplified version of the Usher protein interactome in relation to SANS. Interaction partners of the USH scaffold proteins harmonin, SANS and whirlin were described in detail in Kremer et al. (2006). Recently, whirlin was identified as USH2D (Ebermann et al., 2007) and its binding to MPP1 was more recently shown (Gosens et al., 2007). On the basis of simplification several protein-protein interactions are not shown. Confirmed interaction partners are indicated by solid lines, putative associations by dotted lines.

2. Methods

2.1. Animals and tissue preparation

All experiments described herein conform to the statement by the Association for Research in Vision and Ophthalmology (ARVO) as to care and use of animals in research. Adult C57BL/6J mice, Wistar Kyoto albino rats and *Xenopus laevis* were maintained under a 12 h light–dark cycle, with food and water *ad libitum*. After sacrifice of the animals in CO_2 (rodents) or chloroform (*Xenopus*) and decapitation, subsequently entire eyeballs were dissected or retinas were removed through a slit in the cornea prior to further analysis. For Western blot analyses, appropriate tissues were homogenized in modified RIPA buffer (10 mM Tris, 1 mM $CaCl_2$, 0.5% NP-40, 0.5% desoxycholinacid, 0.1% SDS, 150 mM NaCl,

10 mM NaF, 20 mM β-glycerolphosphate, pH 7.4) containing a protease inhibitor cocktail (Roche Diagnostics, Mannheim, Germany). Pig and bovine eyeballs were obtained from the local slaughterhouse.

2.2. Antibodies

Polyclonal antibodies to SANS were generated in rabbits against a recombinant expressed murine SANS fragment (amino acids 1–46). Expression of the fusion proteins and the purification of antibodies were performed as described elsewhere (Reiners et al., 2003). Antibodies against acetylated α-tubulin, γ-tubulin, actin, and PSD-95 (clone 7E3-1B8) were acquired from Sigma–Aldrich (Deisenhofen, Germany). Anti-cytochrome *c* antibodies (COX IV) were purchased from Invitrogen (Karlsruhe, Germany), anti-synaptophysin (SVP38), and anti-β-catenin antibodies were obtained from Santa Cruz Biotechnology (Santa Cruz, USA). Monoclonal antibodies against centrins (clone 20H5, detecting all four centrin isoforms) and opsin (clone K16-155) were previously described (Adamus, Arendt, Zam, McDowell, & Hargrave, 1988; Adamus, Zans, Arendt, Palczewski, McDowell, & Hargrave, 1991; Wolfrum & Salisbury, 1998; Wolfrum & Schmitt, 2000). Secondary antibodies were purchased from Invitrogen, Sigma–Aldrich or Rockland (Gilbertsville, USA). Preadsorption of anti-SANS antibodies was performed by incubation of antibodies for 1–2 h at room temperature with 1 mg/ml of the specific antigen used for immunization. After short centrifugation preadsorbed antibodies were applied to the retina cryosection or Western blot membrane in the appropriate dilution, and were treated like others.

2.3. Isolation of ROS

Rod outer segments (ROS) were purified from bovine retinas using the discontinuous sucrose gradient method as previously described (Papermaster, 1982; Pulvermüller et al., 2002). Since immunofluorescence microscopy showed no differences between dark and light adaptation, the procedure was performed under light. The purity of ROS was confirmed by Western blot analyses. Briefly, retinas were vortexed in 1.4 ml homogenizing medium (1 M sucrose, 65 mM NaCl, 0.2 mM $MgCl_2$, 5 mM Tris–acetate, pH 7.4) and centrifuged at 2000*g* for 4 min at 4 °C. The supernatant was diluted with twice of its volume in 0.01 M Tris–acetate, pH 7.4, and gently mixed. ROS were pelleted at 2000*g* for 4 min at 4 °C and resuspended in the first density gradient solution (1.10 g/ml sucrose, 0.1 mM $MgCl_2$, 1 mM Tris–acetate, pH 7.4). Crude ROS were carefully overlayed on top of a three-step gradient (1.11, 1.13, and 1.15 g/ml sucrose with 0.1 mM $MgCl_2$, 1 mM Tris–acetate, pH 7.4) and centrifuged at 85,000*g* for 30 min. The interface containing ROS was recovered, diluted with 0.01 mM Tris–acetate, pH 7.4, and ROS were pelleted again at 50,000*g* for 20 min. The pellet containing ROS was resuspended and stored at −80 °C prior to use in Western blot analyses.

2.4. Isolation of the ciliary apparatus by differential density gradient centrifugation

Isolation of ciliary apparati were performed as previously described (Fleischman, 1981; Horst, Forestner, & Besharse, 1987; Schmitt & Wolfrum, 2001; Wolfrum & Schmitt, 2000). Briefly, bovine retinas were isolated and kept at −80 °C. Frozen retinas were thawed in HBS buffer (115 mM NaCl, 2 mM KCl, 2 mM $MgCl_2$, 10 mM Hepes, pH 7), neuronal cells were cracked by gentle shaking for 1 min, filtered (400 μm, Millipore, Schwalbach, Germany) and enriched by a Sorvall RC-5B centrifuge, fixed angle rotor SS34, for 20 min at 4 °C and 48,000*g*. The pellet was resuspended in 50% sucrose (w/v), overlaid by HBS buffer and ultracentrifuged (Beckman-Coulter Optima max, rotor MLS 50) at 4 °C, 31,000*g* for 1 h. Cell fragments on the top of sucrose cushion were collected, added to a continuous sucrose gradient 25–50% and overlaid with buffer. After centrifugation for 2 h at 4 °C, 31,000*g*, two bands were collected. Probes were sedimented by decreasing the sucrose concentration. Pellets were resuspended in cytoskeleton extraction buffer (100 mM Hepes, 10 mM $MgSO_4$, 10 mM EGTA, 100 mM KCl, 5% DMSO, 20 mM DTT, 2% Triton X-100 adjusted to pH 7.5) and extracted on ice for 1 h. Ciliary apparati were separated by centrifugation for 3 h at 4 °C and 31,000*g* on a discontinuous sucrose gradient composed of 40, 50, and 60% (w/v) sucrose in a modified cytoskeleton extraction buffer (100 mM Hepes, 10 mM $MgSO_4$, 10 mM EGTA, 100 mM KCl).

2.5. Isolation of crude synaptosomes

Crude synaptosomes were prepared as described elsewhere (Hirao et al., 1998; Reiners et al., 2003). In brief, the brain of an adult mouse was homogenized in 800 μl extraction buffer (0.32 M sucrose in 4 mM Hepes, pH 7.4) and centrifuged at 800*g* for 10 min at 4 °C. The supernatant was centrifuged at 9200*g* for 15 min at 4 °C. The pellet was resuspended in 800 μl extraction buffer (0.32 M sucrose in 4 mM Hepes, pH 7.4) and centrifuged at 10,200*g* for 15 min at 4 °C. The crude synaptosome fraction was recovered in the pellet and resuspended in 800 μl buffer containing 20 mM Hepes/NaOH (pH 8.0), 100 mM NaCl, 5 mM EDTA, and 1% Triton X-100 and centrifuged at 100,000*g* for 30 min at 4 °C. The supernatant was used in Western blot analyses.

2.6. Serial tangential sectioning

Western blot analyses of serial tangential sections were performed as described by Reiners et al. (2003). Briefly, after removal of the vitreous, dissected rat eye cups were cut at four opposite sites and flat-mounted between two glass slides separated by 0.5 mm spacers. The bottom slide facing the basal membrane of the retina was roughened with sandpaper to improve adhesion. The top slide facing the outer side of the eye cup was covered with teflon spray to improve later release. The glass slide and eye cup sandwich was hold together by two small binder clips and frozen immediately on dry ice. The bottom slide with the eye cup was mounted into a cryomicrotome and sequential 10 μm tangential sections of the eye cups were collected in 100 μl SDS–PAGE sample buffer. Aliquots of 10 μl per lane were subjected to Western blot analyses.

2.7. Western blot analyses

For denaturing gel electrophoresis, the samples were mixed with SDS-PAGE sample buffer (62.5 mM Tris–HCl, pH 6.8; 10% glycerol; 2% SDS; 5% β-mercaptoethanol; 1 mM EDTA; 0.025% bromphenol blue). Twenty-five micrograms of protein extract per lane were separated on 12% polyacrylamide gels and transferred onto PVDF membranes (Millipore). Immunoreactivities were detected with the appropriate primary and corresponding secondary antibodies (IRDye 680 or 800, Rockland) employing the Odyssey infra red imaging system (LI-COR Biosciences, Lincoln, NE, USA). In case of the use of the ECL detection system (Amersham Biotech/GE Healthcare, Freiburg, Germany) donkey anti-rabbit secondary antibodies coupled to horseradish peroxidase were applied to Western blot membranes. Band sizes were calculated using Total Lab software (Phoretics, UK). As a molecular marker a prestained ladder (Sigma–Aldrich), ranging from 11 to 170 kDa was used.

2.8. Immunofluorescence microscopy

Eyes from developing and adult mice were cryofixed directly in melting isopentane and cryosectioned as previously described (Wolfrum, 1991). Cryosections were placed on poly-L-lysine-precoated coverslips and incubated with 0.01% Tween 20 in PBS. PBS washed sections were blocked with blocking solution (0.5% cold water fish gelatin, 0.1% ovalbumin in PBS) for 30 min, and then incubated with primary antibodies in blocking solution overnight at 4 °C. Washed sections were subsequently incubated with secondary antibodies conjugated to Alexa 488 or Alexa 568 (Molecular Probes, Leiden, Netherlands) and DAPI (Sigma–Aldrich) for visualization of the nuclei, in blocking solution for 1–2 h at room temperature in the dark. After washing with PBS, sections were mounted in Mowiol 4.88 (Hoechst, Frankfurt, Germany). In none of the appropriate controls a reaction was observed. Mounted retinal sections were examined with a

Please cite this article in press as: Overlack, N. et al., SANS (USH1G) expression in developing and mature ..., *Vision Research* (2007), doi:10.1016/j.visres.2007.08.021

Leica DMRB microscope (Leica microsystems, Bensheim, Germany). Images were obtained with a Hamamatsu ORCA ER CCD camera (Hamamatsu, Herrsching, Germany) and processed with Adobe Photoshop CS (Adobe Systems, San Jose, USA).

2.9. Cell culture

NIH3T3 cells were cultured in Dulbecco's modified Eagle's medium supplemented with 10% heat-inactivated fetal calf serum (FCS) and 2 mM glutamine. Immunofluorescence analyses were carried out on cells seeded on coverslips, followed by fixation with methanol and proceeded as previously described (Nagel-Wolfrum et al., 2004).

3. Results

3.1. Generation and validation of specific anti-SANS antibodies

Knowledge of expression profiles of proteins and their subcellular localization provide important insights in their specific function. So far, little was known about the expression and subcellular distribution of SANS. We generated a polyclonal antiserum against recombinant expressed murine SANS protein as a tool to study the expression and subcellular localization of SANS. Western blot analyses of mouse retina extracts revealed that affinity purified anti-SANS antibodies decorated a band at approximately 55 kDa (Fig. 2A), corresponding to the predicted size of SANS (52 kDa). To validate the specificity of anti-SANS antibodies, Western blot analyses of extracts of mouse retina were performed with anti-SANS antibodies preadsorbed with the antigen used for immunization. The appropriate band for SANS was abolished (Fig. 2A), indicating the specificity of the anti-SANS antibodies. We further validated the specificity of the affinity purified antibodies on retinal cryosections (Fig. 2C–E). The specific SANS labeling described below was abolished when preadsorbed antibodies were applied to sections (Fig. 2E).

3.2. SANS protein is expressed in ciliated tissues

With these specific anti-SANS antibodies in hand, we analyzed the expression of SANS for the first time on protein level in various murine tissues (Fig. 3). Our Western blot analyses revealed SANS-specific bands of 55 kDa in protein extracts of the retina, the cochlea, the brain, the lung, the testis, the olfactory epithelium and of NIH3T3 cells. In addition to this 55 kDa band, a fade band at

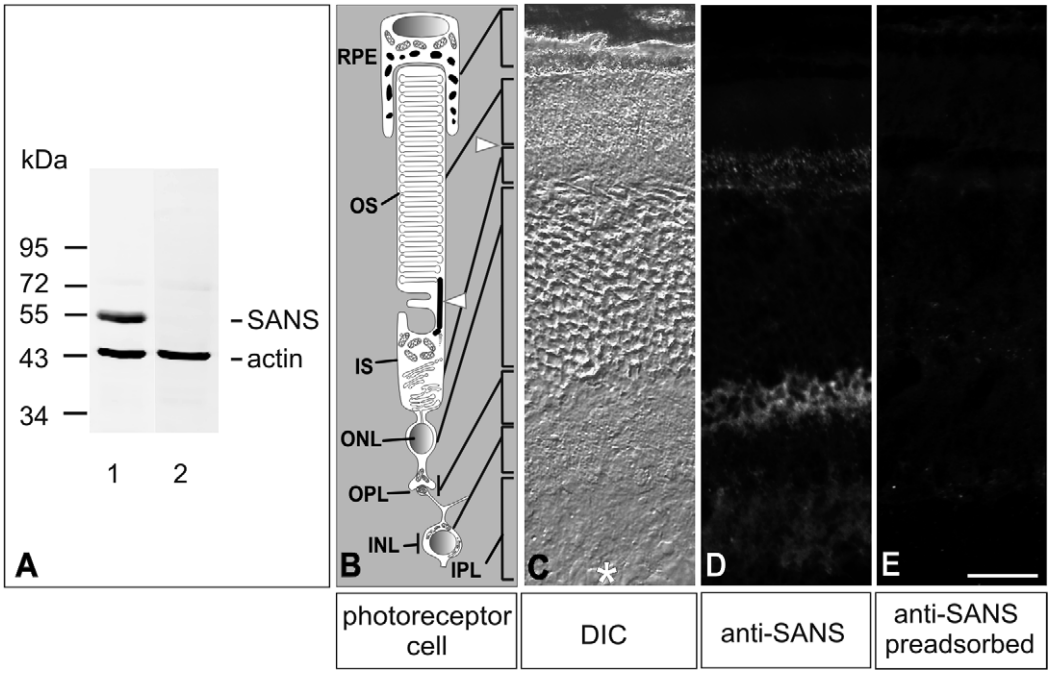

Fig. 2. Validation of anti-SANS antibodies by Western blot analyses and indirect immunofluorescence analyses of mouse retinas. (A) Western blot analysis of protein extract of mature mouse retina with affinity purified antibodies against SANS. A specific band with the molecular weight of approximately 55 kDa was obtained (lane 1). This band was completely abolished after preadsorption of anti-SANS antibodies with the corresponding antigen (lane 2). Coincubation with anti-actin was used as a loading control. (B) Schematic representation of a vertebrate rod photoreceptor cell. Vertebrate photoreceptors are composed of distinct morphological and functional compartments. The photosensitive outer segment (OS) is connected by the connecting cilium (arrowheads) with the biosynthetic active inner segment (IS). The cell body is localized in the outer nuclear layer (ONL) and contains the nucleus (N) and the synaptic terminal in the outer plexiform layer (OPL) of the retina. (C) Differential interference contrast (DIC) image visualizing the different retinal layers. (D) Indirect immunofluorescence analysis of anti-SANS on a longitudinal cryosection through a mature mouse retina. Anti-SANS immunofluorescence was localized in the photoreceptor cell layer and in the plexiform layers. In photoreceptor cells, SANS was detected at the ciliary complex, in the inner segment, the outer limiting membrane and at synapses in the OPL. No labeling was observed in the retinal pigmented epithelium (RPE) and the ganglion cell layer (asterisk in C). (E) Parallel section to (C and D), incubated with preadsorbed anti-SANS antibodies. After preadsorption, anti-SANS staining was abolished. Scale bar: 20 μm.

Please cite this article in press as: Overlack, N. et al., SANS (USH1G) expression in developing and mature ..., *Vision Research* (2007), doi:10.1016/j.visres.2007.08.021

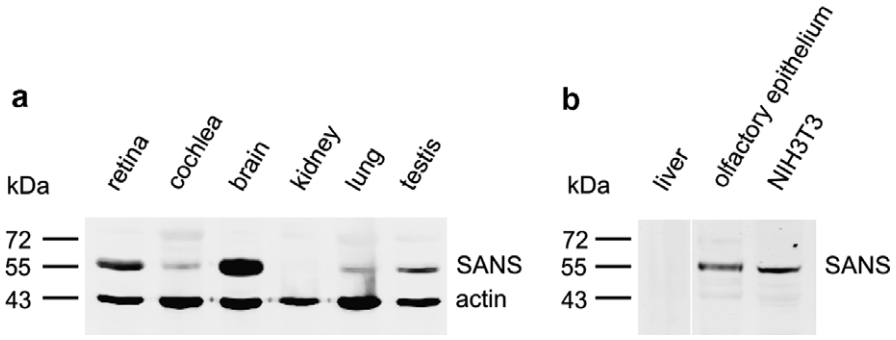

Fig. 3. SANS expression in murine ciliated tissues. (a and b) Western blot analyses of protein extracts of adult murine retina, cochlea, brain, kidney, lung, testis, liver, olfactory epithelium and NIH3T3 cells with anti-SANS antibodies. A specific band with a molecular weight of approximately 55 kDa was detected in NIH3T3 cells and in all analyzed tissues, apart from kidney and liver. The SANS-positive tissues contain ciliated cells. In the Western blots shown in (a), actin was used as loading control.

~72 kDa was reproducible found in cochlea protein extracts. In contrast, no bands were obtained in kidney and liver tissue samples. In conclusion, our data indicate that the SANS protein is preferentially expressed in tissues containing ciliated cells.

3.3. SANS is localized in the photoreceptor cell layer, the inner plexiform layer and the outer plexiform layer of the mammalian retina

To determine the subcellular distribution of SANS in the retina, cryosections through mouse eyes were analyzed by immunofluorescence microscopy using affinity-purified anti-SANS antibodies. SANS expression was present in the photoreceptor cell layer, the outer limiting membrane, the inner plexiform layer and the outer plexiform layer of the retina (Fig. 2D). In contrast, no staining was observed in cells of the retinal pigmented epithelium (Fig. 2D). The same staining pattern by indirect immunofluorescence with anti-SANS antibodies were obtained in cryosections through the mature retina of other mammals, namely rats and pigs (data not shown). Furthermore, SANS expression was found in the photoreceptor cell layer, the outer limiting membrane and the plexiform layers of retinas of the amphibian *X. laevis* (data not shown).

3.4. SANS protein localization at the ciliary apparatus, the outer limiting membrane and the synapse of photoreceptor cells

To analyze the expression of SANS in photoreceptor cells immunohistochemical and biochemical analyses were performed. In a first set of experiments, the subcellular distribution of SANS was elucidated by immunohistochemistry of mature murine photoreceptors (Fig. 4). Immunofluorescence double labeling experiments with antibodies against SANS and marker proteins of subcellular compartments of photoreceptor cells were performed. Labeling with anti-pan-centrin antibodies (marker for the connecting cilium and basal body complex; Gießl et al., 2004) and anti-SANS antibodies revealed partial colocalization (Fig. 4A–C). This indicated SANS as a component of the connecting cilium and of the basal body complex. Furthermore, SANS was colocalized with β-catenin, a marker for the cell–cell adhesion in the inner segment at the outer limiting membrane (Golenhofen & Drenckhahn, 2000; Mehalow et al., 2003; Montonen, Aho, Uitto, & Aho, 2001) (Fig. 4D–F). In addition, antibodies against PSD-95 were applied. Although, PSD-95 is ubiquitously found in the post-synaptic dense differentiations (Kornau, Seeburg, & Kennedy, 1997), PSD-95 is known to be abundantly expressed in pre-synaptic terminals of photoreceptor cells (Koulen, Garner, & Wassle, 1998). Double labeling with anti-PSD-95 and anti-SANS antibodies revealed an overlapping staining pattern at synaptic terminals of photoreceptor cells (Fig. 4G–I). The obtained labeling for SANS was more distinct at the presynapse (Fig. 4G–I), indicating its localization in the synaptic terminal of rod and cone photoreceptor cells. A diminished localization for SANS was observed at postsynapses in second order neurons, in bipolar and horizontal cells.

3.5. SANS presence in subcellular fractionations of synaptosomes and photoreceptor cilia

To occlude the antigen masking occasionally observed in tissue sections we determined the subcellular localization of SANS in photoreceptor cells by Western blot analyses. Therefore, we carried out subcellular fractionations of photoreceptor cells and tangential cryosections through the rat retina. Western blot analyses revealed the presence of SANS in protein extracts of mouse and bovine retinas, in brain synaptosome fraction of mouse and in the ciliary fraction of bovine photoreceptor cells (Fig. 5a). However, in the fraction of isolated rod outer segments (ROS) a weak band was obtained which occurred most likely due to contamination of the ROS fraction with ciliary components. Differential density gradient centrifugation assays revealed that SANS was cosedimented with the ciliary marker acetylated α-tubulin (Fig. 5b).

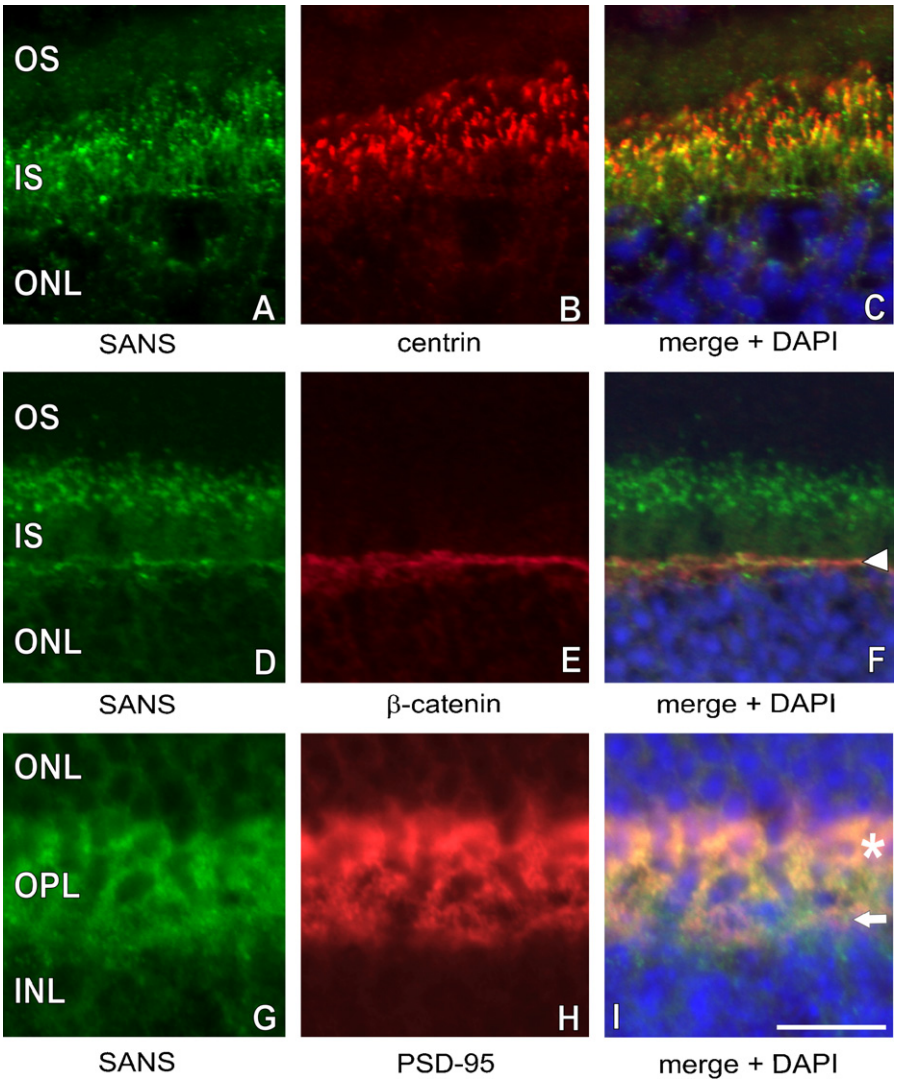

Fig. 4. Double labeling revealed SANS localization in the photoreceptor cilium, the outer limiting membrane and outer plexiform synapses of murine retinas. (A–I) Indirect double immunofluorescence analyses of photoreceptor compartments in retinal cryosections. (A–C) Double labeling with anti-SANS (A) and anti-pan-centrin antibodies (B), a marker for the ciliary apparatus (connecting cilium and the basal body). (C) Merge image of SANS and centrin labeling superposed with the nuclear DNA staining by DAPI. SANS and centrin were partially colocalized in the ciliary apparatus of photoreceptor cells. (D–F) Double labeling of anti-SANS (D) and anti-β-catenin antibodies (E), a molecular marker for the outer limiting membrane. (F) Merge image of SANS and β-catenin labeling superposed with DAPI staining. SANS and β-catenin were colocalized at the outer limiting membrane (arrowhead). (G–I) Double labeling with anti-SANS (G) and anti-PSD-95 antibodies (H), a marker for post-synapses, also staining pre-synaptic terminals in retinas. (I) Merge image of SANS and PSD-95 labeling superposed with DAPI staining. SANS and PSD-95 staining was colocalized in the synaptic terminals of photoreceptor cells (asterisk) and partially overlaps in the post-synaptic region of 2nd order neurons (bipolar cells and horizontal cells) (arrow). Scale bar: 10 μm.

3.6. Analysis of serial tangential cryosections of the retina confirmed SANS localization in the ciliary apparatus and synapse of photoreceptor cells

To validate the localization of SANS in photoreceptor cells we analyzed the protein distribution in serial tangential cryosections through the rat retina by Western blot analyses. For this purpose, we used antibodies against opsin, cytochrome *c*, and synaptophysin as markers to distinguish between the subcellular photoreceptor compartments (Reiners et al., 2003). Our analyses revealed that SANS was localized in the synaptic region and the inner segment, whereas SANS was not detected in the anti-opsin positive outer segment sections (Fig. 5c). Since SANS bands were obtained in sections at the transition of the compartment markers for the inner segment and outer segment, we concluded the presence of SANS in the ciliary apparatus of photoreceptor cells. This conclusion was further supported by the present semi-quantification of SANS protein in serial tangential sections. For this purpose, the optical density of Western blot bands was ascertained. These analyses revealed that SANS was enriched in the ciliary region more than two fold in comparison to other subcompartments of photoreceptor cells (Fig. 5d). The applied

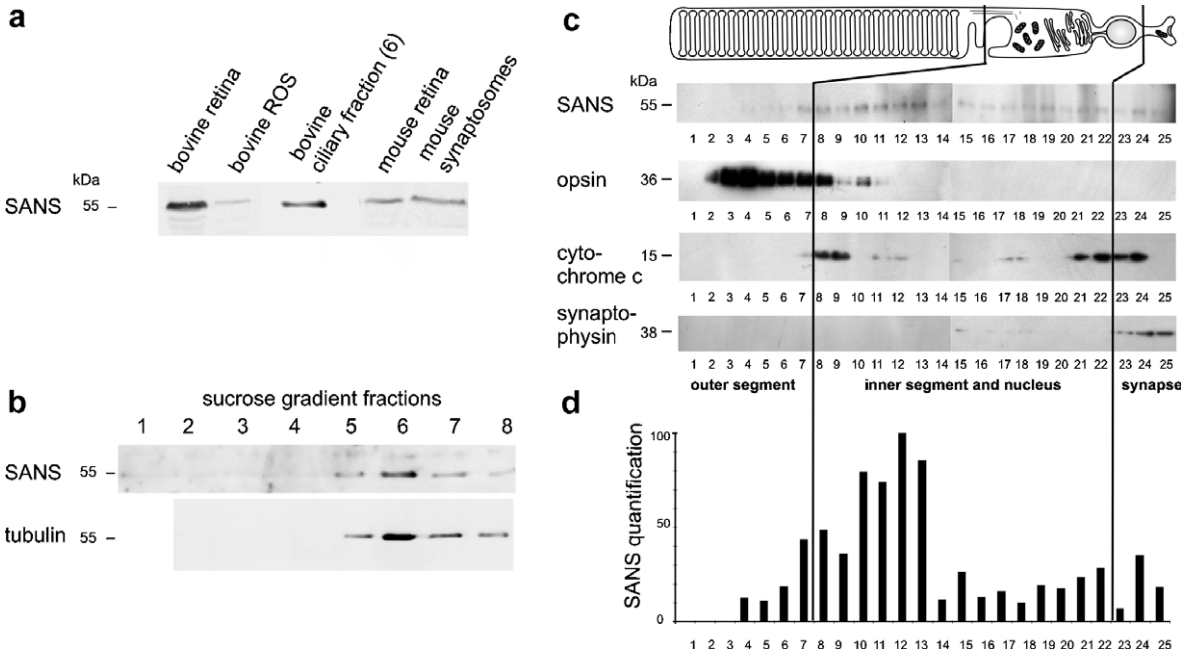

Fig. 5. Biochemical fractionations and analysis of serial tangential sections of retinas confirm SANS subcellular localization in photoreceptor cells. (a) Western blot analyses of subcellular fractions of mouse and bovine retinas. Prominent staining for SANS (~55 kDa) was present in total retina extract and the ciliary fraction of bovine photoreceptor cells (fraction 6 in b), whereas a weak band for SANS was obtained in rod outer segments (ROS). SANS was also detected in retina extract and in the synaptosome fraction of mice brain. (b) Western blot analyses of detergent-lysed bovine ciliary fractions harvested after differential gradient centrifugation. SANS cosediments with the ciliary marker acetylated α-tubulin. (c) Western blot analyses of tangential cryosections through a rat retina. Each lane corresponds to a 10 μm thick slice of the photoreceptor layer. Western blots with antibodies against opsin, cytochrome *c* and synaptophysin were used to determine the photoreceptor compartments assigning the outer segment, the inner segment and the synaptic region. SANS was detected in all tangential sections apart from anti-opsin positive slices of the outer segment. (d) SANS quantification by TotalLab software. The highest SANS protein concentration was present in sections at the transition of the compartment markers for the inner segment (marker: cytochrome *c*) and outer segment (marker: opsin)—the ciliary region of photoreceptor cells.

independent methods confirmed our previous immunohistochemical localization of SANS in the ciliary apparatus and at the synaptic region of mammalian photoreceptor cells.

3.7. SANS protein expression during postnatal maturation of the murine retina

We analyzed the expression and localization of SANS during various developmental stages of postnatal murine retinas. The expression of SANS protein was detected by Western blot analyses in all selected postnatal stages, namely PN0, PN7, PN14, and PN20 (Fig. 6). In addition, we investigated the localization of SANS during retinal development by indirect immunofluorescence and DAPI counterstaining of the nuclear DNA (Fig. 7). Longitudinal sections of PN0 mouse eyes revealed SANS expression at the most apical tip of the neuroblast layer proximal to the retinal pigmented epithelium (Fig. 7A and E). Double labeling with anti-pan-centrin antibodies identified the punctuated anti-SANS stained structures as centrioles and basal bodies in photoreceptor precursors (Fig. 7I and M). The labeling of the differentiating ciliary apparatus of photoreceptor cells persists during all following developmental stages investigated (Fig. 7A–P). In the outer plexiform layer anti-SANS immunofluorescence was observed from PN14 on (Fig. 7C/G and D/H). At this retinal developmental stage synapses are formed in the outer plexiform layer in the mouse retina. SANS was localized at the cell–cell adhesion of the outer limiting membrane not before PN20 (Fig. 7D/H and L/P), when the mouse retina is fully maturated (von Kriegstein & Schmitz, 2003).

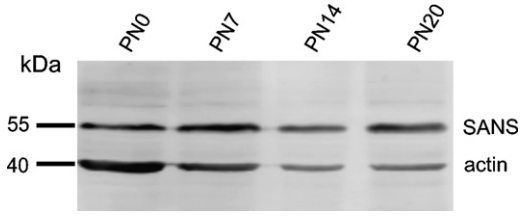

Fig. 6. SANS expression during postnatal differentiation of mouse retina. Western blot analyses with anti-SANS and anti-actin antibodies (loading control) of murine retina at different postnatal developmental stages, namely PN0, PN7, PN14, and PN20. SANS was detected at 55 kDa in all analyzed postnatal developmental stages.

3.8. SANS localization at centrosomes and spindle poles of NIH3T3 cells

Our Western blot analyses revealed SANS expression in NIH3T3 fibroblasts. This prompted us to analyze the sub-

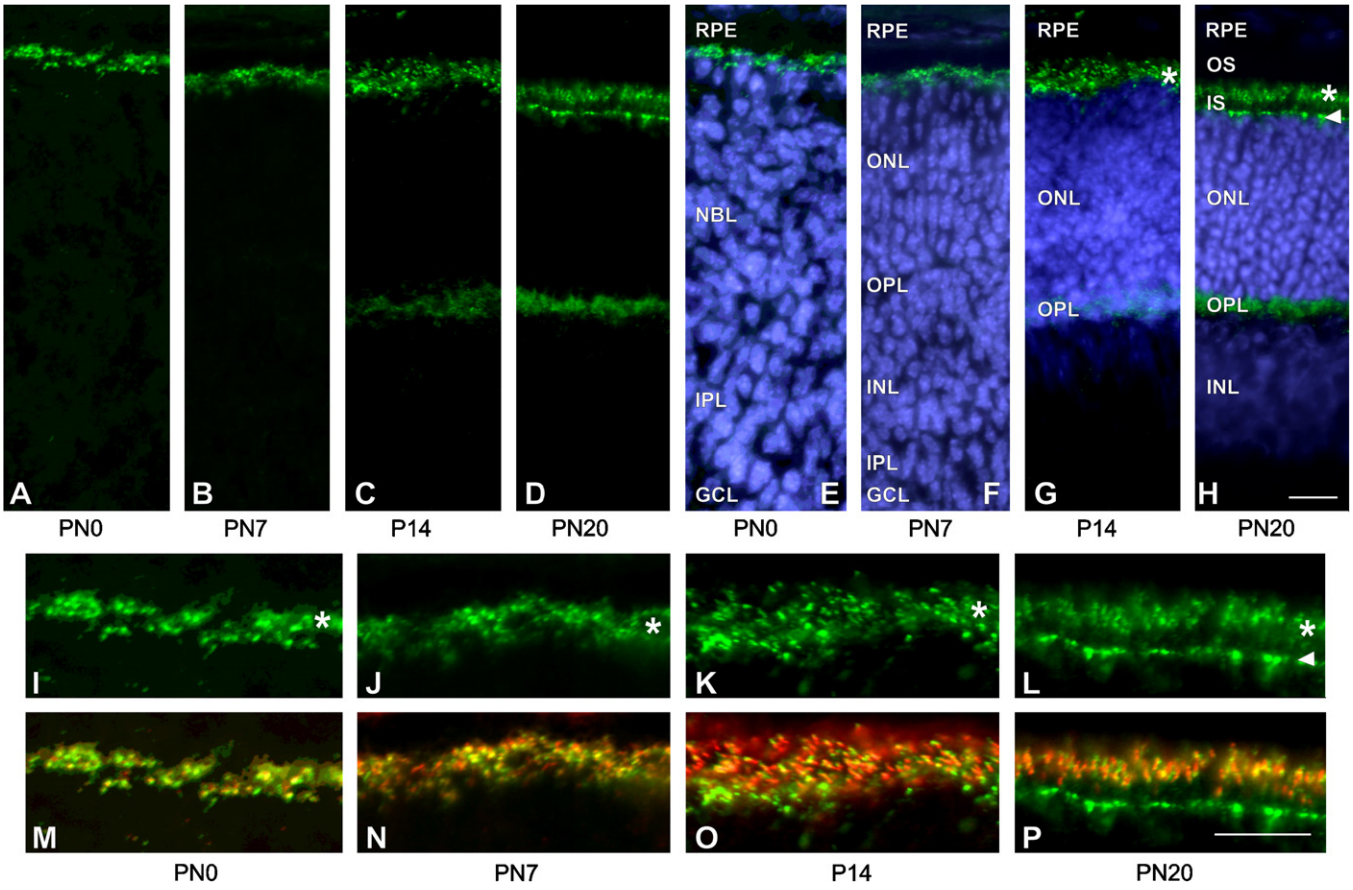

Fig. 7. SANS expression in photoreceptor cells of the maturating retina. (A–H) Indirect immunofluorescence with anti-SANS antibodies in cryosections through mouse retinas at different developmental stages. (E–H) Different nuclear layers in the developing retina were identified by counterstaining with DAPI. (A and E) In the PN0 retina, only the retinal pigmented epithelium (RPE), neuroblast layer (NBL), inner plexiform layer (IPL) and ganglion cell layer (GCL) are distinguishable. SANS labeling showed a punctuated staining pattern in the apical part of the developing retina, beneath the RPE cells. (B and F) In PN7, the neuroblast layer (NBL) is already divided in outer nuclear layer (ONL), the outer plexiform layer (OPL) and the inner nuclear layer (INL). Punctuated SANS staining was visible proximal to the RPE. (C and G) In PN14 eyes, SANS was localized in the ciliary region of photoreceptor cells (asterisk) and in the OPL, where synapses are differentiated. (D and H) In PN20 eyes, SANS labeling was localized at the ciliary region of photoreceptor cells (asterisk), in the OPL and in a thin line underneath the inner segment (IS), representing the outer limiting membrane (arrowhead). Outer segment = OS. (I–P) High magnification analyses of double immunofluorescence of ciliary regions (asterisks) in diverse developmental stages of murine photoreceptor cells shown in (A–H). (I–L) Indirect immunofluorescence of anti-SANS antibodies (green). (M–P) Merged images of anti-SANS (green) and anti-pan-centrin antibodies (red; a frequently used marker for centrioles, basal bodies and cilia of vertebrate photoreceptor cells). (I and M) In PN0 retinas, SANS was partially colocalized with centrins in basal bodies as soon as these are formed, beneath the apical membrane of photoreceptor precursor cells. (J and N) In PN7, SANS labeling revealed partial overlap with centrins in basal bodies and ciliary sprouts present in differentiating photoreceptor cells at this developmental stage. (K and O) In PN14, SANS was partially colocalized with centrins in basal bodies and the developing connecting cilium. (L and P) In PN20, SANS was partially colocalized with centrins in basal bodies and the connecting cilium. In addition, SANS was stained at the outer limiting membrane (arrowhead), which was not stained with anti-pan-centrin antibodies. Scale bars: 10 μm. (For interpretation of the references to the color in this figure legend the reader is referred to the web version of this article.)

cellular localization of SANS in cultured NIH3T3 fibroblasts to gain insight whether SANS has in addition an impact in non specialized cell types. Indirect immunofluorescence microscopy revealed partial colocalization of SANS with the centrosomal marker γ-tubulin at the centrosome of interphase cells (Fig. 8B and D). Further indirect immunocytochemical analyses of mitotic cells indicated that SANS was located at spindle pole bodies, essential for proper cell division (Fig. 8F and G). The obtained data point towards a general function of SANS at centrosome related structures, like basal bodies of cilia or centrioles.

4. Discussion

Recent studies indicated that SANS functions as a scaffold in the USH protein interactome (Adato et al., 2005; Weil et al., 2003; summarized in: Reiners et al., 2006; Kremer et al., 2006). So far, besides SANS homomer formation, interactions with harmonin isoforms a and b (USH1C), myosin VIIa (USH1B), and whirlin (USH2D) have been demonstrated (Adato et al., 2005; van Wijk et al., 2006; Weil et al., 2003; Maerker et al., 2007).

In the present study, we demonstrate that SANS protein expression is not restricted to the tissues mainly affected by

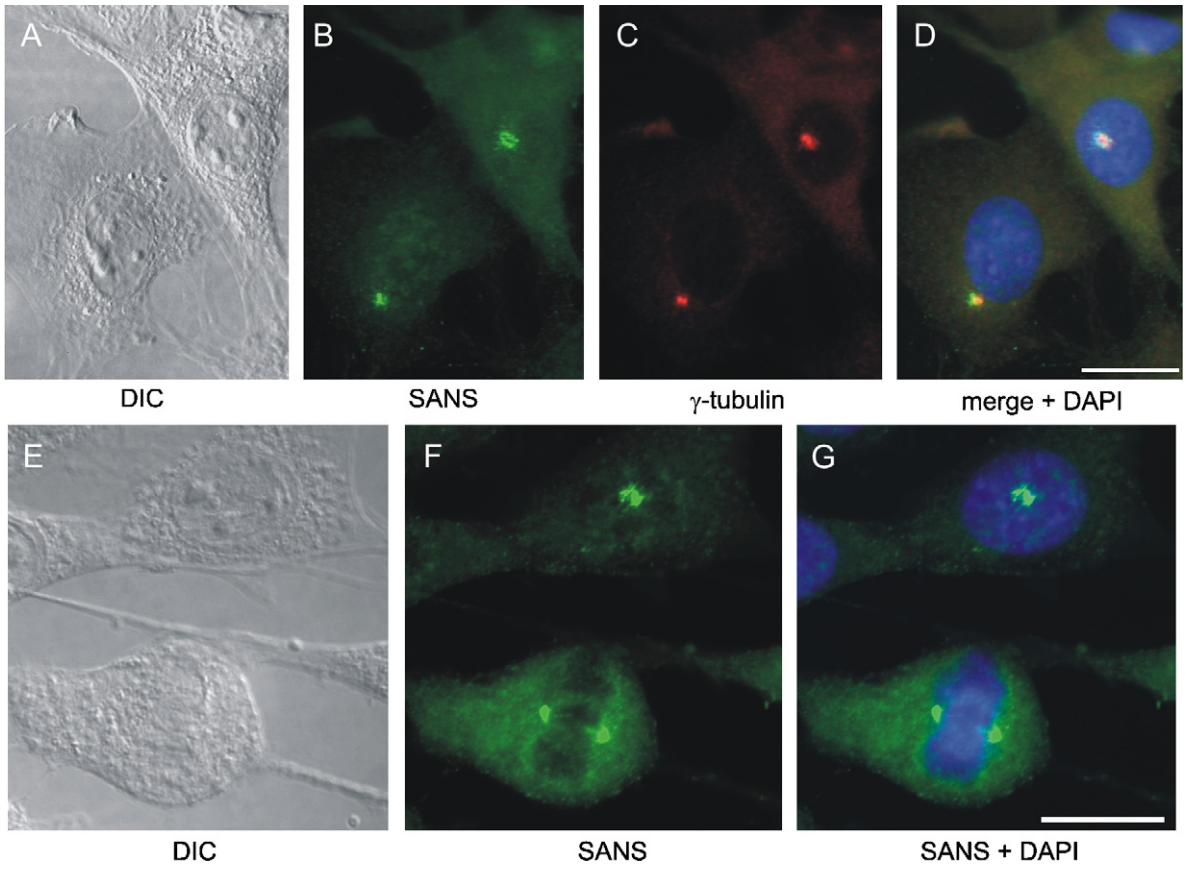

Fig. 8. SANS localization at centrosomes and spindle poles of NIH3T3 cells. (A–D) Double labeling of SANS (B) and γ-tubulin (C) in NIH3T3 cells by indirect immunofluorescence. (A) Differential interference contrast (DIC) image. (B) SANS staining was present throughout the cytoplasm and concentrated in a perinuclear spot. (C) Anti-γ-tubulin antibodies stained centrosomes. (D) Merged immunofluorescence images demonstrated partial colocalization of SANS and γ-tubulin at centrosomes. Nuclear DNA was stained with DAPI. (E–G) Localization of SANS in dividing NIH3T3 cells. (E) Differential interference contrast image. (F) SANS immunofluorescence analysis revealed SANS localization at spindle poles of dividing NIH3T3 cells. (G) Double labeling with anti-SANS antibodies and DAPI. Scale bar: 10 μm.

USH, the retina and inner ear. Western blot analyses revealed SANS specific bands at 55 kDa in further tissues, namely the brain, the lung, the testis and in the olfactory epithelium. Interestingly, we also obtained a band at ~72 kDa in protein extracts of cochleae. So far, we do not know the nature of this protein band. It may result from unspecific cross reactivity of the affinity purified anti-SANS antibody restricted to the cochlea protein extracts. Or, the band may represent the labeling of a higher molecular splice variant of SANS. Such alternatively spliced isoforms are well known from other USH proteins (Kremer et al., 2006; Petit, 2001; Reiners et al., 2006). Nevertheless, the obtained results for SANS protein expression correlate to previous mRNA expression analyses by RT-PCR (Johnston et al., 2004; Weil et al., 2003). All SANS positive tissues have the presence of ciliated cells in common. In SANS negative tissues, kidney and liver which also contain cells with primary cilia the expression of the SANS homologous Harp (harmonin-interacting, ankyrin repeat-containing protein) was shown (Johnston et al., 2004). Thus, Harp may resume the functional role of SANS in these tissues.

The tissue expression of the SANS protein is in line with the rather wide expression profile of other USH1 and 2 proteins (reviewed in: Reiners et al., 2006). This is in agreement with several studies on USH patients which indicate that USH can also affect other tissues, namely brain areas, olfactory and tracheal epithelia as well as sperm cells (see overview in: (Reiners et al., 2006). Such studies gathered histopathological data from USH patients displaying ciliary abnormalities not only in photoreceptor cells but also in olfactory epithelium and sperms. Based on these observations it has been suggested that USH is related to ciliary dysfunction (Arden & Fox, 1979), which is supported by the present study. SANS protein expression in tissues containing ciliated cells indicates that the pathophysiology of USH1G may also encroach cilia in cells of these tissues.

Our data show that SANS is expressed in the photoreceptor cell layer, the inner plexiform layer and the outer plexiform layer of the mammalian retina. Applied subcellular biochemical fractionations and immunological approaches determined the subcellular localization of SANS in photoreceptor cells at the ciliary apparatus and the synapse as well as at adhesion complexes of the outer

Please cite this article in press as: Overlack, N. et al., SANS (USH1G) expression in developing and mature ..., *Vision Research* (2007), doi:10.1016/j.visres.2007.08.021

limiting membrane. Immunofluorescence analyses revealed that SANS was colocalized with markers for these subcellular photoreceptor compartments. Latter data were confirmed by results achieved by Western blot analyses of tangential cryosections. Furthermore, the localization of SANS in the ciliary apparatus and at the synapse of photoreceptor cells was corroborated by the enrichment of SANS in fractions of these compartments obtained by sucrose density gradient centrifugation. In all analyzed subcellular compartments of photoreceptor cells, networks of USH proteins were previously described (reviewed in: (Reiners et al., 2006). SANS may function as an integral component of these USH protein networks in diverse photoreceptor compartments. The integration of SANS in the USH protein interactome is shown in a schematic representation in Fig. 1b. The functional relevance of compartment specific interactions of SANS with its partner proteins will be discussed in the following paragraphs.

The ciliary apparatus of photoreceptor cells consists of a basal body complex from which the non-motile connecting cilium originates (reviewed in: (Besharse & Horst, 1990; Roepman & Wolfrum, 2007). The connecting cilium is placed in a strategic position at the joint between the inner segment and the outer segment of the photoreceptor cell. All exchanges between the inner and outer segment occur through the narrow and slender connecting cilium (Wolfrum, 1995). Currently, two in principle different alternative mechanisms of active transport through the connecting cilium towards the photoreceptor outer segment are discussed (Williams, 2002; Roepman & Wolfrum, 2007): (i) A microtubule-based translocation mediated by kinesin II associated with intraflagellar transport (IFT) complexes (Marszalek et al., 2000; Rosenbaum & Witman, 2002). (ii) Previous studies indicated that the USH network protein myosin VIIa (USH1B) is capable to transport cargo along actin filaments within the ciliary membrane (Liu, Udovichenko, Brown, Steel, & Williams, 1999; Wolfrum & Schmitt, 2000; Maerker et al., 2007; present study). In both alternative transport mechanisms SANS may participate. We have previously shown that SANS directly interacts with myosin VIIa (Adato et al., 2005). Similar localization of both proteins in the connecting cilium (Liu, Vansant, Udovichenko, Wolfrum, & Williams, 1997; Wolfrum & Schmitt, 2000) indicates that these interactions may take place within the ciliary compartment of photoreceptor cells. In this protein complex, SANS may provide the linkage to the prominent microtubule cytoskeleton of the cilium. An association of SANS with microtubules has been previously discussed (Adato et al., 2005; Roepman & Wolfrum, 2007). This is further supported by present results on SANS localization at microtubule organization centers, namely centrosomes and spindle poles in NIH3T3 cells and by a recent study by Maerker et al. (2007).

However, the integration of SANS into a ciliary USH protein network linked by myosin VIIa to actin filaments does not exclude an involvement of SANS in processes related to IFT complexes predominantly associated with microtubules. In photoreceptor cells, SANS and IFT proteins were both detected in the connecting cilium and in the basal body region (present study; Pazour et al., 2002; Maerker et al., 2007). In the basal body region, IFT proteins are thought to recruit cargo from inner segment transport carriers for the transport route through the connecting cilium (Pazour et al., 2002). SANS may also participate in processes of cargo handover between inner segment transport and the delivery through the connecting cilium (Maerker et al., 2007). A role for SANS in the transport of vesicles in inner ear hair cells has been previously suggested, where SANS was found in the periphery of the cuticular plate and in the basal body complex of the kinocilium of outer hair cells (Adato et al., 2005).

Our present study revealed that SANS is not only associated with the cilium of adult photoreceptor cells, but also during maturation of photoreceptor cells. During developmental stages PN0 and PN7, SANS was exclusively present at the apical tip of the neuroblast layer. During this time period ciliogenesis proceeds, basal bodies (centrioles) are placed in the apical inner segments and ciliary sprouts are formed at the photoreceptor apices (Uga & Smelser, 1973; Woodford & Blanks, 1989). Present double immunofluorescence analyses of SANS and centrins indicate that SANS is localized in basal bodies and growing cilia of maturating photoreceptor cells. This is in agreement with an association of SANS with the basal body complex of the kinocilium in differentiating outer hair cells of the inner ear (Adato et al., 2005). The presence of SANS in basal bodies of ciliated cells in tissues is further strengthened by the localization of SANS at the centrosomes and spindle poles of NIH3T3 cells. In general, basal bodies from which cilia arise are homologous to the mother centriole of centrosomes (Dawe, Farr, & Gull, 2007).

The present study revealed the localization of SANS at the outer limiting membrane also known as the *membrana limitans externa* (Spitznas, 1970). The outer limiting membrane is a layer of cell–cell adhesion contacts, mechanically strengthening the adhesion between photoreceptor cells and Mueller glia cells. Previous studies indicated that besides SANS other USH proteins are present in the outer limiting membrane (Ahmed et al., 2003; Reiners, Marker, et al., 2005; van Wijk et al., 2006). Homo- or heterophilic interaction of the ectodomains of protocadherin 15 (USH1F), cadherin 23 (USH1D), USH2A isoform b, and VLGR1b (USH2C) are thought to design connectors between the adjacent membranes of photoreceptor cells and Mueller glia cells. These contacts may be facilitated through intracellular tether of their cytoplasmic domains by parallel direct binding to the PDZ domains 1 and 2 of the scaffold protein whirlin (USH2D) (van Wijk et al., 2006). The direct interaction of SANS with whirlin may provide a conjunction of this protein network at the outer limiting membrane to microtubules.

Recently, we described the direct interaction of whirlin with MPP1, a membrane associated guanylate kinase

Please cite this article in press as: Overlack, N. et al., SANS (USH1G) expression in developing and mature ..., *Vision Research* (2007), doi:10.1016/j.visres.2007.08.021

(MAGUK) protein of the large Crumbs protein complex at the outer limiting membrane (Gosens et al., 2007). Therefore, the USH protein network at the outer limiting membrane may be part of this multiprotein complex mainly organized by Crumbs1 and MPP5 (Gosens et al., 2007; Kantardzhieva et al., 2005). This complex is thought to serve in cell polarity and cell adhesion processes that are intimately connected and governs the formation and maintenance of the layered structure of vertebrate retina (Gosens et al., 2007; Kantardzhieva et al., 2005). The identified USH proteins may contribute to the function of the specialized Crumbs protein cell–cell adhesion complex at the outer limiting membrane. In conclusion, SANS may fulfill a role in bridging this cell–cell adhesion complex to the microtubule cytoskeleton and may participate in transport processes, necessary for the development and maintenance of the outer limiting membrane.

Our previous studies demonstrated localization of all identified USH1 and 2 proteins at photoreceptor and hair cell synapses (Reiners, van Wijk, et al., 2005, Reiners et al., 2006; van Wijk et al., 2006). Here, we confirm SANS as a further molecular component of the ribbon synapse of rod and cone photoreceptor cells. Present studies of developmental stages of the murine retina revealed that SANS protein expression was not found until PN14 when the synaptogenesis of ribbon synapses is terminated (von Kriegstein & Schmitz, 2003). Since our present data did not cover all stages during the critical period of synaptogenesis, we can not state whether or not SANS participates in the latter process. However, our data strengthen that SANS is part of the USH protein network present at the synapse in mature photoreceptor cells (reviewed in (Reiners et al., 2006). The current data set indicates that the PDZ domain containing USH scaffold proteins, harmonin and whirlin target the network components to the specialized ribbon synapses and tether their physiologic function there (Reiners et al., 2003, Reiners, van Wijk, et al., 2005; van Wijk et al., 2006). In the pre- and post-synaptic membrane of specialized photoreceptor synapses USH cadherins, cadherin 23, and protocadherin 15, as well as the transmembrane proteins USH2A and VLGR1b are thought to interact via their extracellular domains and keep the synaptic membranes in spatial proximity (Reiners et al., 2006). As in synapses in general, cytoplasmic scaffold proteins may anchor these adhesion molecules, but also transmembrane proteins as well as channels and receptors into the synaptic membrane (Garner, Nash, & Huganir, 2000). Our present results suggest that SANS is also part of this scaffolding machinery in ribbon synapses. By direct binding to the USH proteins harmonin, whirlin and myosin VIIa (see Fig. 1b) (Adato et al., 2005; van Wijk et al., 2006), SANS may connect the synaptic USH protein network with the microtubule cytoskeleton. However, in this association with microtubules, SANS may also participate in synaptic molecule trafficking and serve in the molecular handover from the long range microtubule-based neuronal transport system to the actin filament associated short range transport system of the synaptic terminal, probably governed by the actin-based molecular motor myosin VIIa.

In conclusion, the scaffold protein SANS is a crucial component of photoreceptor cells involved in various structural and developmental processes associated with the microtubule cytoskeleton. Our data indicate that SANS participates in ciliogenesis during outer segment differentiation, in formation and maintenance of retina and photoreceptor cell polarity and in functions in the ribbon synapse of photoreceptor cells. For its essential specific functions SANS is integrated in protein networks in the ciliary apparatus, the outer limiting membrane and the ribbon synapse of photoreceptor cells. Defects of SANS may cause dysfunctions of entire USH protein networks and may lead overall to degeneration of the sensory systems in the inner ear and retina, symptoms characteristic for USH patients.

Acknowledgements

This work was supported by the DFG GRK 1044 (to U.W.), Forschung contra Blindheit—Initative Usher Syndrom (to T.M. and U.W.), the FAUN-Stiftung, Nürnberg (to U.W.). Authors thank Gabi Stern-Schneider and Ulrike Maas for skillful technical assistance, Philipp Trojan for critical reading of the manuscript and J. Salisbury and P. Hargrave for providing us with anti-pan-centrin and anti-opsin antibodies.

References

Adamus, G., Arendt, A., Zam, Z. S., McDowell, J. H., & Hargrave, P. A. (1988). Use of peptides to select for anti-rhodopsin antibodies with desired amino acid sequence specificities. *Peptide Research, 1*, 42–47.

Adamus, G., Zam, Z. S., Arendt, A., Palczewski, K., McDowell, J. H., & Hargrave, P. A. (1991). Anti-rhodopsin monoclonal antibodies of defined specificity: characterization and application. *Vision Research, 31*, 17–31.

Adato, A., Michel, V., Kikkawa, Y., Reiners, J., Alagramam, K. N., Weil, D., et al. (2005). Interactions in the network of Usher syndrome type 1 proteins. *Human Molecular Genetics, 14*, 347–356.

Ahmed, Z. M., Riazuddin, S., Riazuddin, S., & Wilcox, E. R. (2003). The molecular genetics of Usher syndrome. *Clinical Genetics, 63*, 431–444.

Arden, G. B., & Fox, B. (1979). Increased incidence of abnormal nasal cilia in patients with Retinitis pigmentosa. *Nature, 279*, 534–536.

Besharse, J. C., & Horst, C. J. (1990). The photoreceptor connecting cilium—a model for the transition zone. In R. A. Bloodgood (Ed.), *Ciliary and flagellar membranes* (pp. 389–417). New York: Plenum.

Boeda, B., El-Amraoui, A., Bahloul, A., Goodyear, R., Daviet, L., Blanchard, S., et al. (2002). Myosin VIIa, harmonin and cadherin 23, three Usher 1 gene products that cooperate to shape the sensory hair cell bundle. *EMBO Journal, 21*, 6689–6699.

Dawe, H. R., Farr, H., & Gull, K. (2007). Centriole/basal body morphogenesis and migration during ciliogenesis in animal cells. *Journal of Cell Science, 120*, 7–15.

Davenport, S. L. H., Omenn, G. S., (1977). The heterogeneity of Usher syndrome. *Fifth international conference on birth defects*, Montreal.

Ebermann, I., Scholl, H. P., Charbel, I. P., Becirovic, E., Lamprecht, J., Jurklies, B., et al. (2007). A novel gene for Usher syndrome type 2: Mutations in the long isoform of whirlin are associated with retinitis pigmentosa and sensorineural hearing loss. *Human Genetics, 121*, 203–211.

Fleischman, D. (1981). Rod guanylate cyclase located in axonemes. *Current Topics in Membranes and Transport, 15*, 109–119.

Garner, C. C., Nash, J., & Huganir, R. L. (2000). PDZ domains in synapse assembly and signalling. *Trends in Cell Biology, 10*, 274–280.

Gießl, A., Pulvermüller, A., Trojan, P., Park, J. H., Choe, H.-W., Ernst, O. P., et al. (2004). Differential expression and interaction with the visual G-protein transducin of centrin isoforms in mammalian photoreceptor cells. *Journal of Biological Chemistry, 279*, 51472–51481.

Golenhofen, N., & Drenckhahn, D. (2000). The catenin, p120ctn, is a common membrane-associated protein in various epithelial and non-epithelial cells and tissues. *Histochemistry and Cell Biology, 114*, 147–155.

Gosens, I., van Wijk, E., Kersten, F. F., Krieger, E., van der, Z. B., Marker, T., et al. (2007). MPP1 links the Usher protein network and the Crumbs protein complex in the retina. *Human Molecular Genetics*, Epub ahead of print.

Hirao, K., Hata, Y., Ide, N., Takeuchi, M., Irie, M., Yao, I., et al. (1998). A novel multiple PDZ-domain-containing molecule interacting with *N*-methyl-D-aspartate receptors and neuronal cell adhesion proteins. *Journal of Biological Chemistry, 273*, 21105–21110.

Horst, C. J., Forestner, D. M., & Besharse, J. C. (1987). Cytoskeletal-membrane interactions: Between cell surface glycoconjugates and doublet microtubules of the photoreceptor connecting cilium. *Journal of Cell Biology, 105*, 2973–2987.

Johnston, A. M., Naselli, G., Niwa, H., Brodnicki, T., Harrison, L. C., & Gonez, L. J. (2004). Harp (harmonin-interacting, ankyrin repeat-containing protein), a novel protein that interacts with harmonin in epithelial tissues. *Genes to Cells, 9*, 967–982.

Kantardzhieva, A., Gosens, I., Alexeeva, S., Punte, I. M., Versteeg, I., Krieger, E., et al. (2005). MPP5 recruits MPP4 to the CRB1 complex in photoreceptors. *Investigative Ophthalmology & Visual Science, 46*, 2192–2201.

Kikkawa, Y., Shitara, H., Wakana, S., Kohara, Y., Takada, T., Okamoto, M., et al. (2003). Mutations in a new scaffold protein Sans cause deafness in Jackson shaker mice. *Human Molecular Genetics, 12*, 453–461.

Kornau, H. C., Seeburg, P. H., & Kennedy, M. B. (1997). Interaction of ion channels and receptors with PDZ domain proteins. *Current Opinion in Neurobiology, 7*, 368–373.

Koulen, P., Garner, C. C., & Wassle, H. (1998). Immunocytochemical localization of the synapse-associated protein SAP102 in the rat retina. *Journal of Comparative Neurology, 397*, 326–336.

Kremer, H., van Wijk, E., Märker, T., Wolfrum, U., & Roepman, R. (2006). Usher syndrome: Molecular links of pathogenesis, proteins and pathways. *Human Molecular Genetics, 15*(Suppl. 2), R262–R270.

Liu, X., Udovichenko, I. P., Brown, S. D., Steel, K. P., & Williams, D. S. (1999). Myosin VIIa participates in opsin transport through the photoreceptor cilium. *Journal of Neuroscience, 19*, 6267–6274.

Liu, X. R., Vansant, G., Udovichenko, I. P., Wolfrum, U., & Williams, D. S. (1997). Myosin VIIa, the product of the Usher 1B syndrome gene, is concentrated in the connecting cilia of photoreceptor cells. *Cell Motility and the Cytoskeleton, 37*, 240–252.

Marszalek, J. R., Liu, X., Roberts, E. A., Chui, D., Marth, J. D., Williams, D. S., et al. (2000). Genetic evidence for selective transport of opsin and arrestin by kinesin-II in mammalian photoreceptors. *Cell, 102*, 175–187.

Maerker, T., van Wijk, E., Overlack, N., Kersten, F. F. J., McGee, J., Goldmann, T., et al. (2007). A novel Usher protein network at the periciliary reloading point between molecular transport machineries in vertebrate photoreceptor cells. *Human Molecular Genetics*, accepted for publication.

Mehalow, A. K., Kameya, S., Smith, R. S., Hawes, N. L., Denegre, J. M., Young, J. A., et al. (2003). CRB1 is essential for external limiting membrane integrity and photoreceptor morphogenesis in the mammalian retina. *Human Molecular Genetics, 12*, 2179–2189.

Montonen, O., Aho, M., Uitto, J., & Aho, S. (2001). Tissue distribution and cell type-specific expression of p120ctn isoforms. *Journal of Histochemistry & Cytochemistry, 49*, 1487–1496.

Nagel-Wolfrum, K., Buerger, C., Wittig, I., Butz, K., Hoppe-Seyler, F., & Groner, B. (2004). The interaction of specific peptide aptamers with the DNA binding domain and the dimerization domain of the transcription factor Stat3 inhibits transactivation and induces apoptosis in tumor cells. *Molecular Cancer Research, 2*, 170–182.

Nourry, C., Grant, S. G., & Borg, J. P. (2003). PDZ domain proteins: plug and play! *Science's STKE, 2003*, RE7.

Papermaster, D. S. (1982). Preparation of retinal rod outer segments. *Methods in Enzymology, 81*, 48–52.

Pazour, G. J., Baker, S. A., Deane, J. A., Cole, D. G., Dickert, B. L., Rosenbaum, J. L., et al. (2002). The intraflagellar transport protein, IFT88, is essential for vertebrate photoreceptor assembly and maintenance. *Journal of Cell Biology, 157*, 103–113.

Petit, C. (2001). Usher syndrome: From genetics to pathogenesis. *Annual Review of Genomics and Human Genetics, 2*, 271–297.

Pulvermüller, A., Gießl, A., Heck, M., Wottrich, R., Schmitt, A., Ernst, O. P., et al. (2002). Calcium dependent assembly of centrin/G-protein complex in photoreceptor cells. *Molecular and Cellular Biology, 22*, 2194–2203.

Reiners, J., Marker, T., Jurgens, K., Reidel, B., & Wolfrum, U. (2005). Photoreceptor expression of the Usher syndrome type 1 protein protocadherin 15 (USH1F) and its interaction with the scaffold protein harmonin (USH1C). *Molecular Vision, 11*, 347–355.

Reiners, J., van Wijk, E., Maerker, T., Zimmermann, U., Juergens, K., te Brinke, H., et al. (2005). Scaffold protein harmonin (USH1C) provides molecular links between Usher syndrome type 1 and type 2. *Human Molecular Genetics, 14*, 3933–3943.

Reiners, J., Nagel-Wolfrum, K., Jurgens, K., Marker, T., & Wolfrum, U. (2006). Molecular basis of human Usher syndrome: deciphering the meshes of the Usher protein network provides insights into the pathomechanisms of the Usher disease. *Experimental Eye Research, 83*, 97–119.

Reiners, J., Reidel, B., El-Amraoui, A., Boeda, B., Huber, I., Petit, C., et al. (2003). Differential distribution of harmonin isoforms and their possible role in Usher-1 protein complexes in mammalian photoreceptor cells. *Investigative Ophthalmology & Visual Science, 44*, 5006–5015.

Roepman, R., & Wolfrum, U. (2007). Protein networks and complexes in photoreceptor cilia. In E. Bertrand & M. Faupel (Eds.). *Subcellular proteomics from cell deconstruction to system reconstruction* (Vol. 43, pp. 209–235). New York: Springer, Chapter 10.

Rosenbaum, J. L., & Witman, G. B. (2002). Intraflagellar transport. *Nature Reviews. Molecular Cell Biology, 3*, 813–825.

Schmitt, A., & Wolfrum, U. (2001). Identification of novel molecular components of the photoreceptor connecting cilium by immunoscreens. *Experimental Eye Research, 73*, 837–849.

Sedgwick, S. G., & Smerdon, S. J. (1999). The ankyrin repeat: A diversity of interactions on a common structural framework. *Trends in Biochemical Sciences, 24*, 311–316.

Siemens, J., Kazmierczak, P., Reynolds, A., Sticker, M., Littlewood Evans, A., & Müller, U. (2002). The Usher syndrome proteins cadherin 23 and harmonin form a complex by means of PDZ-domain interactions. *Proceedings of the National Academy of Sciences of the United States of America, 99*, 14946–14951.

Spitznas, M. (1970). The fine structure of the so-called outer limiting membrane in the human retina. *Albrecht von Graefes Archin fur Klinische Experimentelle Ophthalmologie, 180*, 44–56.

Stapleton, D., Balan, I., Pawson, T., & Sicheri, F. (1999). The crystal structure of an Eph receptor SAM domain reveals a mechanism for modular dimerization. *Nature Structure Biology, 6*, 44–49.

Uga, S., & Smelser, G. K. (1973). Electron microscopic study of the development of retinal Mullerian cells. *Investigative Ophthalmology, 12*, 295–307.

van Wijk, E., van der Zwaag, B., Peters, T., Zimmermann, U., te Brinke, H., Kersten, F. F., et al. (2006). The DFNB31 gene product whirlin connects to the Usher protein network in the cochlea and retina by direct association with USH2A and VLGR1. *Human Molecular Genetics, 15*, 751–765.

Please cite this article in press as: Overlack, N. et al., SANS (USH1G) expression in developing and mature ..., *Vision Research* (2007), doi:10.1016/j.visres.2007.08.021

von Kriegstein, K., & Schmitz, F. (2003). The expression pattern and assembly profile of synaptic membrane proteins in ribbon synapses of the developing mouse retina. *Cell and Tissue Research, 311*, 159–173.

Weil, D., El-Amraoui, A., Masmoudi, S., Mustapha, M., Kikkawa, Y., Lainé, S., et al. (2003). Usher syndrome type I G (USH1G) is caused by mutations in the gene encoding SANS, a protein that associates with the USH1C protein, harmonin. *Human Molecular Genetics, 12*, 463–471.

Williams, D. S. (2002). Transport to the photoreceptor outer segment by myosin VIIa and kinesin II. *Vision Research, 42*, 455–462.

Wolfrum, U. (1991). Tropomyosin is co-localized with the actin filaments of the scolopale in insect sensilla. *Cell and Tissue Research, 265*, 11–17.

Wolfrum, U. (1995). Centrin in the photoreceptor cells of mammalian retinae. *Cell Motility and the Cytoskeleton, 32*, 55–64.

Wolfrum, U., & Salisbury, J. L. (1998). Expression of centrin isoforms in the mammalian retina. *Experimental Cell Research, 242*, 10–17.

Wolfrum, U., & Schmitt, A. (2000). Rhodopsin transport in the membrane of the connecting cilium of mammalian photoreceptor cells. *Cell Motility and the Cytoskeleton, 46*, 95–107.

Woodford, B. J., & Blanks, J. C. (1989). Localization of actin and tubulin in developing and adult mammalian photoreceptors. *Cell and Tissue Research, 256*, 495–505.

Please cite this article in press as: Overlack, N. et al., SANS (USH1G) expression in developing and mature ..., *Vision Research* (2007), doi:10.1016/j.visres.2007.08.021

II Maerker, T., van Wijk, E., Overlack, N., Kersten, F. F. J., McGee, J., Goldmann, T., Sehn, E., Roepman, R., Walsh, E.J., Kremer, H., Wolfrum, U. (2007) A novel Usher protein network at the periciliary reloading point between molecular transport machineries in vertebrate photoreceptor cells. *Hum Mol Genet.*, Epub ahead of print

HMG Advance Access published September 28, 2007

A novel Usher protein network at the periciliary reloading point between molecular transport machineries in vertebrate photoreceptor cells

Tina Maerker[1], Erwin van Wijk[2,3], Nora Overlack[1], Ferry F.J. Kersten[2,3,4,5], JoAnn McGee[6], Tobias Goldmann[1], Elisabeth Sehn[1], Ronald Roepman[3,5], Edward J. Walsh[6], Hannie Kremer[2] and Uwe Wolfrum[1]*

[1]Department of Cell and Matrix Biology, Institute of Zoology, Johannes Gutenberg University of Mainz, 55099 Mainz, Germany
[2]Department of Otorhinolaryngology [3]Department of Human Genetics and [4]Department of Ophthalmology, Radboud University Nijmegen Medical Centre, [5]Nijmegen Centre for Molecular Life Sciences, 6500 HB Nijmegen, The Netherlands
[6]Developmental Auditory Physiology Laboratory, Boys Town National Research Hospital, Omaha, Nebraska 68131, U.S.A

***Corresponding author:** Uwe Wolfrum, Johannes Gutenberg University Mainz, Institute of Zoology, Department of Cell and Matrix Biology, Muellerweg 6, D-55099 Mainz, Germany.
Tel.: +49-6131-39-25148; Fax: +49-6131-39-23815;
E-mail: ***wolfrum@uni-mainz.de***

Abstract

The human Usher syndrome (USH) is the most frequent cause of combined deaf-blindness. USH is genetically heterogeneous with at least 12 chromosomal loci assigned to three clinical types, USH1-3. Although these USH types exhibit similar phenotypes in human, the corresponding gene products belong to very different protein classes and families.

The scaffold protein harmonin (USH1C) was shown to integrate all identified USH1 and USH2 molecules into protein networks. Here, we analyzed a protein network organized in the absence of harmonin by the scaffold proteins SANS (USH1G) and whirlin (USH2D). Immunoelectron microscopic analyses disclosed the colocalization of all network components in the apical inner segment collar and the ciliary apparatus of mammalian photoreceptor cells. In this complex, whirlin and SANS directly interact. Furthermore, SANS provides a linkage to the microtubule transport machinery, whereas whirlin may anchor USH2A isoform b and VLGR1b via binding to their cytodomains at specific membrane domains. The long ectodomains of both transmembrane proteins extend into the gap between the adjacent membranes of the connecting cilium and the apical inner segment. Analyses of Vlgr1/del7TM mice revealed the ectodomain of VLGR1b as a component of fibrous links present in this gap. Comparative analyses of mouse and *Xenopus* photoreceptors demonstrated that this USH protein network is also part of the periciliary ridge complex in *Xenopus*. Since this structural specialization in amphibian photoreceptor cells defines a specialized membrane domain for docking and fusion of transport vesicles, we suggest a prominent role of the USH proteins in cargo shipment.

Introduction

Vertebrate rod and cone photoreceptor cells are highly polarized neurons, which consist of morphological and functional distinct cellular compartments. A light sensitive outer segment is linked via a non-motile connecting cilium with an inner segment which contains the organelles typical for the metabolism of eukaryotic cells. The outer segment is characterized by specialized flattened disk-like membranes, where all components of the visual transduction cascade are arranged. These phototransductive membranes in the outer segment are continually renewed throughout lifetime. Newly synthesized membranes are added at the base of the outer segment, whereas disks at the outer segment apex are phagocytosed by cells of the retinal pigment epithelium (1). All molecular components of the outer segment machinery are synthesized in organelles located in the basal part of the inner segment and are vectorially transported in the inner segment and through the connecting cilium to the outer segment (2-4). On its route, the cargo has to be reloaded from inner segment transport carriers to ciliary transport systems in a specialized compartment of the apical inner segment (5). In our present study, we identified a protein network which participates in the cargo delivery from the inner segment to the outer segment of vertebrate photoreceptor cells. Interestingly, the proteins of this network are encoded by genes related to the human Usher syndrome.

The Usher syndrome (USH) is an autosomal recessive disorder characterized by combined hearing loss and retinal degeneration. USH is genetically heterogeneous with at least 12 chromosomal loci involved. Depending on their clinical features (onset, severity and progression) three USH types can be distinguished (6-8). Patients suffering from USH1, the most severe form, exhibit profound congenital hearing loss and constant vestibular dysfunction, combined with pre-pubertal onset of retinitis pigmentosa. In USH2, the most frequent type, congenital hearing loss is milder; the onset of retinitis pigmentosa is during or after puberty and vestibular function remains normal. USH3 is only relatively frequent in specific populations and characterized by progressive hearing loss with variability in vestibular dysfunction and in the onset of retinitis pigmentosa.

The gene products of identified USH genes belong to various protein classes and families as recently reviewed in Reiners et al., (2006) and Kremer et al., (2006): USH1B encodes the molecular motor myosin VIIa; harmonin (USH1C), SANS (scaffold protein containing ankyrin repeats and SAM domain, USH1G) and whirlin, more recently identified as USH2D (9) belong to the group of scaffold proteins (Fig. 1A); cadherin 23 (USH1D) and protocadherin 15 (USH1F) represent cell-cell adhesion proteins, whereas USH2A and USH2C

encode the large transmembrane protein USH2A isoform b and seven transmembrane receptor VLGR1b (very large G-protein coupled receptor 1b), respectively (Fig. 1A). The four-transmembrane-domain protein clarin-1 (USH3A) is so far the only member of USH3.

Previous molecular analyses revealed that the USH1C scaffold protein harmonin integrates all USH1 and USH2 proteins into USH protein networks (see recent reviews: (10, 11)). In hair cells of the inner ear, harmonin mediated USH protein networks are thought to be essential for stereocilia development and may participate in synaptic function as well as in mechano-electric signal transduction (6,10,11). In the retina, the function of these protein networks is mainly assumed to maintain synaptic integrity and function (10).

However, the USH proteins SANS and whirlin were already suggested as scaffold proteins organizing additional protein networks in the inner ear and the retina (11-14). SANS forms homodimers and directly interacts with harmonin and myosin VIIa (12). In the present study, direct binding of SANS and whirlin was confirmed as originally suggested (11,14). In addition, we found evidence for the association of SANS with the microtubule cytoskeleton. In previous studies, we demonstrated direct interaction of whirlin with the cytoplasmic domains of USH2A isoform b and VLGR1b (11,14). The latter transmembrane proteins were proposed as molecular components of fibrous ankle links between adjacent stereocilia of mechanosensitive hair cells (13,15). A more recent study demonstrated whirlin as the major scaffold protein of a USH protein network in the ankle link complex of inner ear hair cells (16). Immunological analyses indicated that the ankle links between neighboring stereocilia of hair cells share antigens with fibrous links localized in the gap between the adjacent membranes of the inner segment apex and the connecting cilium of vertebrate photoreceptor cells (15,17,18). Here, we describe a novel USH protein network in the periciliary region of vertebrate photoreceptor cells which has a molecular composition comparable to the ankle link complex. We show that the ectodomain of VLGR1b is an essential component of the fibrous links connecting the adjacent membranes in the ciliary region of photoreceptor cells. Furthermore, our comparative analyses of mouse and *Xenopus* photoreceptor cells provide strong indications for an important role of this novel periciliary USH protein complex in the delivery of cargo to the outer segment of vertebrate photoreceptor cells in general.

Results

The USH1G protein SANS directly interacts with the USH2D protein whirlin.

Yeast two-hybrid screens were performed to identify proteins interacting with the USH1G protein SANS. For this, the C-terminus of human SANS (aa 400-465) containing a SAM domain (sterile alpha motif) and a class I PDZ binding motif (PBM) (Fig. 1A) was used as a bait to screen a bovine retina cDNA library. Of the 40 positive clones encoding potential interaction partners 33 encoded the N-terminal region of whirlin. Reciprocal yeast two-hybrid assays confirmed specific interaction between whirlin and the C-terminus of SANS and pinpointed the binding site of the whirlin molecule to its PDZ domains 1 and 2 (Fig. 1B).

In order to validate the SANS-whirlin interaction, different recombinantly expressed domains of both proteins were used to carry out GST (glutathione S-transferase) pull-down assays. Incubation of GST-tagged whirlin PDZ domains, namely PDZ1, PDZ2, PDZ1 and 2, PDZ3 or GST alone with FLAG-tagged full length SANS identified whirlin's PDZ1 and 2 as the binding sites for SANS (Fig. 1C). Interaction of FLAG-tagged SANS and whirlin´s PDZ3 or GST alone could not be detected. In GST pull-down assays with the FLAG-tagged C-terminal SAM domain of SANS lacking the PBM motif (FLAG-SANS SAMΔPBM) the interaction was abolished (Fig. 1C). Since the N-terminal 400 amino acids of SANS were not present in the bait construct used in our initial yeast-two hybrid screen these findings strongly support that SANS directly interacts via its C-terminal PBM motif with PDZ1 and PDZ2 of whirlin.

To confirm this interaction *in vivo*, COS-1 cells were cotransfected with plasmids encoding full length SANS and the long isoform of whirlin fused to eCFP or mRFP, respectively (Fig. 1D). In mRFP-whirlin transfected COS-1 cells, the mRFP-fluorescence was present in the entire cytoplasm with a concentration in the perinuclear area (Fig. 1D, upper panel). eCFP-SANS single transfected cells expressed the fusion protein in granulous aggregates in the periphery of the nucleus (Fig. 1D, middle panel). In cotransfected COS-1 cells, mRFP-whirlin and eCFP-SANS were colocalized in these granules in the periphery of the nucleus (Fig. 1D, lower panel) indicating a recruitment of mRFP-whirlin towards the nucleus through its interaction with eCFP-SANS. To evaluate whether the interaction between SANS and whirlin also occurs in the retina, coimmunoprecipitations were performed. For this purpose, extracts of mouse retinas were incubated with anti-whirlin antibodies immobilized on agarose beads. Western blot analysis of the immunoprecipitates with anti-SANS antibodies revealed coimmunoprecipitation of SANS with whirlin (Fig. 1E). In conclusion, the results of

the present protein-protein interaction analyses indicate specific binding of SANS via its C-terminal class I PBM to the PDZ domains 1 and 2 of whirlin.

Subcellular colocalization of the USH scaffold proteins SANS and whirlin in the ciliary region of mouse photoreceptor cells.

In situ protein-protein interaction of SANS and whirlin should imply colocalization of both binding partners in tissue. To validate this, we carried out indirect immunofluorescence double labeling experiments with anti-SANS and anti-whirlin antibodies in murine retinal cryosections. Double immunofluorescence labeling revealed colocalization of SANS and whirlin at the synapses in the outer plexiform layer, in the outer limiting membrane, the inner segment and the ciliary region of photoreceptor cells (Fig. 2C-E). For further confirmation of the localization SANS and whirlin in the ciliary apparatus of photoreceptor cells, immunofluorescence double labeling with antibodies against SANS or whirlin, respectively, and anti-pan-centrin antibodies, a well characterized molecular marker for the photoreceptor ciliary apparatus (19,20), was performed. High resolution analyses of double immunofluorescences revealed colocalization of SANS and whirlin in the connecting cilium and the basal body complex of photoreceptor cells (Fig. 2F-H).

To elucidate the subcellular distribution of SANS and whirlin more precisely in mouse photoreceptors, we performed immunoelectron microscopy. Pre-embedding immunolabeling with anti-SANS and anti-whirlin antibodies confirmed the localization of both proteins in the connecting cilium, the basal body complex and in the apical inner segment of mouse photoreceptor cells (Fig. 3). It is important to note, that the pre-embedding immunoelectron microscopy analyses of SANS and whirlin in the connecting cilium depended on the depth of the antibody penetration into the connecting cilium. Therefore, concentrations of antibody staining were found in the proximal and apical portion of the cilium to which the antibodies were able to freely diffuse (Figs. 3, 4). However, since the ciliary membrane turned out to be often resistant to the cracking procedure and detergent treatments applied (21), antibodies were unable to penetrate the ciliary membrane and therefore the middle portion of the cilium was seldom stained. Nevertheless, in other photoreceptor cells the ciliary region was more perforated. In those cases, antibodies were able to reach the ciliary cytoplasm and the antigen epitopes present in the cilium were detected (Fig. 3 B, C, E, F). Exploiting the high resolution of the electron microscope we demonstrated labeling of SANS and whirlin pronounced in the cytoplasm of the apical inner segment extension (Figs. 3A, C, D). This extension forms a

collar alongside the connecting cilium and is different from calycal processes, which project as slender elongations of the inner segment apex along the outer segment (22).

Since harmonin was previously shown as the major scaffold protein organizing USH protein networks (10,11), we analyzed the subcellular localization of harmonin by a spectrum of equivalent methods. Immunofluorescence analyses and immunelectron microscopy after pre-embedding labeling confirmed our previous results (23). Harmonin was localized at the synaptic region, in the inner segment and the outer segment, but was absent from in the apical collar of the inner segment and in the connecting cilium of mouse photoreceptor cells (supplementary material Fig. 1).

Subcellular colocalization of SANS and whirlin with the cytoplasmic domains of USH2A isoform b and VLGR1b in the connecting cilium and apical inner segment collar of mouse photoreceptor cells.

The USH2 proteins USH2A isoform b and VLGR1b (USH2C) are transmembrane proteins composed of a very short intracellular cytoplasmic domain and a very long extracellular ectodomain (Fig 1A). The expression of USH2A isoform b and VLGR1b in mouse retina and previous immunofluorescence studies indicated their localization in the outer plexiform layer, the inner segment and more interestingly also in the region of the connecting cilium (10,14). Furthermore, direct association of USH2A isoform b and VLGR1b with whirlin was demonstrated (13,14). Therefore, we investigated the subcellular localization of these USH2 transmembrane proteins by high resolution immunofluorescence and immunoelectron microscopy. High magnification immunofluorescence images of double labeling of USH2A isoform b or VLGR1b, respectively and the ciliary molecular marker centrin revealed partial colocalization (supplementary material Fig. 2). Immunofluorescence labeling of USH2A isoform b was found in the connecting cilium and the basal body complex, while VLGR1b staining was present in the connecting cilium. These results confirmed USH2A isoform b and VLGR1b as components of the ciliary apparatus (10,24).

Pre-embedding immunoelectron microscopy analyses demonstrated localization of both transmembrane proteins, SANS and whirlin in the same compartments of the photoreceptor cell, indicating the colocalization of all four proteins. Anti-USH2A antibodies directed against the intracellular domain of USH2A isoform b detected USH2A at the basal body complex, the connecting cilium and the adjacent collar of the apical inner segment of photoreceptor cells (Figs. 4A-D). Unfortunately, antibodies raised against the extracellular domain of USH2A isoform b which previously stained the ciliary region of photoreceptor

cells by indirect immunofluorescence (10, 14, 24) did not work in our pre-embedding labeling protocol for immunoelectron microscopy analyses (data not shown). The antibodies directed against intracellular domains of VLGR1b labeled VLGR1b at the apical membrane of the inner segment and the connecting cilium of mouse photoreceptor cells (Figs. 4E, F). VLGR1b and USH2A isoform b labeling of cross-sections through connecting cilia confirmed their ciliary localization (Figs. 4D, F). Nevertheless, the staining of VLGR1b and USH2A isoform b in the connecting cilium was incomplete (see Figs. 4C, B, E) due to the methodological limitations discussed above for immunoelectron microscopy analyses for SANS and whirlin.

Ectodomains of VLGR1b are components of fibrous links bridging the ciliary and apical inner segment membrane of photoreceptor cells.

The subcellular distribution of the long extracellular domain of VLGR1b was analyzed with specific antibodies directed against ectodomains of VLGR1b. Immunoelectron microscopy analyses using these antibodies revealed exclusive decoration of fibrous links localized within the gap between the membranes of the connecting cilium and the periciliary inner segment collar (Fig. 4G).

It has been demonstrated, that fibrous links in photoreceptor cells as well as the homologous ankle links in inner ear hair cells are sensitive to the calcium chelator BAPTA (17,18). This prompted us to test, whether the ectodomains of VLGR1b are BAPTA sensitive. For this purpose we treated retina cryosections with 0.5 mM BAPTA in PBS previous to immunohistochemical analyses with anti-ecto-VLGR1b or control antibodies. The VLGR1b ectodomains were BAPTA sensitive and could no longer be detected by anti-ecto-VLGR1b antibodies after treatment with BAPTA for 30 minutes (Fig. 5D, F). In contrast, the staining with control antibodies to whirlin and to the cytoplasmic domain of VLGR1b remained unaffected (see whirlin staining in Fig. 5E, F). These findings strengthened the hypothesis, that the ectodomains of VLGR1b are components of fibrous membrane linkages in photoreceptor cells.

Fibrous links between the ciliary and apical inner segment membrane are absent in Vlgr1/del7TM mice.

These results encouraged us to analyze the organization of the periciliary apparatus in VLGR1b deficient (Vlgr1/del7TM) mice. Transmission electron microscopy was used to examine the distribution of fibrous membrane linkers in retinal photoreceptor cells of wild type and homozygous Vlgr1/del7TM mice (25). In photoreceptor cells of wild type mice,

fibrous membrane linkers were readily visible spanning the gap between the adjacent membranes (Fig. 5G, H). In contrast, these fibrous links were not detected in any of the photoreceptor cells examined from homozygous Vlgr1/del7TM mice, neither in rod (Fig. 5I, J), nor in cone photoreceptor cells (data not shown). In longitudinal ultrathin sections through the photoreceptor cells of homozygous Vlgr1/del7TM mice the membranes of the connecting cilium and the inner segment collar were no longer closely opposed (Fig. 5J). These findings support the results described above, further strengthening the hypothesis that VLGR1b is a component of fibrous membrane linkers within the newly identified periciliary network in photoreceptor cells.

SANS, whirlin, USH2A isoform b and VLGR1b colocalize in the periciliary ridge complex of *Xenopus* photoreceptor cells.

Our results from protein-protein interaction assays (14) and our immunoelectron microscopical data indicate the localization of an USH protein complex, composed of SANS, whirlin, USH2A isoform b and VLGR1b in the connecting cilium and in the adjacent collar-like extension of the apical inner segment in mouse photoreceptor cells. To date, little was known about structural and molecular specializations in the apical inner segment subarea of mammalian photoreceptor cells. However, in amphibians, Papermaster and co-workers previously described the so-called periciliary ridge complex as a highly specialized subcellular compartment in the apex of the photoreceptor cell inner segment (26-28). A schematic representation of the periciliary ridge complex is shown in the supplemental material figure 3. The topologic parallels of the periciliary ridge complex to the apical inner segment membrane in mouse photoreceptor cells prompted us to analyze the subcellular distribution of SANS, whirlin, USH2A isoform b and VLGR1b in photoreceptor cells of *Xenopus laevis* by immunoelectron microscopy. Our studies revealed the localization of all four analyzed USH proteins in the ciliary apparatus and the periciliary ridge complex of *Xenopus* rod and cone photoreceptor cells (Figs. 6 and 7; supplemental material Fig. 3). In the ciliary apparatus immunolabelings were obtained in the cytoplasm of the connecting cilium and its apical projection into the outer segment (Figs. 6A-C, 7A-D). Furthermore, SANS, whirlin and USH2A isoform b were found at the basal body at the base of the connecting cilium (Figs. 6A-C, 7A). In the periciliary ridge complex, labeling was predominantly present in the ridges (Figs. 6D, 7B, D). From these ridges fibrous links bridge to the ciliary membrane (Figs. 6D, 7B, D). In contrast, the intercalating periciliary grooves which are thought to

constitute the docking sites for transport vesicles were not stained by any of the antibodies (Fig. 6D).

The observed colocalization of SANS, whirlin, USH2A isoform b and VLGR1b in mouse and *Xenopus* photoreceptors confirms the presence of a periciliary USH protein network at adjacent membranes of the connecting cilium and a specialized micro compartment of the apical inner segment (Fig. 9, supplemental material Fig. 3). Furthermore, we found first evidence for the presence of this USH protein network in calycal processes of *Xenopus* rod and cone photoreceptor cells (data not shown).

SANS is associated with microtubules in NIH3T3 and retinal photoreceptor cells.

Findings from previous studies in which SANS was localized in microtubule-rich regions of inner ear hair cells and in cultured cells (12,29) prompted us to analyze a potential connection of SANS to microtubules. To illuminate the possible association of SANS with microtubules we treated cultured cells and organotypic retina cultures with microtubule destabilizing drugs. Immunofluorescence analyses of NIH3T3 cells revealed localization of endogenously expressed SANS in a perinuclear region at the centrosome of the cell (Fig. 8A; see also 29). Treatment with either colchicine or thiabendazole resulted in the degradation of the microtubule cytoskeleton (Figs. 8 B, C) and caused apparent changes of the cellular distribution of SANS (Figs. 8 B, C). SANS staining was no longer present at centrosomes, but was dispersed throughout the entire cytoplasm (Fig. 8B) or even found in nuclei of NIH3T3 cells (Fig. 8C).

Since our interest focused on a possible SANS association with microtubules in the retinal photoreceptor cells, we analyzed the distribution of SANS in DMSO treated and cytoskeletal drug treated organotypic cultures of mature mouse retinas which we recently introduced (30). Indirect immunofluorescence of cryosections through cultured mouse retinas stained by anti-SANS and anti-α-tubulin antibodies revealed a partially overlapping staining pattern of microtubules and SANS in DMSO treated control retinas (Fig. 8D). As expected, microtubules were depolymerized after application of thiabendazole to cultured retinas (Fig. 8E, middle panel). In addition, treatments with the microtubule destabilization drug resulted in an altered distribution of SANS or even in fading of the SANS staining in photoreceptor cells (Fig. 8E). The localization of SANS in microtubule-rich regions of different cell types and its microtubule-dependent cellular distribution indicated a direct or indirect association of SANS with the microtubule cytoskeleton.

Discussion

USH1 and USH2 proteins are organized in an interactome of multiprotein scaffolds (10,11,16). We and others have identified the USH1C protein harmonin as the major scaffold protein networking USH proteins (10). The localization of all identified components of the USH proteins in the synaptic region of photoreceptor cells indicated the existence of an USH protein network positioned at cone and rod photoreceptor synapses (10). In the present study, we discovered a protein network composed of USH1 and USH2 proteins in the absence of harmonin (supplementary material Fig. 1) (23) in the periciliary collar of the apical inner segment and the adjacent connecting cilium of mammalian photoreceptor cells. This protein network is organized by two other USH scaffold proteins, namely SANS (USH1G) and whirlin (USH2D) (Fig. 9). In addition, we found an association of SANS with microtubules suggesting an important side branch of USH protein networks to the microtubule cytoskeleton and hence to microtubule-associated intracellular transport processes.

Our yeast two-hybrid screens and subsequent protein-protein interaction assays revealed direct interaction of SANS with whirlin. These findings were confirmed by preliminary data obtained from reciprocal yeast two-hybrid assays using whirlin as bait (14). The validation of this interaction by GST pull-downs demonstrated that SANS binds directly to the PDZ1 and 2 but not to the PDZ3 domain of whirlin. Furthermore, our findings indicate that this interaction is most probably mediated through binding of the C-terminal PBM of SANS. A semiquantitative analysis of these associations indicates higher affinity of the SANS-C-terminus to PDZ1 than to PDZ2 of whirlin. Nevertheless, the three amino acids of the C-terminal PDZ-binding motif are essential for the interaction of SANS to whirlin´s PDZ1 and PDZ2. This is in contrast to the previously identified interaction of SANS with harmonin which is dependent on a larger C-terminal domain of SANS (12).

Several USH1 proteins, namely the cadherins CDH23 (USH1D) and PCDH15 (USH1F), myosin VIIa (USH1B) and SANS were previously identified as binding partners for whirlin (11,14,16,31). In the latter protein network, whirlin, myosin VIIa and SANS have the potential for homodimerization and interaction with each other (12,31,32). In addition, specific binding of whirlin and myosin VIIa to the large transmembrane proteins USH2A isoform b and VLGR1b was reported (13,14,16). In inner ear hair cells, several lines of evidence support the hypothesis that a supra-molecular protein complex scaffolded by whirlin plays an important role in the ankle link formation at the base of stereocilia (12-16). These ankle links are extracellular fibrous structures which connect neighboring stereocilia as well

as stereocilia with the adjacent kinocilium and are essential for correct differentiation and organization of hair cell bundles. Recent data indicated that ankle link fibers are composed of the ectodomains of USH2A isoform b and VLGR1b (13,15,16). It has been suggested that the ankle link complex in hair cells is homologous to the periciliary complex localized to the membranes of the connecting cilium and the collar-like extension of the apical inner segment in photoreceptor cells (15,17,18,33). This is in full agreement with our present data. We show that the molecular composition of the ankle link complex in hair cells and the periciliary complex in photoreceptor cells is conserved. Immunoelectron microscopy demonstrated colocalization of the cytoplasmic domains of the transmembrane proteins USH2A isoform b and VLGR1b with whirlin and SANS in the connecting cilium and in the adjacent apical inner segment collar of mammalian photoreceptor cells. The direct binding to the scaffold protein whirlin most probably anchors both transmembrane proteins within the cytoplasm of these subcellular compartments. The distinct labeling of epitopes by antibodies directed against the ectodomain of VLGR1b in the extracellular gap between the membranes of the cilium and the collar-like extension of the apical inner segment strongly suggests that the extracellular domains of VLGR1b are components of fibrous links which interconnect adjacent plasma membranes. The absence of these fibers in photoreceptor cells of homozygous Vlgr1/del7TM mice and the BAPTA sensitivity of the ectodomains of VLGR1b further confirmed VLGR1b as an essential component of these fibrous links.

The structures of USH2A isoform b and VLGR1b (see Fig. 1A) are consistent with the hypothesis that both USH2 proteins are substantial components of these fibrous membrane links in vertebrate photoreceptor cells. Estimations of the large ectodomains in both USH2 molecules reveal a length of ~ 150 nm (13,34) which is in the range of the distance between the ciliary membrane and the adjacent inner segment membrane in photoreceptor cells (over 125 nm). There are several possibilities how USH2A isoform b and VLGR1b are arranged within these fibrous links. It is conceivable that USH2A isoform b and VLGR1b form homomers or heteromers mediated by direct interaction of their long ectodomains (13-15). In VLGR1b, CalX-β repeats which are frequently present in the ectodomain were suggested as protein binding domains (15). Such dimerizations may be facilitated through an intracellular tether by parallel binding of their cytoplasmic PBM sites to the PDZ domains 1 and 2 of whirlin. Homo- or heteromers may bridge the extracellular cleft between the adjacent membranes according to mechanisms known from cell-cell adhesion molecules e.g. conventional cadherins in cell-cell attachments (35). The absence of fibers in homozygous Vlgr1/del7TM mice further indicates that USH2A isoform b homomers are not sufficient for

formation and maintenance of these fibers. Nevertheless, recent retinal analyses of USH2A knock-out mice demonstrated the essential impact of USH2A isoform b for the maintenance of photoreceptor cell survival (33).

Cell-cell adhesion complexes including membrane-spanning structures supported by cytoplasmic scaffolds often define specialized regions of the plasma membrane. Such organizations are well known from the plasma membrane specializations of the active zone in presynaptic boutons of axons (36) or the division in the apical and baso-lateral membrane of epithelial cells. Present analyses revealed a periciliary USH protein network situated at adjacent membranes of the inner segment collar and the connecting cilium of mouse photoreceptor cells. So far, little was known about the periciliary structural membrane specialization in the apical inner segment of mammalian photoreceptor cells. In a study, parallel to the present, on USH2A knock out mice (33), it has been suggested that the membrane domain of the apical inner segment collar corresponds to the periciliary ridge complex, previously described by Papermaster and co-workers in amphibian photoreceptor cells (26-28). However, experimental data supporting this hypothesis were nonexistent until now. Here, we provide for the first time molecular and ultrastructural evidence indicating the homology between both structures in mammalian and amphibian photoreceptor cells. We demonstrated the localization of the molecular components of the periciliary USH protein network in the connecting cilium and apical inner segment collar in mouse photoreceptor cells and in the periciliary ridge complex of *Xenopus* photoreceptor cells. The USH proteins SANS, whirlin, USH2A isoform b and VLGR1b are localized in the ridges of the periciliary complex and in the connecting cilium of *Xenopus* photoreceptor cells. As in the mouse, extracellular fibrous links project from the tip of each ridge to the membrane of the connecting cilium. These are most probably also composed of the long ectodomains of the transmembrane proteins USH2A isoform b and VLGR1b. As we discussed for mouse photoreceptor cells above, the latter transmembrane proteins may be anchored with their cytodomains via the scaffold proteins whirlin and SANS in the cytoplasm of the two adjacent cellular compartments in *Xenopus* photoreceptor cells. The congruence in the cellular topology and the molecular composition of these membrane associated periciliary protein complexes strongly supports structural and functional homology in mammalian and *Xenopus* photoreceptor cells.

What is the function of these periciliary complexes in vertebrate photoreceptor cells? In amphibian photoreceptor cells, the membrane subdomains in the grooves of the periciliary ridge complex are thought to constitute docking sites for inner segment transport vesicles

which contain cargo molecules for the outer segment (27,28,37). Independent immunoelectron microscopy analyses revealed association of opsin-laden transport vesicles with the grooves but not with the ridges (26,27,37-39). These vesicles originate from the trans-Golgi network of the cell (4,40). After Golgi budding, cargo vesicles are subsequently transported along microtubules by cytoplasmic dynein to the apical inner segment (2) (Fig. 9B, C). At the apical inner segment membrane the transport carriers are supposed to dock and fuse with designated plasma membrane domains (4,28,41). In amphibian photoreceptor cells, designated membrane domains are present in the grooves of the periciliary ridge complex (28) (supplemental material Fig. 3). In mammalian photoreceptors, the membrane domains of the apical inner segment collar localized alongside the connecting cilium correspond to these membrane micro domains (33). In both cases, the USH protein network may structurally support the specialized membrane micro domains by bridging adjacent membranes and anchoring the transmembrane proteins in the cytoplasm of both the inner segment and the connecting cilium.

However, this does not exclude participation of the periciliary protein network in vesicle targeting and guiding as well as in the adjustment of vesicle docking and fusion to designated membrane areas. In particular, the association of SANS with microtubules may affiliate the microtubule routes for the vesicular transport with predefined target membranes in the apical inner segment collar. Indeed previously obtained data indicate that microtubules project into the collar-like extension of the inner segment apex and that cargo vesicles are present at the target membrane (2) (B.Reidel, T.Goldmann, A.Gießl, and U.Wolfrum, submitted). Since tethering and fusion of rhodopsin transport carriers is thought to be regulated by phosphatidylinositol-4,5-bisphosphate, moesin, actin, and rac1 acting in concert with rab8 (42), future efforts are necessary to provide more insights into molecular links between the structural support function of the USH protein network and transport processes.

In addition, our present data indicate the localization of a USH protein network in the ciliary apparatus of mouse and amphibian photoreceptor cells. In the photoreceptor connecting cilium, SANS may anchor the membrane associated USH protein network, composed of SANS, whirlin, USH2A isoform b and VLGR1b to the ciliary microtubule doublets. A solid SANS association with the ciliary cytoskeleton of photoreceptor cells was recently confirmed by the recovery of SANS in the detergent insoluble cytoskeleton fraction of enriched photoreceptor cilia (29). Furthermore, the USH1B protein myosin VIIa is capable of direct binding to all proteins of the present network (12,16).

The molecular motor myosin VIIa can have a dual function in the connecting cilium: After the fusion of membranous vesicles with the apical surface of the inner segment discussed above, the membrane incorporated cargo translocates in the ciliary membrane to the outer segment. We previously indicated that myosin VIIa mediates the transport of membrane cargo along actin filaments in the membrane of photoreceptor cilia (3). The direct binding of myosin VIIa to the proteins of the ciliary USH protein network may connect this transport system through SANS to the prominent microtubule cytoskeleton of the cilium (29). Furthermore, the regulation of myosin VIIa mediated molecular trafficking by the interaction with SANS was previously suggested for the delivery of proteins to stereovilli in inner ear hair cells (12).

However, myosin VIIa and the transmembrane protein vezatin, identified as one of the first interaction partners of myosin VIIA, are present in the connecting cilium (43) (Wolfrum unpublished data) and directly interact with the cytoplasmic domains of transmembrane proteins USH2A isoform b and VLGR1b (16). Thus, it has to be considered that the motor protein myosin VIIa could actively support the protein network at the ciliary membrane by force generation at the cytoplasmic domains of the transmembrane proteins (43).

In conclusion, our data show that an USH protein network is localized at the interface of the inner segment and the light sensitive outer segment of rod and cone vertebrate photoreceptor cells. The cooperation of the network members may contribute to the regulation of cargo transfer from inner segment transport carriers to the ciliary transport system. Dysfunction or absence of any of the proteins in the ciliary-periciliary USH protein network may lead to the disruption of the entire network function and may cause degeneration of the neuronal retina, the clinical retinal symptom characteristic for USH patients.

Material and Methods

Yeast two-hybrid-assays. The GAL4-based yeast two-hybrid system (HybriZAP, Stratagene, La Jolla, USA) was used to identify the interactions between SANS, whirlin and putative interactors as previously described (44). The DNA binding domain (pBD) fused to either the SAMPBM domain of SANS, or PDZ 1 and 2 or PDZ 3 of whirlin respectively, was used as a bait on a bovine oligo-dT primed retinal cDNA library. The yeast strain *PJ69-4A* was used as a host, which carried the *HIS3* (histidine), *ADE2* (adenine), *MEL1* (α-galactosidase) and *LacZ* (β-galactosidase) reporter genes. Interactions were analyzed by assessment of reporter gene activation, using growth on selective media (*HIS3* and *ADE2* reporter genes), X-α-gal

colorimetric plate assays (*MEL1* reporter gene) and X-β-gal colorimetric filter lift assays (*LacZ* reporter gene). To map the interacting domains of SANS and whirlin, constructs fused to the DNA activation domain (pAD) and pBD were co-transformed in *PJ694α*. If yeast clones grew on selection plates and were stained in the α- and β-galactosidase activity assays, an interaction between a protein pair was indicated.

GST pull-down assays. Constructs encoding human whirlin domains were cloned in the pDEST15 vector (Gateway cloning system, Invitrogen, Karlsruhe, Germany). GST-fusion proteins were produced by transforming BL21-DE3 cells with pDEST15-whirlin PDZ 1 (aminoacids (aa) 45-141), PDZ 2 (aa 187-268), PDZ 1+2 (aa 45-268) and PDZ 3 (aa 469-814). Cells were induced at 30°C with 0.5 mM IPTG overnight and subsequently lysed with STE buffer (1% Sarkosyl, 1% Triton-X-100, 5 mM 1,4-dithiothreitol (DTT)) supplemented with complete protease inhibitor cocktail (Roche Diagnostics, Mannheim, Germany). Lysates were incubated with glutathione-Sepharose 4B beads (Amersham Biosciences, Freiburg, Germany). The GST-fusion proteins bound to the beads were washed with lysis buffer and TBSTD (TBS with 1% Triton-X-100 and 2 mM DTT). The amount of bound GST-fusion protein was verified on a NUPAGE Novex 4-12% Bis-Tris SDS-PAGE gel and stained with SimplyBlue SafeStain (Invitrogen). FLAG-tagged human SANS full length (aa 1-461) and FLAG-tagged SANS SAMΔPBM (aa 385-455) were produced by transfection of COS-1 cells with the appropriate vectors, using Effectene as a transfection reagent (QIAGEN, Hilden, Germany) according to the manufacturer's instruction. 24 hours after transfection cells were washed with phosphate-buffered saline (PBS) and subsequently lysed on ice in lysis buffer (50 mM Tris-HCL pH 7.5, 150 mM NaCl, 0.5% Triton-X-100). The cell supernatant was incubated overnight at 4°C with equal amounts of beads pre-incubated either with GST or with GST-fusion proteins. Beads were washed and precipitated protein complexes were eluted with SDS sample buffer and subjected to SDS-PAGE and Western blot analysis.

Animals and tissue preparation. All experiments conformed to the statement by the Association for Research in Vision and Ophthalmology (ARVO) regarding the care and use of animals in research. Mature C57BL/6J and Vlgr1/del7TM mice, previously described by McMillan and White (2004), and adult *Xenopus laevis* were maintained on a 12-hour light–dark cycle, with food and water *ad libitum*. After sacrifice of the animals by sodium pentobarbital overdoses (mice) or chloroform (*Xenopus*) and decapitation, subsequently entire

eyeballs were dissected or retinas were removed through a slit in the cornea prior to further analyses.

Fluorescence microscopical analysis of cotransfected COS-1 cells. Full length whirlin was cloned in pDEST 733 resulting in an N-terminal fused mRFP and full length SANS was cloned in pDEST 501 resulting in an N-terminal fused eCFP-protein. Both constructs were transfected individually or in combination by using Effectene transfection reagent (QIAGEN) according to the manufacturer´s instructions. After 24 hours cells were washed in PBS and fixed with 3.7% paraformaldehyde, mounted with vectashield containing DAPI (Vector Laboratories Inc., Peterborough, UK) and analyzed by epifluorescence microscopy.

Coimmunoprecipitation. Retina lysate was prepared in HNTG buffer (20 mM Hepes, 150 mM NaCl, 0.1% Triton-X-100, 6 mM EDTA, 10% glycerol, pH 7.4). 35 µl AG-Beads (PIERCE, Rockford, USA) were washed with HNTG buffer and displaced with 5 µl anti-whirlin antibodies per reaction. As a negative control beads were incubated without antibodies. All mixtures were incubated at 4°C for 4-5 h. To remove unbound antibodies beads were washed several times with HNTG buffer. Afterwards retina extracts were applied to the beads in equal amounts and incubated at 4°C overnight. Beads were washed and precipitated protein complexes were eluted with SDS sample buffer and subjected to SDS-PAGE and Western blot analysis.

Western blot analyses. For Western blot analyses, the appropriate tissues were homogenized in buffer containing a protease inhibitor cocktail (Roche Diagnostics). Samples were prepared in either RIPA buffer (50 mM Tris-HCl, 150 mM NaCl, 0.1% SDS, 2 mM EDTA, 1% NP-40, 0.5% sodium-deoxycholate, 1 mM sodium-vanadate, 30 mM sodium-pyrophosphate, pH 7.4) or HNTG buffer (20 mM Hepes, 150 mM NaCl, 0.1% Triton-X-100, 6 mM EDTA, 10% glycerol, pH 7.4). For denaturing gel electrophoresis, samples were mixed with SDS-PAGE sample buffer (62.5 mM Tris-HCl pH 6.8, 10% glycerol, 2% SDS, 5% mercaptoethanol, 1 mM EDTA and 0.025 mM bromphenol blue). 25 µg protein extract per lane was separated on a 12% polyacrylamide gel and transferred onto polyvinylidene difluoride (PVDF) membranes (Millipore, Schwalbach, Germany). After blocking the membrane with Applichem blocking reagent (Applichem, Darmstadt, Germany) for 2 h at room temperature, immunoreactivities were detected by applying primary and appropriate secondary antibodies (IRDye 680 or 800, Rockland, Gilbertsville, USA) employing the Odyssey infra red imaging system (LI-COR

Biosciences, Lincoln, USA). As a molecular marker a prestained ladder (Sigma-Aldrich, Deisenhofen, Germany) was used, ranging from 11-170 kDa.

Constructs for expression of cDNA. cDNAs for expression of proteins were obtained by RT-PCR or from EST-clones and subcloned into the appropriate expression vectors as previously described (14,23). The numbers of the given amino acids are according to the following Genbank entries. SANS (murine) AF_176847, SANS (human) AF_775748, USH2A isoform b (human), NP_99681; VLGR1b (human), NP_115495.

Antibodies and fluorescent dyes. Polyclonal antibodies against SANS generated against a murine fragment (aa 1-46) and raised in rabbit was previously characterized (29). The anti-whirlin antibodies were raised in guinea pig against a GST-fusion protein encoding the human amino acid region 701-765 of the long isoform of whirlin (14). The antibodies against VLGR1b were either generated against the cytoplasmic tail (aa 6198-6307) (24) or against a GST-fusion protein of the extracellular region (aa 3249-3425) (kindly provided by Dr. Dominic Cosgrove (Omaha, USA)) both of murine origin and raised in rabbit. Anti-USH2A antibodies were generated against FN (fibronectin) type III domains of mouse USH2A (aa 1359-1443) raised in guinea pig and against a 139 aa fragment encoding the cytoplasmic tail of human USH2A, raised in rabbit (24). Monoclonal antibodies against centrins (clone 20H5, detecting all four centrin isoforms) have previously been characterized (45). Specific antibodies against harmonin (aa 1-89) raised in rabbit were characterized before (23). Expression of the fusion proteins and purification of the antibodies were performed as previously described (23). The anti-α-tubulin and anti-FLAG-tag antibodies were acquired from Sigma-Aldrich. The secondary antibodies were purchased from Invitrogen or Rockland.

Immunofluorescence microscopy. Eyes of adult wild type mice were cryofixed in melting isopentane and cryosectioned as described elsewhere (46). Cryosections were placed on poly-L-lysine-precoated coverslips and incubated subsequently with 0.01% Tween 20 in PBS for 20 min. After several PBS washing steps sections were covered with blocking solution (0.5% cold-water fish gelatin plus 0.1% ovalbumin in PBS) and incubated for a minimum of 30 min followed by an overnight incubation with primary antibodies, diluted in blocking solution at 4°C. Washed cryosections were incubated with secondary antibodies conjugated to Alexa 488 or Alexa 568 (Invitrogen, Germany) in PBS with DAPI (4',6-Diamidin-2'-phenylindoldihydrochlorid) (Sigma-Aldrich) to stain the DNA of the cell nuclei, for a

minimum of 1.5 hours at room temperature in the dark. After repeated washing with PBS sections were mounted in Mowiol 4.88 (Hoechst, Frankfurt, Germany). Mounted retina cryosections were analyzed by microscopy (DMRB; Leica microsystems, Bensheim, Germany). Images were obtained with a charge-coupled device camera (ORCA ER; Hamamatsu, Herrsching, Germany) and processed with Adobe Photoshop CS (Adobe Systems, San Jose, USA).

Immunoelectron microscopy. Isolated mouse and *Xenopus* eye balls were placed in 4% paraformaldehyde (PFA) in Soerensen buffer (0.1 M disodiumhydrogenphophate, 0.1 M potassiumdihydrogenphosphate, pH 7.3), perforated with an injection needle and the lens was removed. Then the eye-cups were prefixed in 4% in 0.1 M Soerensen buffer (pH 7.3) for 50 min. After washing in Soerensen buffer retinas were dissected from the eye-cups in 10% sucrose in Soerensen buffer from the eye-cups and incubated in 10% and 20% sucrose in Soerensen buffer for 2 h in each case and in 30% sucrose in Soerensen buffer overnight. In one experiment we dissected the retina in PBS and treated it with 0.5% Triton in PBS for 3 min. After that the retina was fixed for 50 min in 4% PFA and further treated as above. After four cycles of freezing (-196°C) and thawing (37°C) the retinas were washed in PBS and embedded in buffered 2% Agar (Sigma-Aldrich). Agar blocks were sectioned by a vibratome (Leica, Wetzlar, Germany) in 50 µm slices. Vibratome sections were blocked for 2 h in 10% NGS (normal goat serum), 1% BSA (bovine serum albumin) in PBS and subsequently incubated with primary antibodies against SANS, whirlin, USH2A isoform b, VLGR1b or harmonin in 3% NGS, 1% BSA in PBS for 4 days at 4°C. After washing with PBS the appropriate biotinylated secondary antibodies (Vector Laboratories) were applied to the sections for 2 h at room temperature. Following several washing steps with PBS a complex consisting of avidin and biotinylated horseradish peroxidase (Vectastain ABC-Kit, Vector Laboratories) was added to the sections and incubated for 1.5 h in the dark. After incubation with DAB (diaminobenzidine) the precipitate was fixed in 2.5% glutaraldehyde in 0.1 M Cacodylate buffer (pH 7.3) for 1 h. After silverenhancement sections were fixed in 0.5% OsO_4 in 0.1 M Cacodylate buffer (pH 7.3) on ice, dehydrated and embedded in araldite. Ultrathin sections were cut and microscopical analysis was performed using a Tecnai 12 BioTwin transmission electron microscope (FEI, Eindhoven, NL).

BAPTA treatment. To examine the effects of the calcium chelator BAPTA (1,2-bis(o-aminophenoxy)ethane-N,N,N',N'-tetraacetic acid) (Sigma-Aldrich) mouse retina cryosections

were incubated with Ca^{2+}-free PBS containing 5 mM BAPTA for 30 min at room temperature. After BAPTA incubation of cryosections were washed several times with PBS and processed for immunofluorescence microscopy as described above.

Organotypic retina culture. The elaboration of the retina culture system was previously described (30). Intact eyes removed from sacrificed C57BL/6J mice on postnatal day 16-19 were incubated in 1.2 mg/ml proteinase K (Sigma-Aldrich) for 15 min at 37°C. Proteinase K activity was stopped by application of Dulbecco's Modified Eagle's Medium with F12 supplement (DMEM–F12) with 10% fetal calf serum for 5 min. After rinsing the eyes in serum-free medium retinas were dissected following removal of the sclera, the ocular tissue and the hyaloid vessel. Specimens were cultured with the retinal pigmented epithelial cells facing down on ME 25/31 culture membranes (Whatman, Dassel, Germany) in DMEM–F12 and 10% fetal calf serum, L-glutamine, penicillin and streptomycin (Sigma-Aldrich) at 37°C in a 5% CO_2 atmosphere. Retinas were mounted and frozen as previously described (30) and processed for immunofluorescence microscopy as described above.

Application of cytoskeletal drugs. Thiabendazole (Fluka, Seelze, Germany) and colchicine (Sigma-Aldrich) were diluted in 1% dimethyl sulfoxide (DMSO). The applied end concentration of thiabendazole was 1.5 mM to organotypic retina culture medium and 0.5 mM to NIH3T3 cell culture medium; colchicine was applied in an end concentration of 125 nM to NIH3T3 cell culture medium for 2 h at 37°C and 5% CO_2. Controls were incubated with 1% DMSO under the same conditions and processed as described for organotypic retina culture.

Acknowledgements

This work was supported by the DFG (to U.W.), Forschung contra Blindheit - Initative Usher Syndrom (to H.K., T.M., U.W.), ProRetina Deutschland (to U.W.), the FAUN-Stiftung, Nürnberg (U.W.), the Nijmegen ORL Research Fund (to H.K.), the Heinsius Houbolt Foundation (to H.K.) the BRPS (to H.K. and R.R), and the NIH EY016247 (to Perrin White, E.J.W. and J.M.). Authors thank Gabi Stern-Schneider and Ulrike Maas for technical assistance, Dr. Dominic Cosgrove (Boys Town National Research Hospital, Omaha, NE) for providing us with anti-VLGR1b antibodies and Drs. Kerstin Nagel-Wolfrum and Martin Latz for critical reading of the manuscript.

Conflicts of Interest

No conflict of interest

References

1. Young, R.W. (1976) Visual cells and the concept of renewal. *Invest. Ophthalmol. Vis. Sci.*, **15**, 700-725.

2. Tai, A.W., Chuang, J.Z., Bode, C., Wolfrum, U., Sung, C.H. (1999) Rhodopsin´s carboxy-terminal cytoplasmic tail acts as a membrane receptor for cytoplasmic dynein by binding to the dynein light chain Tctex-1. *Cell*, **97**, 877-887.

3. Wolfrum, U., Schmitt, A. (2000) Rhodopsin transport in the membrane of the connecting cilium of mammalian photoreceptor cells. *Cell Motil. Cytoskeleton*, **46**, 95-107.

4. Deretic, D. (2006) A role for rhodopsin in a signal transduction cascade that regulates membrane trafficking and photoreceptor polarity. *Vision Res.*, **46**, 4427-4433.

5. Roepman, R., Wolfrum, U. (2007) Protein networks and complexes in photoreceptor cilia. In Faupel, M., Bertrand, E. (eds.), *Subcellular Fractionation and Proteomics*. Springer, NY

6. Petit, C. (2001) Usher syndrome: from genetics to pathogenesis. *Annu. Rev. Genomics Hum. Genet.*, **2**, 271-297.

7. Ahmed, Z.M., Riazuddin, S., Riazuddin, S., Wilcox, E.R. (2003) The molecular genetics of Usher syndrome. *Clin. Genet.*, **63**, 431-444.

8. Davenport, S.L.H., Omenn, G.S. (1977) The heterogeneity of Usher syndrome. *Vth Int. Conf. Birth Defects, Montreal*.

9. Ebermann, I., Scholl, H.P., Charbel, I.P., Becirovic, E., Lamprecht, J., Jurklies, B., Millan, J.M., Aller, E., Mitter, D., Bolz, H. (2007) A novel gene for Usher syndrome type 2: mutations in the long isoform of whirlin are associated with retinitis pigmentosa and sensorineural hearing loss. *Hum. Genet.*, **121**, 203-211.

10. Reiners, J., Nagel-Wolfrum, K., Jurgens, K., Märker, T., Wolfrum, U. (2006) Molecular basis of human Usher syndrome: deciphering the meshes of the Usher protein network provides insights into the pathomechanisms of the Usher disease. *Exp. Eye Res.*, **83**, 97-119.

11. Kremer, H., van Wijk, E., Märker, T., Wolfrum, U., Roepman, R. (2006) Usher syndrome: molecular links of pathogenesis, proteins and pathways. *Hum. Mol. Genet.,* **15**, 262-270.

12. Adato, A., Michel, V., Kikkawa, Y., Reiners, J., Alagramam, K.N., Weil, D., Yonekawa, H., Wolfrum, U., El Amraoui, A., Petit, C. (2005) Interactions in the network of Usher syndrome type 1 proteins. *Hum. Mol. Genet.*, **14**, 347-356.

13. Adato, A., Lefevre, G., Delprat, B., Michel, V., Michalski, N., Chardenoux, S., Weil, D., El Amraoui, A., Petit, C. (2005) Usherin, the defective protein in Usher syndrome type IIA, is likely to be a component of interstereocilia ankle links in the inner ear sensory cells. *Hum. Mol. Genet.*, **14**, 3921-3932.

14. van Wijk, E., van der Zwaag, B., Peters, T., Zimmermann, U., te Brinke, H., Kersten, F.F., Märker, T., Aller, E., Hoefsloot, L.H., Cremers, C.W., et al. (2006) The DFNB31 gene product whirlin connects to the Usher protein network in the cochlea and retina by direct association with USH2A and VLGR1. *Hum. Mol. Genet.*, **15**, 751-765.

15. McGee, J., Goodyear, R.J., McMillan, D.R., Stauffer, E.A., Holt, J.R., Locke, K.G., Birch, D.G., Legan, P.K., White, P.C., Walsh, E.J., et al. (2006) The very large G-protein-coupled receptor VLGR1: a component of the ankle link complex required for the normal development of auditory hair bundles. *J. Neurosci.*, **26**, 6543-6553.

16. Michalski, N., Michel, V., Bahloul, A., Lefevre, G., Barral, J., Yagi, H., Chardenoux, S., Weil, D., Martin, P., Hardelin, J.P., et al. (2007) Molecular characterization of the ankle-link complex in cochlear hair cells and its role in the hair bundle functioning. *J. Neurosci.*, **27**, 6478-6488.

17. Goodyear, R., Richardson, G. (1999) The ankle-link antigen: an epitope sensitive to calcium chelation associated with the hair-cell surface and the calycal processes of photoreceptors. *J. Neurosci.*, **19**, 3761-3772.

18. Goodyear, R.J., Richardson, G.P. (2003) A novel antigen sensitive to calcium chelation that is associated with the tip links and kinocilial links of sensory hair bundles. *J. Neurosci.*, **23**, 4878-4887

19. Wolfrum, U. (1995) Centrin in the photoreceptor cells of mammalian retinae. *Cell Motil. Cytoskeleton*, **32**, 55-64.

20. Gießl, A., Pulvermüller, A., Trojan, P., Park, J.H., Choe, H.W., Ernst, O.P., Hofmann, K.P., Wolfrum, U. (2004) Differential expression and interaction with the visual G-protein transducin of centrin isoforms in mammalian photoreceptor cells. *J. Biol. Chem.*, **279**, 51472-51481.

21. Besharse, J.C., Horst, C.J. (1990) The photoreceptor connecting cilium - a model for the transition zone. In Bloodgood, R.A. (ed.), *Ciliary and Flagellar Membranes*. Plenum, New York, pp. 389-417.

22. Pagh-Roehl, K., Wang, E., Burnside, B. (1992) Shortening of the calycal process actin cytoskeleton is correlated with myoid elongation in teleost rods. *Exp. Eye Res.*, **55**, 735-746.

23. Reiners, J., Reidel, B., El Amraoui, A., Boeda, B., Huber, I., Petit, C., Wolfrum, U. (2003) Differential distribution of harmonin isoforms and their possible role in Usher-1 protein complexes in mammalian photoreceptor cells. *Invest. Ophthalmol. Vis. Sci.*, **44**, 5006-5015.

24. Reiners, J., van Wijk, E., Märker, T., Zimmermann, U., Jurgens, K., te Brinke, H., Overlack, N., Roepman, R., Knipper, M., Kremer, H., et al. (2005) Scaffold protein harmonin (USH1C) provides molecular links between Usher syndrome type 1 and type 2. *Hum. Mol. Genet.*, **14**, 3933-3943.

25. McMillan, D.R., White, P.C. (2004) Loss of the transmembrane and cytoplasmic domains of the very large G-protein-coupled receptor-1 (VLGR1 or Mass1) causes audiogenic seizures in mice. *Mol. Cell Neurosci.*, **26**, 322-329.

26. Peters, K.R., Palade, G.E., Schneider, B.G., Papermaster, D.S. (1983) Fine structure of a periciliary ridge complex of frog retinal rod cells revealed by ultrahigh resolution scanning electron microscopy. *J. Cell Biol.*, **96**, 265-276.

27. Papermaster, D.S., Schneider, B.G., DeFoe, D., Besharse, J.C. (1986) Biosynthesis and vectorial transport of opsin on vesicles in retinal rod photorecptors. *J. Histochem. Cytochem.*, **34**, 5-16.

28. Papermaster, D.S. (2002) The birth and death of photoreceptors: the Friedenwald Lecture. *Invest. Ophthalmol. Vis. Sci.*, **43**, 1300-1309.

29. Overlack, N., Märker, T., Latz, M., Nagel-Wolfrum, K., Wolfrum, U. (2007) SANS (USH1G) expression in developing and mature mammalian retina. *Vision Res.,* in press.

30. Reidel, B., Orisme, W., Goldmann, T., Smith, C.W., Wolfrum, U. (2006) Photoreceptor vitality in organotypic cultures of mature vertebrate retinas validated by light-dependent molecular movements. *Vision Res.*, **46**, 4464-4471.

31. Delprat, B., Michel, V., Goodyear, R., Yamasaki, Y., Michalski, N., El Amraoui, A., Perfettini, I., Legrain, P., Richardson, G., Hardelin, J.P., et al. (2005) Myosin XVa and whirlin, two deafness gene products required for hair bundle growth, are located at the stereocilia tips and interact directly. *Hum. Mol. Genet.*, **14**, 401-410.

32. Udovichenko, I.P., Gibbs, D., Williams, D.S. (2002) Actin-based motor properties of native myosin VIIa. *J. Cell Sci.*, **115**, 445-450.

33. Liu, X., Bulgakov, O.V., Darrow, K.N., Pawlyk, B., Adamian, M., Liberman, M.C., Li, T. (2007) Usherin is required for maintenance of retinal photoreceptors and normal development of cochlear hair cells. *Proc. Natl. Acad. Sci. USA*, **104**, 4413-4418.

34. McMillan, D.R., Kayes-Wandover, K.M., Richardson, J.A., White, P.C. (2002) Very large G protein-coupled receptor-1, the largest known cell surface protein, is highly expressed in the developing central nervous system. *J. Biol. Chem.*, **277**, 785-792.

35. Bolz, H., Reiners, J., Wolfrum, U., Gal, A. (2002) The role of cadherins in Ca^{2+}-mediated cell adhesion and inherited photoreceptor degeneration. *Adv. Exp. Med. Biol.*, **514**, 399-410.

36. Zhen, M., Jin, Y. (2004) Presynaptic terminal differentiation: transport and assembly. *Curr. Opin. Neurobiol.*, **14**, 280-287.

37. Papermaster, D.S., Schneider, B.G., Besharse, J.C. (1985) Vesicular transport of newly synthesized opsin from the Golgi apparatus toward the rod outer segment. *Invest. Ophthalmol. Visual Sci.*, **26**, 1386-1404.

38. Besharse, J.C., Pfenninger, K.H. (1980) Membrane assembly in retinal photoreceptors. I. Freeze-fracture analysis of cytoplasmic vesicles in relationship to disc assembly. *Cell Biol.*, **87**, 451-463.

39. Schneider, B.G., Papermaster, D.S. (1983) Immunocytochemistry of retinal membrane protein biosynthesis at the electron microscopic level by the albumin embedding technique. *Methods Enzymol.*, **96**, 485-495.

40. Deretic, D., Williams, A.H., Ransom, N., Morel, V., Hargrave, P.A., Arendt, A. (2005) Rhodopsin C terminus, the site of mutations causing retinal disease, regulates trafficking by binding to ADP-ribosylation factor 4 (ARF4). *Proc. Natl. Acad. Sci. USA*, **102**, 3301-3306.

41. Sung, C.H., Tai, A.W. (2000) Rhodopsin trafficking and its role in retinal dystrophies. *Int. Rev. Cytol.*, **195**, 215-267.

42. Deretic, D., Traverso, V., Parkins, N., Jackson, F., Rodriguez de Turco, E.B., Ransom, N. (2004) Phosphoinositides, ezrin/moesin, and rac1 regulate fusion of rhodopsin transport carriers in retinal photoreceptors. *Mol. Biol. Cell*, **15**, 359-370.

43. Küssel-Andermann, P., El-Amraoui, A., Safieddine, S., Nouaille, S., Perfettini, I., Lecuit, M., Cossart, P., Wolfrum, U., Petit, C. (2000) Vezatin, a novel transmembrane protein, bridges myosin VIIA to the cadherin-catenins complex. *EMBO J.*, **19**, 6020-6029.

44. Roepman, R., Schick, D., Ferreira, P.A. (2000) Isolation of retinal proteins that interact with retinitis pigmentosa GTPase regulator by interaction trap screen in yeast. *Methods Enzymol.*, **316**, 688-704.

45. Wolfrum, U., Salisbury, J.L. (1998) Expression of centrin isoforms in the mammalian retina. *Exp. Cell Res.*, **242**, 10-17.

46. Wolfrum, U. (1991) Tropomyosin is co-localized with the actin filaments of the scolopale in insect sensilla. *Cell Tissue Res.*, **265**, 11-17.

Figure Legends

Figure 1. Validation of the SANS - whirlin interaction.

(**A**) Schematic representation of SANS, whirlin, USH2A isoform b and VLGR1b. SANS is composed of 3 ankyrin repeats (ANK) at the N-terminus, a central domain (CEN) followed by a sterile alpha motif (SAM) and a PDZ binding motif (PBM) at the C-terminus indicated by an *asterisk*. Whirlin contains three PDZ domains and a proline-rich region (PR). The extracellular domain of the USH2A isoform b (USH2A) contains a laminin G-like domain (LamGL), an N-terminal laminin domain (LamNT), 10 laminin-type EGF-like modules (EGF-Lam), 32 fibronectin type III (FN3) repeats (4 + 28) spaced by two laminin G domains (LamG) followed by a transmembrane region (TM) and the intracellular C-terminal domain containing a PBM. VLGR1b (very large G-protein coupled receptor 1b, USH2C) consists of extracellular N-terminal extensions with a LamG/TspN/PTX-homologous domain, seven EAR/EPTP repeats, 35 Ca^{2+}-binding calcium exchanger β (CalX-β) modules, one 7-transmembrane domain (TM) as well as a short intracellular domain containing a PBM.

(**B**) Reciprocal yeast two-hybrid interaction assays were performed with the SANS C-terminus containing the SAM and PBM domains and whirlin´s PDZ1+2 or PDZ3 fused to the activation domain (AD) or the DNA-binding domain (BD) of the GAL4 reporter gene, respectively. SANS interacts with whirlin´s PDZ1+2, but not with the PDZ3 domain.

(**C**) GST pull-down assays were performed: ***upper panel***, FLAG-tagged SANS is incubated with immobilized GST-whirlin PDZ domains, or GST alone. Anti-FLAG Western blot reveals recovery of SANS with whirlin PDZ1, PDZ2 and PDZ1+2, but not with whirlin PDZ3 or GST alone. ***Lower panel***, FLAG-tagged SANS C-terminus lacking the PBM (SAMΔPBM) is assayed with each of the immobilized GST-tagged PDZ-domains of whirlin or GST protein alone and analyzed by anti-FLAG Western blot analysis. Binding of SANS to whirlin is abolished.

(**D**) Colocalization of recombinant mRFP-whirlin and eCFP-SANS in COS-1 cells. (***upper panel***) overexpressed mRFP-whirlin (red) is localized to the cytoplasm but not to the DAPI stained nucleus in single transfected cells. (***middle panel***) overexpressed eCFP-SANS (green) is localized to punctuated structures in the periphery of the nucleus. (***lower panel***) In mRFP-whirlin and eCFP-SANS double transfected COS-1 cells, overexpressed eCFP-SANS (green) recruits mRFP-whirlin (red) to the perinuclear punctuated structures. Scale bar: 10 μm.

(**E**) Immunoprecipitation (IP) with anti-whirlin antibodies of protein extract of mouse retinas. Anti-SANS Western blot analysis (WB) demonstrates that SANS is coimmunoprecipitated with whirlin. In protein AG-Beads (Beads) incubated retinal extracts SANS is not recovered.

Figure 2. SANS and whirlin colocalize in mouse photoreceptor cells.

(**A**) Schematic representation of a rod photoreceptor cell. Vertebrate photoreceptors are composed of a light-sensitive outer segment (OS) linked via a connecting cilium (CC) to an inner segment (IS), containing all organelles for biosynthesis. N = nucleus localized in the outer nuclear layer (ONL); S = synaptic terminal located in the outer plexiform layer (OPL) of the retina. *Arrowhead* points to outer limiting membrane (OLM). 2^{nd} = second order neurons, bipolar or horizontal cells, respectively. RPE = retinal pigment cells.

(B–E) Indirect immunofluorescence double labeling of SANS and whirlin counterstained with DAPI in a longitudinal cryosection through a mouse retina. (**B**) Differential interference contrast (DIC) image of C – E. (**C, D**) Indirect immunofluorescence of SANS (green) (**C**) and whirlin (red) (**D**). (**E**) Merge image of SANS and whirlin labeling superposed with the nuclear DNA staining by DAPI. The yellow color indicates SANS and whirlin colocalization in the CC, the IS, the OLM and the OPL in photoreceptor cells. (**F**) Schematic representation of the ciliary apparatus composed of the connecting cilium (CC) and the basal body complex (BB) in a rod photoreceptor cell. CP, calycal processes. (**G, H**) High magnification fluorescence microscopy analyses of double immunofluorescence with anti-SANS or anti-whirlin, respectively, and anti-pan-centrin antibodies (marker for the ciliary apparatus: CC and BB) in longitudinal cryosections through the ciliary part of mouse photoreceptor cells. (**G**) Double labeling of SANS (green) and centrins (red). (**H**) Double labeling of whirlin (green) and centrins (red). Merged images indicate partial colocalization of SANS and whirlin with centrins in the CC and the BB. The periciliary collar-like inner segment (IS) extension is indicated by an *asterisk*. Scale bars: E: 20 μm, G, H: 0.2 μm.

Figure 3. Immunoelectron microscopic localization of SANS and whirlin in mouse photoreceptor cells.

(**A-C**) Electron micrographs of anti-SANS labeling in longitudinal (**A**, **C**) and cross-sections (**B**) through parts of mouse photoreceptor cells. SANS localization is found in the apical inner segment (IS) in the periciliary collar-like extension (*asterisk*) and at the basal body complex (*arrow heads*). In some longitudinal sections (**C**) and in cross-sections (**B**), SANS is also detected in the connecting cilium (CC). (**D-F**) Electron micrographs of anti-whirlin labeling in

longitudinal (**D**, **E**) and cross-sections (**F**) through parts of mouse photoreceptor cells. Whirlin is localized in the apical IS in the periciliary collar-like IS extension (*asterisk*) and at the basal body complex (*arrow heads*). In some longitudinal sections (**E**) and in cross-sections (**F**), whirlin is also detected in the CC. Scale bars: A: 0.25 µm, B: 0.1 µm, C: 0.25 µm, D: 0.5 µm E: 0.25 µm, F: 0.2 µm.

Figure 4. Immunoelectron microscopic localization of USH2A isoform b and VLGR1b in mouse photoreceptor cells.

(**A-D**) Electron micrographs of anti-USH2A isoform b immunolabeling in longitudinal (**A-C**) and cross-sections (**D**) through parts of mouse photoreceptor cells. (**A-D**) USH2A isoform b localization is found in the apical inner segment (IS) in the periciliary collar-like extension (*asterisk*) and at the basal body complex (*arrow heads* in **C**). In some longitudinal sections (**A**) and in cross-sections (**D**) USH2A isoform b is also detected in the connecting cilium (CC).

(**E-G**) Electron micrographs of anti-VLGR1b labeling in longitudinal (**E, G**) and cross-sections (**F**) through parts of mouse photoreceptor cells. In longitudinal sections VLGR1b labeling by antibodies directed against the intracellular domain is found in the periciliary collar-like IS extension (*asterisk*) and in the CC (**E**). Staining in the CC is also observed in cross-sections (**F**). (**G**) Anti-VLGR1b antibodies directed against the extracellular domain reveal VLGR1b localization in the gap (*arrows*) between membranes of the periciliary collar-like IS extension (*asterisk*) and the CC. Scale bars: A: 0.25 µm, B: 0.5 µm, C: 0.2 µm, D: 0.25 µm, E G: 0.1 µm.

Figure 5. BAPTA sensitivity of VLGR1b ectodomains and fibrous link distribution in wild type and Vlgr1/del7TM mouse photoreceptor cells.

(**A-F**) BAPTA sensitivity of VLGR1b ectodomains in retinal cryosections of mouse retinas. (**A-C**) Double immunofluorescence labeling with antibodies directed against extracellular domains of VLGR1b and anti-whirlin antibodies of retinal cryosections, control treated with PBS. (**A**) Indirect immunofluorescence of anti-VLGR1b and (**B**) anti-whirlin antibodies. (**C**) Merged image of anti-VLGR1b and anti-whirlin staining superposed with nuclear DNA staining by DAPI. Anti-VLGR1b and anti-whirlin staining are localized in the ciliary region. (**D-F**) Double immunofluorescence labeling with antibodies directed against extracellular domains of VLGR1b and anti-whirlin antibodies of retinal cryosections after treatment with 5 mM BAPTA in PBS. (**D**) Indirect immunofluorescence of anti-VLGR1b and (**E**) anti-whirlin antibodies. (**F**) Merged image of anti-VLGR1b and anti-whirlin staining superposed with the

nuclear staining by DAPI. After BAPTA treatment, the staining of the extracellular domain of VLGR1b is completely vanished, while anti-whirlin staining persists in the ciliary region.
(**G-J**) Electron microscopical analyses of fibrous links in wild type and Vlgr1/del7TM mouse photoreceptor cells. (**G, H**) Electron micrographs of ultrathin cross-sections (**G**) and longitudinal sections (**H**) through the ciliary region of wild type mouse photoreceptor cells. *Arrows* point to the fibrous links between the adjacent membranes of the apical inner segment collar (*asterisk*) and the connecting cilium (CC). (**I, J**) Electron micrographs of ultrathin cross-sections (**I**) and longitudinal sections (**J**) through the ciliary region of homozygous Vlgr1/del7TM mouse photoreceptor cells. Fibrous links are not detectable, neither in cross-sections nor in longitudinal sections through the ciliary region of photoreceptor cells of homozygous Vlgr1/del7TM mice. Scale bars: C, F: 20 µm; G: 0.1 µm; H-J: 0.2 µm.

Figure 6. Subcellular localization of SANS and whirlin in *Xenopus* retina.

(**A, B**) Electron micrographs of anti-SANS labeling in longitudinal sections of *Xenopus* photoreceptor cells. SANS localization is found in the apical inner segment (IS), in the periciliary ridge complex (PRC) at the base of the connecting cilium (CC), in the CC, in the basal body complex (BB) and in the axonemal extension of the CC (*arrow head*). (**C, D**) Electron micrographs of anti-whirlin labeling in a longitudinal section (**C**) and a slightly oblique cross-section through the CC and the PRC (**D**) of *Xenopus* photoreceptor cells. Whirlin labeling is predominantly found in the ridges of the PRC and to lesser extent in the IS and the CC. Arrows indicate the ridges of the PRC. OS, outer segment. Scale bars: A: 0.25 µm, B: 0.2 µm, C: 0.25 µm, D: 0.5 µm.

Figure 7. Subcellular localization of USH2A isoform b and VLGR1b in *Xenopus* photoreceptor cells.

(**A, B**) Electron micrographs of anti-USH2A isoform b labeling in a longitudinal section (**A**) and an oblique cross-section through the connecting cilium (CC) and the periciliary ridge complex (PRC) (**B**) of *Xenopus* photoreceptor cells. USH2A isoform b localization is restricted to the apical inner segment in the PRC, at the base of the CC, in the CC, in the basal body complex (BB) and in the axonemal extension of the CC (**A**) (*arrow head*). (**C, D**) Electron micrographs of anti-VLGR1b-cytoplasmic domain labeling in a longitudinal section (**C**) and an oblique cross-section through the CC and the PRC (**D**) of *Xenopus* photoreceptor cells. VLGR1b is detected in the apical inner segment in the PRC at the base of the

connecting cilium (CC), in the CC and in the axonemal extension of the CC (*arrow head*). Scale bars: A-D: 0.2 µm

Figure 8. SANS distribution is dependent on microtubules in NIH3T3 cells and organotypic mouse retina culture

(**A-C**) SANS distribution after DMSO, colchicine or thiabendazole treatment in NIH3T3 cells. Immunohistochemical localization of SANS (green) and α-tubulin (red) in control cells incubated with DMSO **(A)** and NIH3T3 cells treated with colchicine (**B**) or thiabendazole (**C**). After drug treatment the microtubule network stained by anti-α-tubulin antibodies is destroyed (**B, C, middle panels**), the anti-SANS punctuated centrosomal labeling (**A, left panel**, *arrows*) is abolished and SANS is distributed throughout the cytoplasm (**B**) or even found in the nucleus (**C**). (**D, E**) SANS distribution in photoreceptor cells after DMSO or thiabendazole treatment of organotypic cultures of mouse retinas. Immunohistochemical localization of SANS (green) and α-tubulin (red) in control retinal cultures incubated with DMSO **(D)** and after thiabendazole treatment (**E**). In control retinal cultures, SANS staining overlaps with the microtubule cytoskeleton in photoreceptor cells. After thiabendazole treatment microtubules are depolymerized and SANS distribution is altered and staining intensity is reduced. Scale bars: A-C: 10 µm, E: 20 µm

Figure 9. Schematic representation of the protein interactions involved in the ciliary/ periciliary protein network of photoreceptor cells.

(**A**) Schematic representation of the interactions within ciliary/pericilary protein network. Ectodomains of USH2A isoform b and VLGR1b connect the membranes of the connecting cilium and the inner segment. Both are anchored via whirlin at the USH protein network in the cytoplasm of the adjacent domains. Direct protein-protein interactions are indicated by solid lines. Doted lines indicate putative interaction. *Asterisk* indicates inner segment collar.

(**B, C**) Schematic arrangement of the ciliary/periciliary USH protein network and its relation to transport vesicle delivery in a mammalian rod photoreceptor cell. Note: a schematic representation of a *Xenopus* rod cell is presented in the supplement material Fig. 3. (**B**) Longitudinal section and (**C**) Cross-section. Cytoplasmic dynein mediates vesicle transport along microtubule to the apical inner segment collar (*asterisk*). Docking and fusion membrane sites (indicated in red) are predefined by USH protein network arrangement.

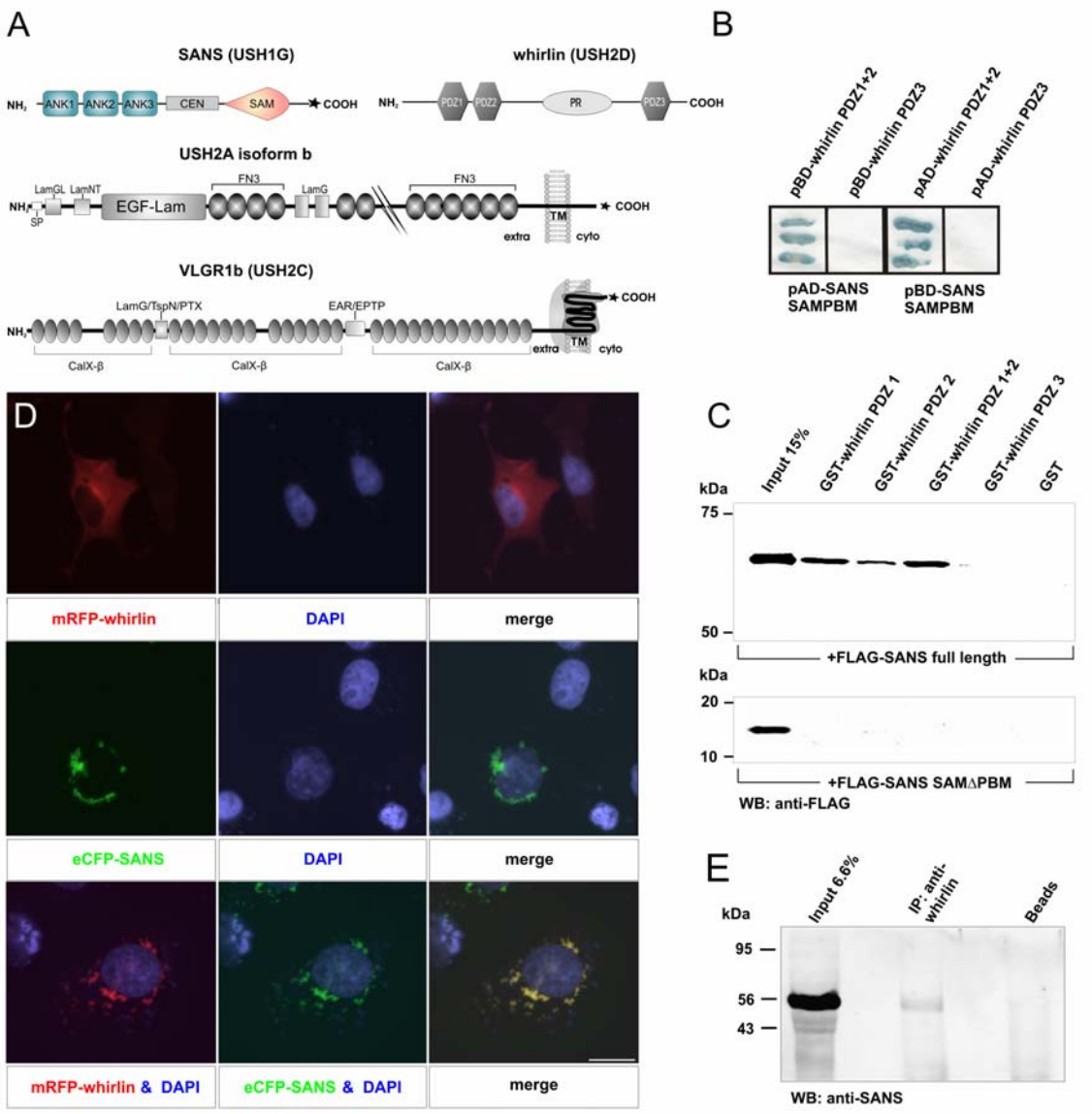

Fig.1. **Validation of the SANS - whirlin interaction.**

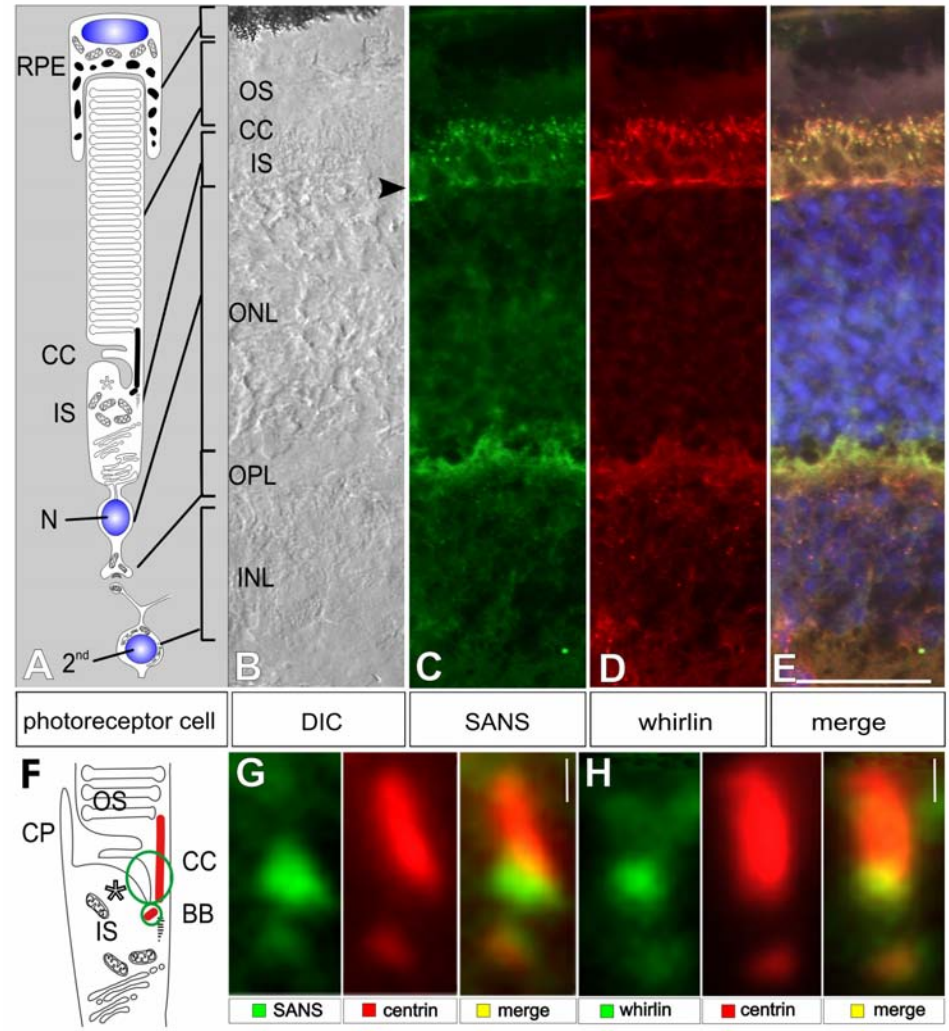

Fig.2. **SANS and whirlin colocalize in mouse photoreceptor cells.**

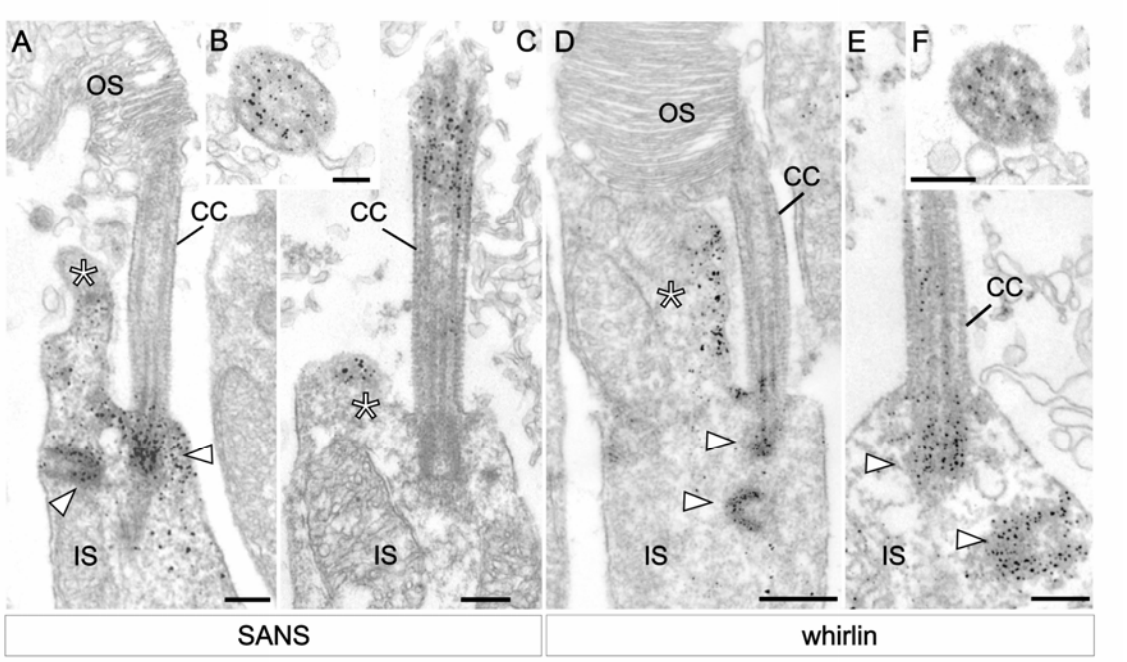

Fig.3. **Immunoelectron microscopic localization of SANS and whirlin in mouse photoreceptor cells.**

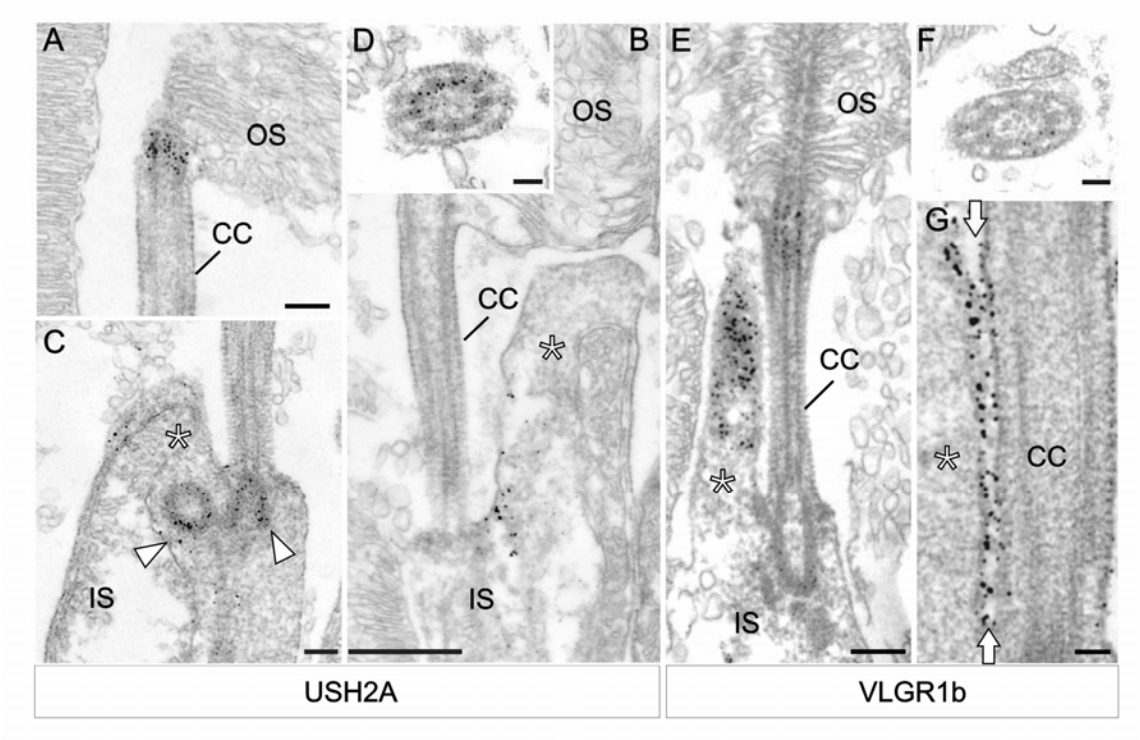

Fig.4. **Immunoelectron microscopic localization of USH2A isoform b and VLGR1b in mouse photoreceptor cells.**

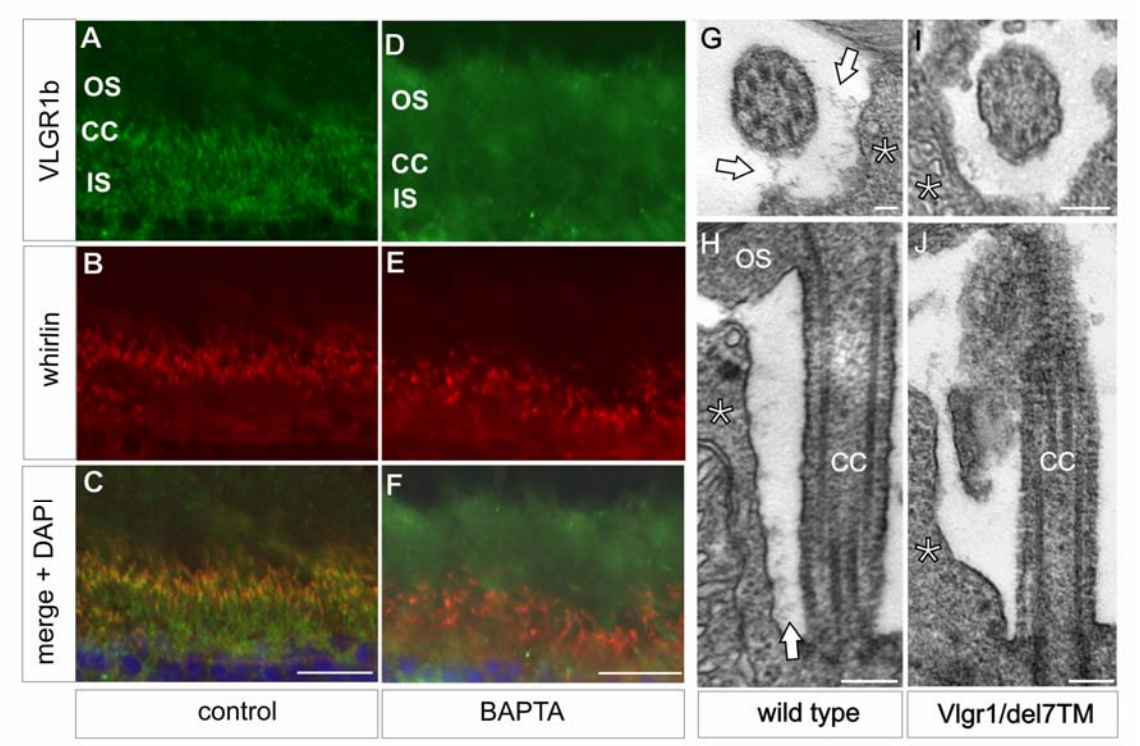

Fig.5. **BAPTA sensitivity of VLGR1b ectodomains and fibrous link distribution in wild type and Vlgr1/del7TM mouse photoreceptor cells.**

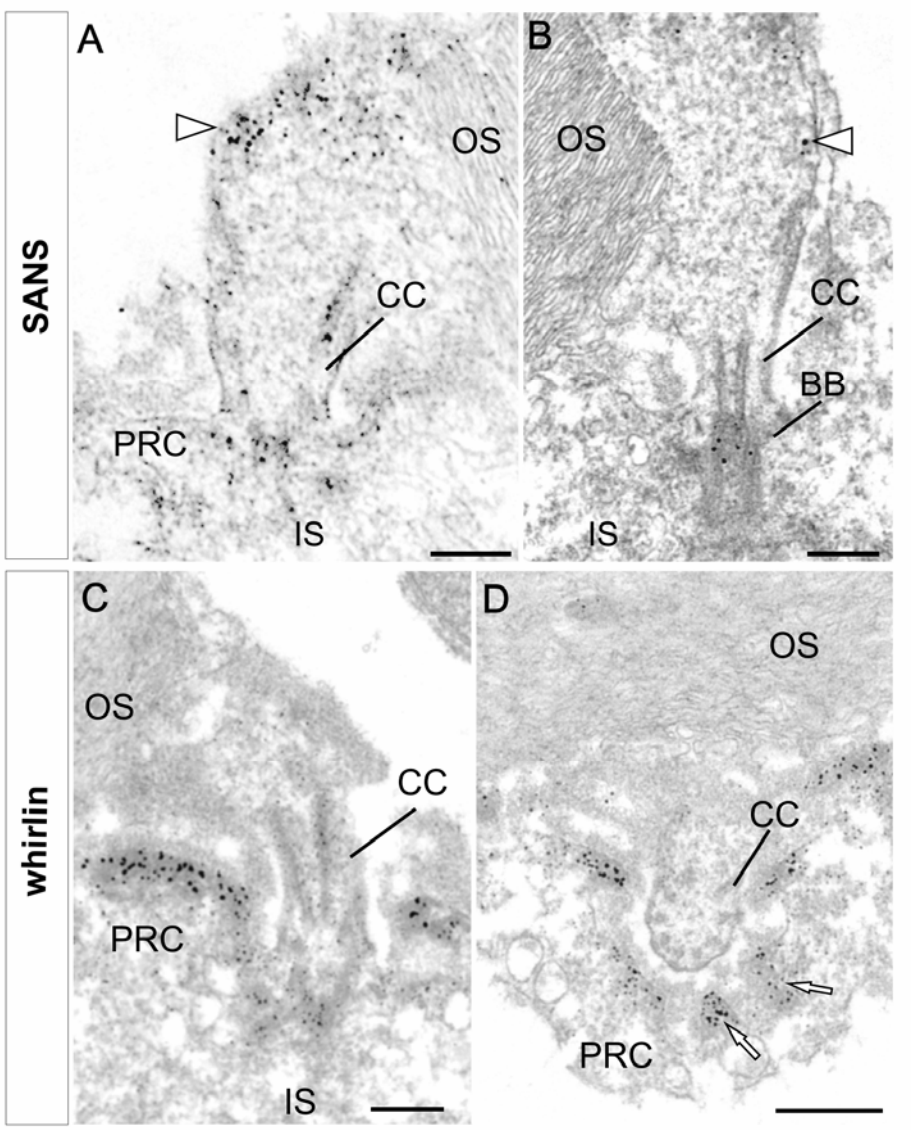

Fig.6. **Subcellular localization of SANS and whirlin in *Xenopus* retina.**

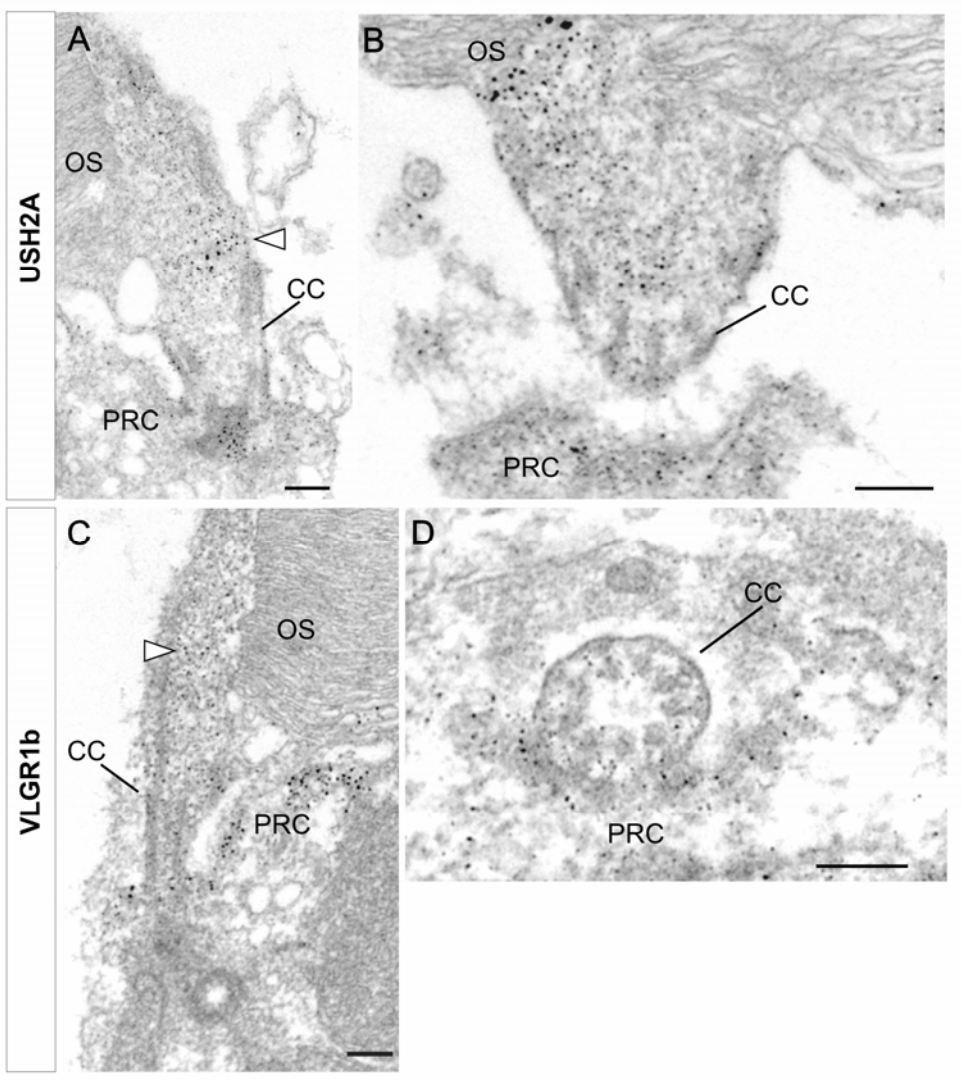

Fig.7. **Subcellular localization of USH2A isoform b and VLGR1b in *Xenopus* photoreceptor cells.**

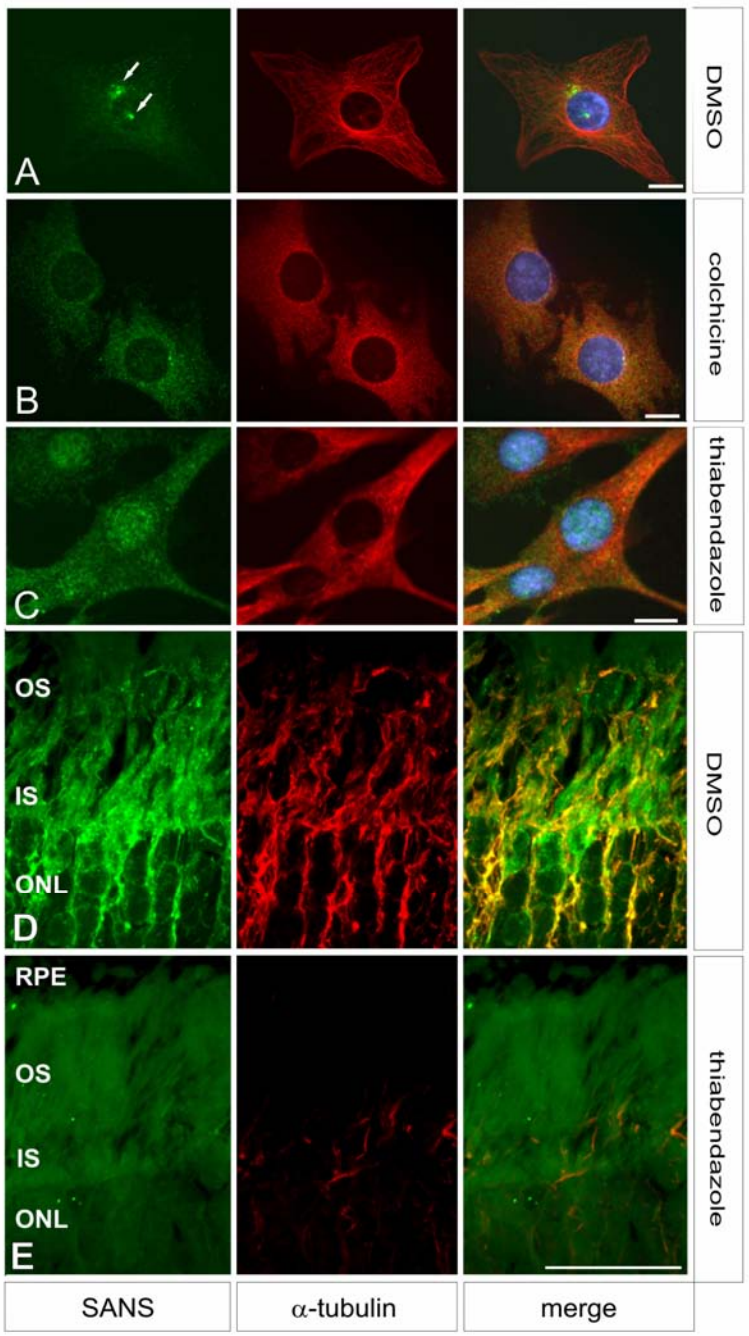

Fig.8. **SANS distribution is dependent on microtubules in NIH3T3 cells and organotypic mouse retina culture.**

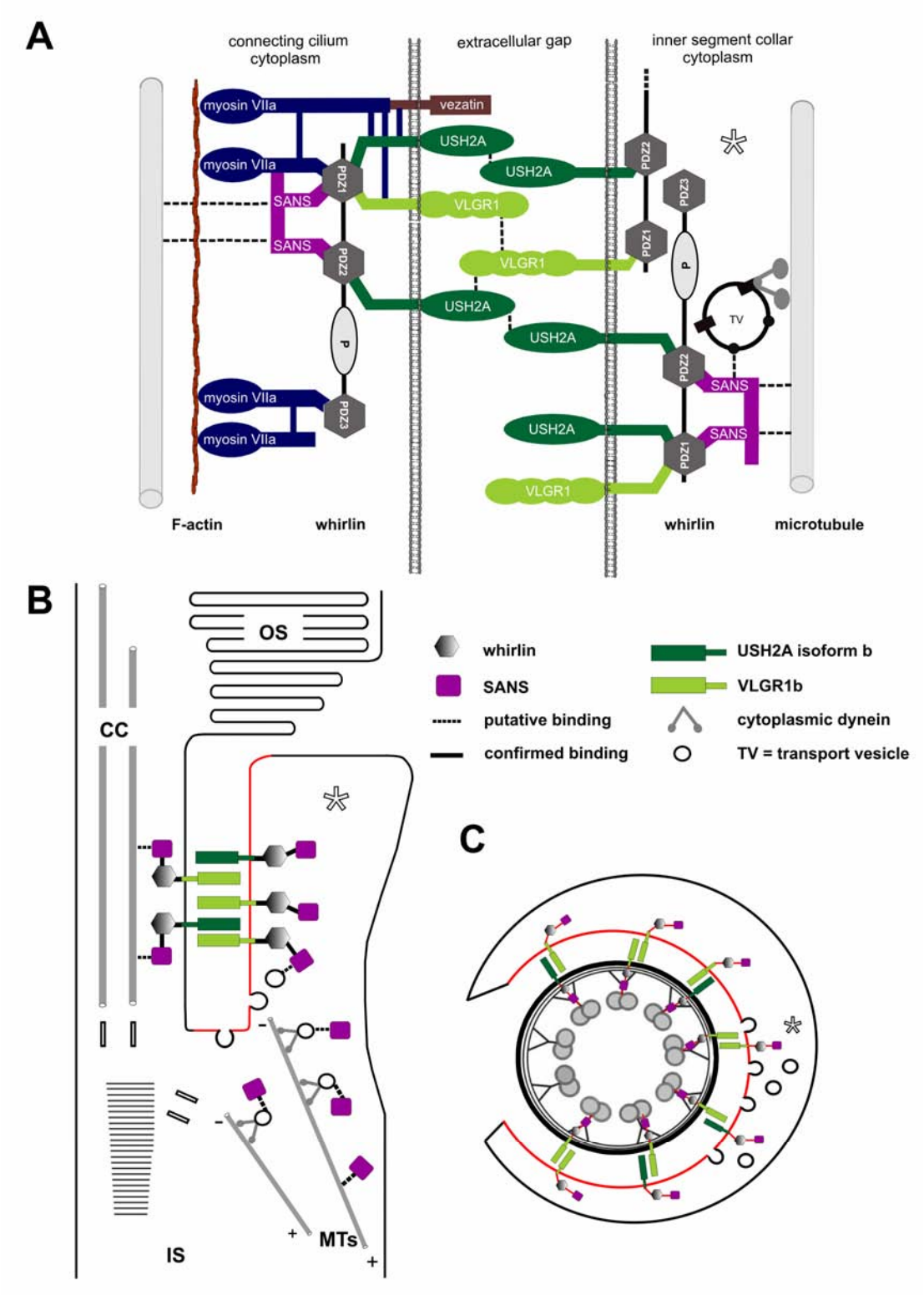

Fig.9. **Schematic representation of the protein interactions involved in the ciliary/ periciliary protein network of photoreceptor cells.**

Abbreviations

BAPTA, 1,2-bis(o-aminophenoxy)ethane-N,N,N',N'-tetraacetic acid; DAPI, 4',6-Diamidin-2'-phenylindoldihydrochlorid; DMSO, dimethyl sulfoxide; eCFP, enhanced cyan fluorescent protein; GST, Glutathion-S-transferase; mRFP, monomeric red fluorescent protein; PBM, PDZ binding motif; PDZ domain, domain present in postsynaptic density 95, discs large, zonula occludens-1; PRC, periciliary ridge complex; SAM, sterile alpha motif; SANS, scaffold protein containing ankyrin repeats and SAM domain; USH, Usher syndrome; VLGR1b, very large G-protein coupled receptor 1b; Vlgr1/del7TM, deletion of the 7 transmembrane domains and of the cytoplasmic C-terminus of VLGR1.

Supplementary material

Supplementary material figure 1. Harmonin is not localized in the ciliary apparatus or in the periciliary inner segment collar of mouse photoreceptor cells.

(**A - C**) Indirect immunofluorescence double labeling of harmonin (green) and centrins (red) in longitudinal cryosections of mouse retina. Harmonin is predominantly localized in outer segments (OS) with a weaker staining in inner segments (IS) and the outer plexiform layer of photoreceptor cells, which is conform with previous data (10,23). (**B**) Anti-pan-centrin antibodies used as a molecular marker for the ciliary region stain the connecting cilium and the basal body complex of mouse photoreceptor cells. (**C**) Merged image of harmonin and centrins indicated slight colocalization in the ciliary region of photoreceptor cells. (**D, E**) Immunoelectron microscopical analysis of photoreceptor cells with anti-harmonin antibodies. (**D**) A longitudinal section through the ciliary part of a photoreceptor cell and (**E**) a cross-section through the photoreceptor connecting cilium. In contrast to the immunofluorescence analysis, Harmonin staining is exclusively detected in the OS. In the connecting cilium (CC) and the IS harmonin is not obtained. *Asterisk* indicates the apical inner segment collar. Scale bars: C: 10 µm; D: 0.5 µm; E: 0.1.µm.

Supplementary material figure 2. High magnification immunofluorescence analyses of USH2A isoform b and VLGR1b localization in the connecting cilium of mouse photoreceptor cells.

Indirect immunofluorescence double labeling with (**A**) anti-USH2A isoform b (green) or (**B**) anti-VLGR1b-cytodomain antibodies (green), respectively and anti-pan-centrin antibodies (red) (marker for the connecting cilium and the basal body complex) of photoreceptor cilia in retinal cryosections analyzed by fluorescence microscopy. Merged images of USH2A isoform b and centrin labeling reveal a partial colocalization of USH2A isoform b in the connecting cilium and the basal body complex. (**B**) Merged images of VLGR1b and centrin labeling show partial colocalization in the connecting cilium but not in the basal body complex. Scale bars: 0.2 µm.

Supplementary material figure 3. Schematic representation of the periciliary ridge complex of *Xenopus* photoreceptor cells.

(**A**) Cross-section through the periciliary ridge complex (PRC). (**B**) Longitudinal section of the apical part of a frog photoreceptor cell (section plane of A is indicated by green arrows). The PRC is a plasma membrane specialization of the apical inner segment (IS) in frog photoreceptor cells (26-28). The PRC consists of nine alternating ridges (R) and invaginations termed grooves (G) surrounding the base of the connecting cilium (CC). Its nine-fold symmetry apparently reflects the 9 + 0 microtubule duplet organization of the CC. The membrane domains of the grooves (indicated in red) are sites for docking and fusion of inner segment transport vesicles. The USH proteins whirlin and SANS as well as the cytodomains of USH2A isoform b and VLGR1b are localized in the ridges. Ectodomains of USH2A isoform b and VLGR1b form extracellular fibers projecting from the top edges of the ridges to the adjacent ciliary membrane. Cytoplasmic dynein mediates vesicle transport along microtubule to the PRC. Direct protein-protein interactions are indicated by solid lines, dotted lines indicate putative interactions. OS, outer segment; CP, calycal processes.

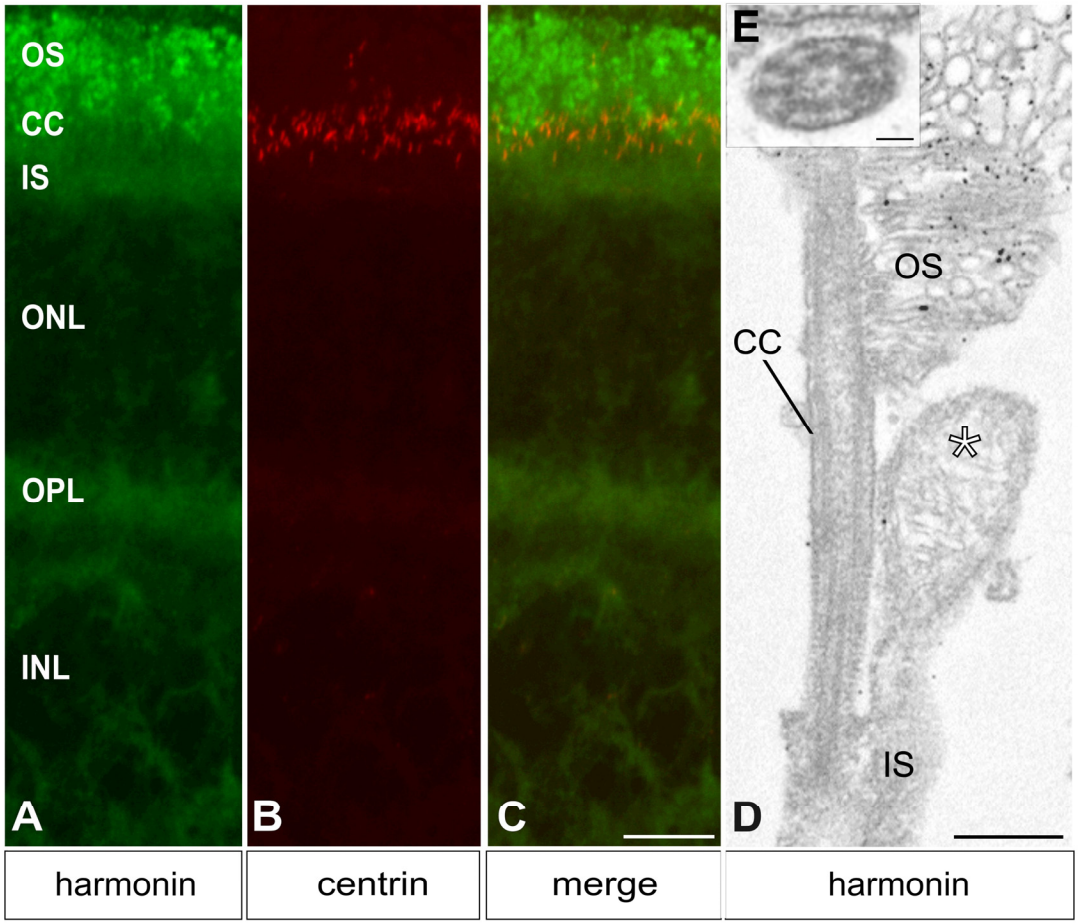

Supplementary material figure 1. Harmonin is not localized in the ciliary apparatus or in the periciliary inner segment collar of mouse photoreceptor cells.

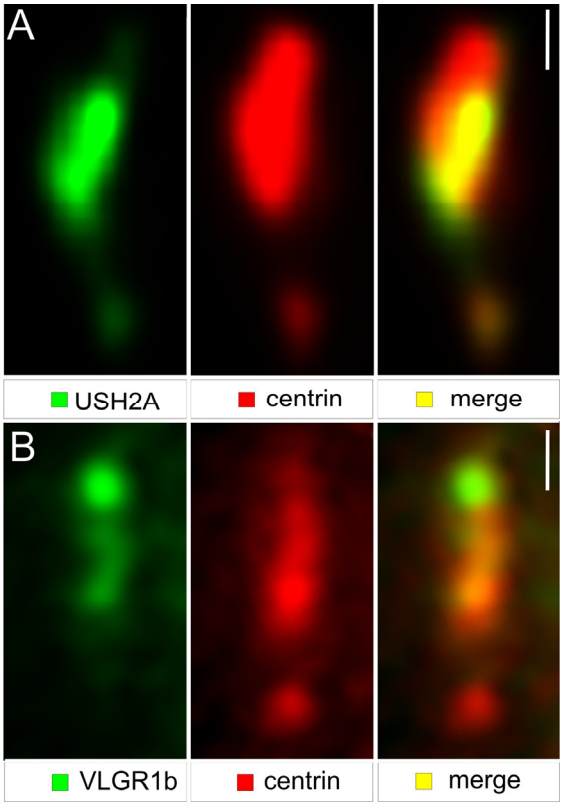

Supplementary material figure 2: High magnification immunofluorescence analyses of USH2A isoform b and VLGR1b localization in the connecting cilium of mouse photoreceptor cells.

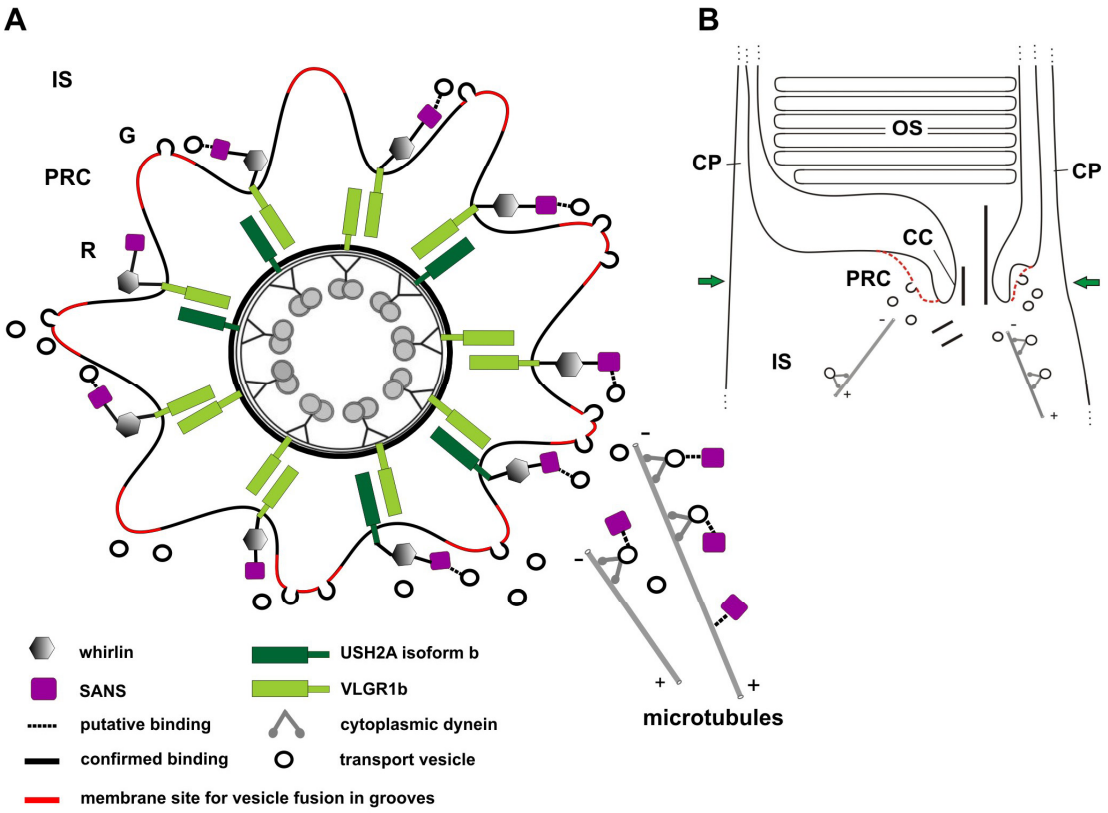

Supplementary material figure 3: Schematic representation of the periciliary ridge complex of *Xenopus* photoreceptor cells.

3. Zusammenfassung der Ergebnisse

Durch die im Rahmen der vorliegenden Arbeit generierten und charakterisierten spezifischen Antikörper gegen SANS („Scaffold protein containing Ankyrin repeats and SAM domain“) waren erstmals Analysen auf Proteinniveau möglich. Die Expression von SANS konnte neben den mit einem USH Phänotypen ausgeprägten Geweben, Retina und Cochlea, auch in weiteren cilientragenden Geweben, wie im Gehirn, in der Lunge, in Testis und im olfaktorischen Epithel nachgewiesen werden (Dissertation Publikation I). In der Retina konnte SANS in der äußeren und inneren plexiformen Schicht sowie in der Photorezeptorzellschicht detektiert werden (Dissertation Publikation I). Eine Vielzahl biochemischer und molekularbiologischer Methoden hat gezeigt, dass SANS im Bereich der Photorezeptorzellsynapsen, der *Membrana limitans externa*, des Innensegments sowie des Verbindungsciliums lokalisiert ist (Dissertation Publikation I, II). Die subzelluläre Lokalisation von SANS konnte auf den Basalkörperkomplex, das Verbindungscilium und das apikale Innensegment eingegrenzt werden (Dissertation Publikation II). Um die zelluläre Funktion von SANS näher charakterisieren zu können war es essentiell, neue Interaktionspartner von SANS zu eruieren. Zur Identifikation neuer Bindepartner von SANS wurde im Rahmen dieser Arbeit ein Hefe-2-Hybrid „Screen“ mit dem C-Terminus von SANS (SAM Domäne und PDZ-Bindemotiv) als „Köder“ und einer bovinen Retina cDNA Bibliothek als „Beute“ durchgeführt. Die Resultate dieser Hefe-2-Hybrid Analysen sind in Tabelle 3 zusammenfasst.

Protein	#	Funktion	Expression	Lokalisation	Referenzen
Whirlin	33	Stereocilienelongation, Organisation von Proteinnetzwerken	Retina, Cochlea, Niere,Gehirn, Lunge	CC, IS, OLM, OPL Cochlea	Mburu *et al.*, 2003,2006 van Wijk *et al.*, 2006* Ebermann *et al.*, 2007
MAGI-2	3	Proteinwechselwirkung, Organisation von Multiproteinkomplexen	Gehirn		Hirao *et al.*, 1998
PDZRN4 (PDZ domain containing RING finger protein-4)	2	Ubiquitin-Protein Ligase	Gehirn, Pankreas, Testis	intrazellulär extrazellulär nukleär	Katoh und Katoh, 2004

Tabelle 3. Übersicht der mittels Hefe-2-Hybrid Analysen identifizierten Interaktionspartner des C-Terminus von SANS. CC = Verbindungscilium, IS = Innensegment, OLM = *Membrana limitans externa*, OPL = äußere plexiforme Schicht, # = Häufigkeit der im Hefe-2-Hybrid „Screen“ identifizierten Interaktionspartner.

Neben der Identifikation des Gerüstproteins Whirlin (USH2D) (insgesamt 33 mal), konnten das MAGUK-(„Membrane Associated Guanylate Kinase“) Protein MAGI-2 („Membrane-Associated Guanylate Kinase Inverted-2“) sowie das Protein PDZRN4 („PDZ domain

containing RING finger protein 4“) als neue Interaktionspartner von SANS in der Retina identifiziert werden (Dissertation Publikation II). Die Resultate der vorliegenden Arbeit konnten Whirlin als Bindepartner von SANS validieren (Dissertation Publikation II). Darüber hinaus konnten das MAGUK-Protein MPP1 („Membrane Palmitoylated Protein 1“) und die USH2 Transmembranproteine USH2A Isoform b und VLGR1b im Rahmen dieser Arbeit als weitere Bindepartner von Whirlin in der Retina validiert werden (van Wijk *et al.*, 2006*****; Gosens *et al.*, 2007*****). Ferner war es möglich mittels Immunelektronenmikroskopie erstmals die Kolokalisation von SANS, Whirlin, USH2A Isoform b und VLGR1b in Photorezeptorzellen auf subzellulärem Niveau zu veranschaulichen (Dissertation Publikation II). SANS und alle USH2-Proteine konnten im Verbindungscilium sowie im benachbarten apikalen Innensegment in Photorezeptoren der Maus lokalisiert werden. In *Xenopus laevis* konnte die Kolokalisation der vier USH-Proteine in homologen Strukturen zum apikalen Innensegment und Verbindungscilium, dem so genannten „periciliary ridge complex“, bestätigt werden. Des Weiteren war es möglich, die Ektodomänen von VLGR1b als Komponente von filamentösen Strukturen im extrazellulären Bereich zwischen Verbindungscilium und apikalem Innensegment zu identifizieren (Dissertation Publikation II). Diese Resultate sprechen für die Existenz eines ciliären-periciliären USH-Proteinnetzwerkes bestehend aus SANS, Whirlin, USH2A Isoform b und VLGR1b in Photorezeptorzellen der Maus und des Frosches. Ferner wurde die Assoziation von SANS zum Mikrotubulicytoskelett aufgezeigt, was eine potentielle Beteiligung von SANS an Transportmechanismen in Photorezeptorzellen ermöglichen würde.

3.1. Weiterführende Analysen

3.1.1. Identifikation und Charakterisierung von MAGI-2 als Interaktionspartner von SANS

Neben dem mehrfach identifizierten USH2D-Protein Whirlin konnte in den durchgeführten Hefe-2-Hybrid Analysen das Protein MAGI-2 als ein weiterer viel versprechender Bindepartner von SANS eruiert werden (Hirao *et al.*, 1998). MAGI-2 besteht aus sechs PDZ Domänen, zwei Tryptophanresten sowie einer Guanylat Kinase (GuK) Domäne und gehört zur Proteinfamilie der MAGUK-Proteine (Woods and Bryant, 1991; Anderson, 1996). Alle in MAGI-2 enthaltenen Proteindomänen sind in Protein-Proteinwechselwirkungen involviert (Kim *et al.*, 1997; Satoh *et al.*, 1997; Takeuchi *et al.*, 1997). MAGUK-Proteine sind

Gerüstproteine, die in der Lage sind mit dem C-Terminus von Transmembranproteinen zu interagieren sowie weitere Mitglieder der MAGUK Proteinfamilie zu rekrutieren (Fanning *et al.*, 1998; Dimitratos *et al.*, 1999; Leonoudakis *et al.*, 2004). Diese Assoziationen ermöglichen die Organisation von Multiproteinkomplexen in Regionen der Synapse (Fanning et al,. 1998; Deng et al., 2006). Ein weiteres Charakteristikum von MAGUK-Proteinen ist Proteinkomplexe am Aktincytoskelett zu verankern sowie die extrazelluläre Umgebung mit intrazellulären Signalwegen zu verbinden (Anderson, 1996). MAGI-2 spielt eine Rolle bei der Regulation von Signalkaskaden in neuronalen Zellen und wurde als Interaktionspartner von N-Methyl-D-Aspartat-Rezeptoren und neuronalen Zelladhäsionsproteinen, wie PSD-95 und β-Catenin an „Synaptic Junctions“ identifiziert (Hirao *et al.*, 1998; Hirao *et al.*, 2000; Shoji *et al.*, 2000; Nishimura *et al.*, 2002; Abb. 8.).

3.1.2. Zelluläre und subzelluläre Lokalisation von MAGI-2 in der Retina

Zur Validierung der potentiellen Interaktion von SANS mit MAGI-2 wurden zunächst Immunfluoreszenzanalysen auf Kryostatschnitten von Mausretina durchgeführt. In der Retina konnte MAGI-2 im Innensegment, an der *Membrana limitans externa*, in der äußeren plexiformen Schicht, etwas schwächer in der inneren nukleären Schicht sowie in der inneren plexiformen Schicht und im Bereich der Ganglienzellschicht detektiert werden (nicht gezeigt). Zur weiteren Untersuchung der subzellulären Lokalisation von MAGI-2 wurden Kolokalisationsstudien mit Antikörpern gegen MAGI-2 sowie gegen Markerproteine unterschiedlicher Zellkompartimente von Photorezeptorzellen durchgeführt. In der Übereinanderlagerung konnte die partielle Kolokalisation von MAGI-2 mit PSD-95, β-Catenin und Centrinen (Markerproteine für die Prä- und Postsynapse, die *Membrana limitans externa* sowie das Verbindungscilium) dargestellt werden (Abb. 4. C,F,I). Durch diese Analysen konnte die Lokalisation von MAGI-2 auf den Bereich der Synapsen, der *Membrana limitans externa*, des Innensegments sowie auf die Region des Verbindungsciliums von Photorezeptorzellen eingegrenzt werden (Abb. 4. C,F,I).

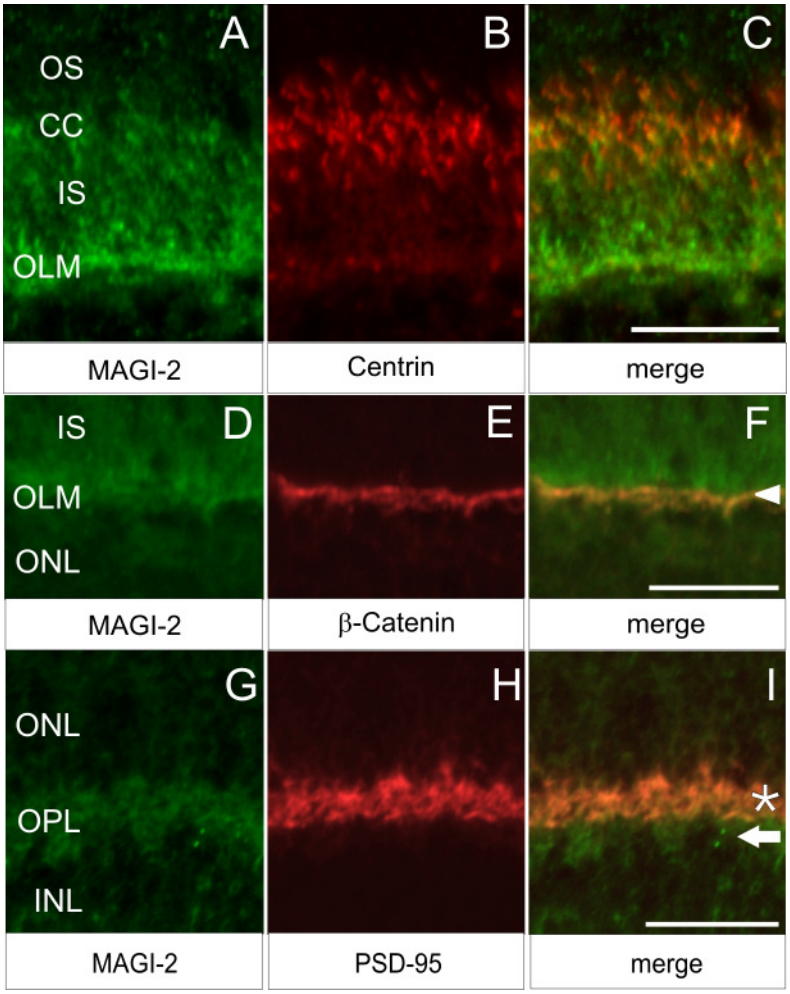

Abb. 4. Lokalisation von MAGI-2 in Mausretina. **(A-I)** Indirekte Immunfluoreszenzanalyse von Doppelmarkierungen auf Kryostatschnitten durch Mausretina. **(A-C)** Doppelmarkierung mit anti-MAGI-2 (**A**) und anti-pan-Centrin (**B**) Antikörpern (Klon 20H5; Marker für Verbindungscilien). (**C**) Die Übereinanderlagerung von A und B zeigt eine partielle Kolokalisation von MAGI-2 und Centrinen in Verbindungscilien (CC) von Photorezeptorzellen. Darüber hinaus konnte MAGI-2 im Innensegment (IS) detektiert werden. **(D-F)** Doppelmarkierung mit anti-MAGI-2 (**D**) und anti-β-Catenin (**E**) Antikörpern (Marker für die *Membrana limitans externa,* OLM). (**F**) Die Übereinanderlagerung der Markierungen für MAGI-2 und β-Catenin zeigt eine deutliche Kolokalisation an der OLM (Pfeilkopf). **(G-I)** Doppelmarkierung mit anti-MAGI-2 (**G**) und anti-PSD-95 (**H**) Antikörpern (Marker für Post-Synapsen und Prä-Synapsen in der Retina). (**I**) Die Übereinanderlagerung der Immunfluoreszenzen für MAGI-2 und PSD-95 zeigt eine partielle Kolokalisation in Post-Synapsen von Photorezeptorzellen und Prä-Synapsen (Stern) von nachgeschalteten Synapsen. MAGI-2 ist darüber hinaus in der inneren nukleären Schicht (INL) lokalisiert (Pfeil). OS = Außensegment, ONL = äußere nukleäre Schicht, INL = innere nukleäre Schicht. Größenbalken: 10 µm.

Die ermittelte Lokalisation von MAGI-2 in Photorezeptorzellen ist mit der Markierung für SANS konsistent (Dissertation Publikation I, II). Kolokalisationsanalysen mit Antikörpern gegen SANS und MAGI-2 waren bisher nicht möglich, da die zur Verfügung stehenden Antikörper aus dem gleichen Tier stammten.

Neben der Kolokalisation von MAGI-2 und SANS wurde erstmals Kolokalisation von MAGI-2 mit dem USH2D Protein Whirlin im Bereich des Verbindungsciliums, des

Innensegments, der *Membrana limitans externa* sowie an den Synapsen von Photorezeptorzellen und der inneren nukleären Schicht in der Retina visualisiert (Abb. 5.).

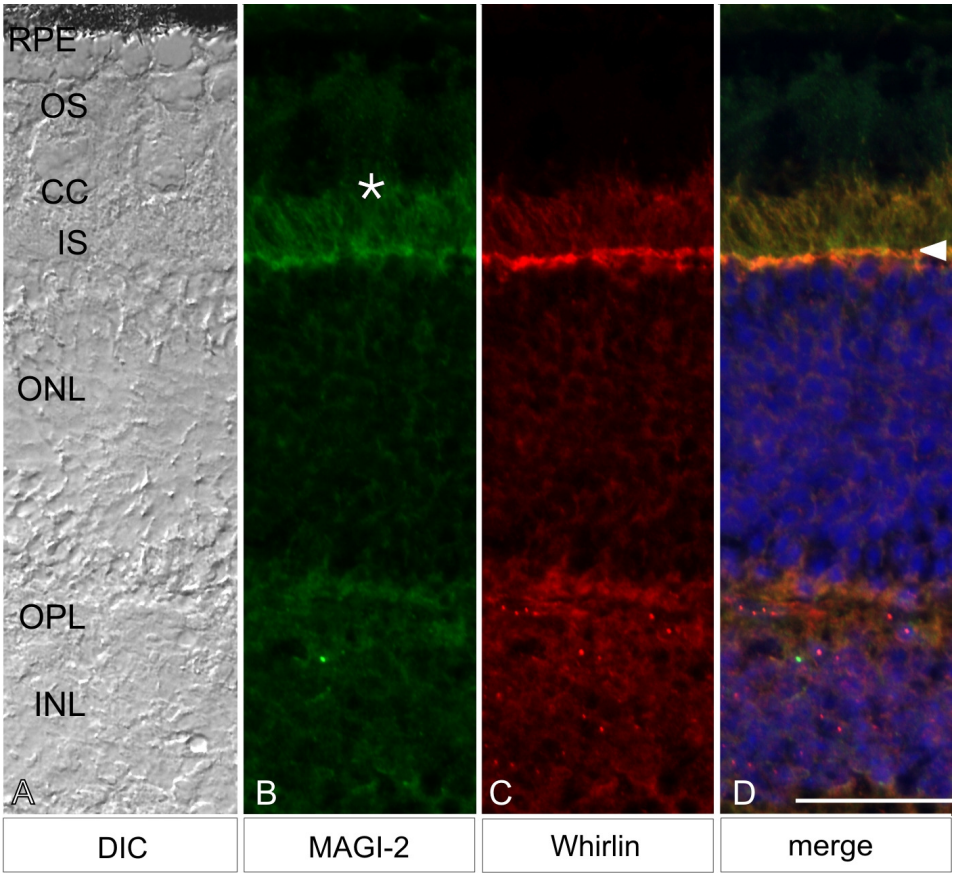

Abb. 5. Lokalisation von MAGI-2 und Whirlin in Mausretina. (A) Lichtmikroskopische Aufnahme eines untersuchten retinalen Kryostatschnittes im differenziellen Interferenzkontrast (DIC). **(B)** Indirekte Immunfluoreszenzmarkierung mit Antikörpern gegen MAGI-2. MAGI-2 ist im Verbindungscilium (CC, Stern), im Innensegment (IS), an der *Membrana limitans externa* (OLM, Pfeilkopf), in der äußeren plexiformen Schicht (OPL) sowie in der inneren nukleären Schicht (INL) lokalisiert. **(C)** Indirekte Immunfluoreszenzmarkierung mit Antikörpern gegen Whirlin. Anti-Whirlin Antikörper detektieren Whirlin im Bereich des CC, des IS, der OLM sowie an der OPL von Photorezeptorzellen. Whirlin wurde auch in der INL sowie im Bereich der dort lokalisierten Centrosomen als punktförmige Markierung visualisiert. **(D)** Übereinanderlagerung von B und C mit der DAPI gefärbten Zellkernschicht. Die Übereinanderlagerung der Markierungen für MAGI-2 und Whirlin zeigt eine deutliche Kolokalisation im CC, IS, OLM sowie in der OPL und INL. RPE = Retinales Pigmentepithel, OS = Außensegment, ONL = äußere nukleäre Schicht. Größenbalken: 20 µm.

Um die Lokalisation von MAGI-2 in Photorezeptorzellen auf subzellulärem Niveau zu analysieren, wurde die Methode der „pre-embedding“ Elektronenmikroskopie angewandt. Immunelektronenmikroskopische Daten zeigen eine subzelluläre Lokalisation von MAGI-2 an der Basis des Außensegmentes (Abb. 6. A,D) sowie eine Assoziation von MAGI-2 mit Transportvesikeln im apikalen Innensegment (Abb. 6. B,C) in Photorezeptorzellen der Maus. Darüber hinaus wurde MAGI-2 in Longitudinal- und Querschnitten durch das

Verbindungscilium (Abb. 6. E,F) sowie im Bereich der *Membrana limitans externa* lokalisiert (Abb. 6. G).

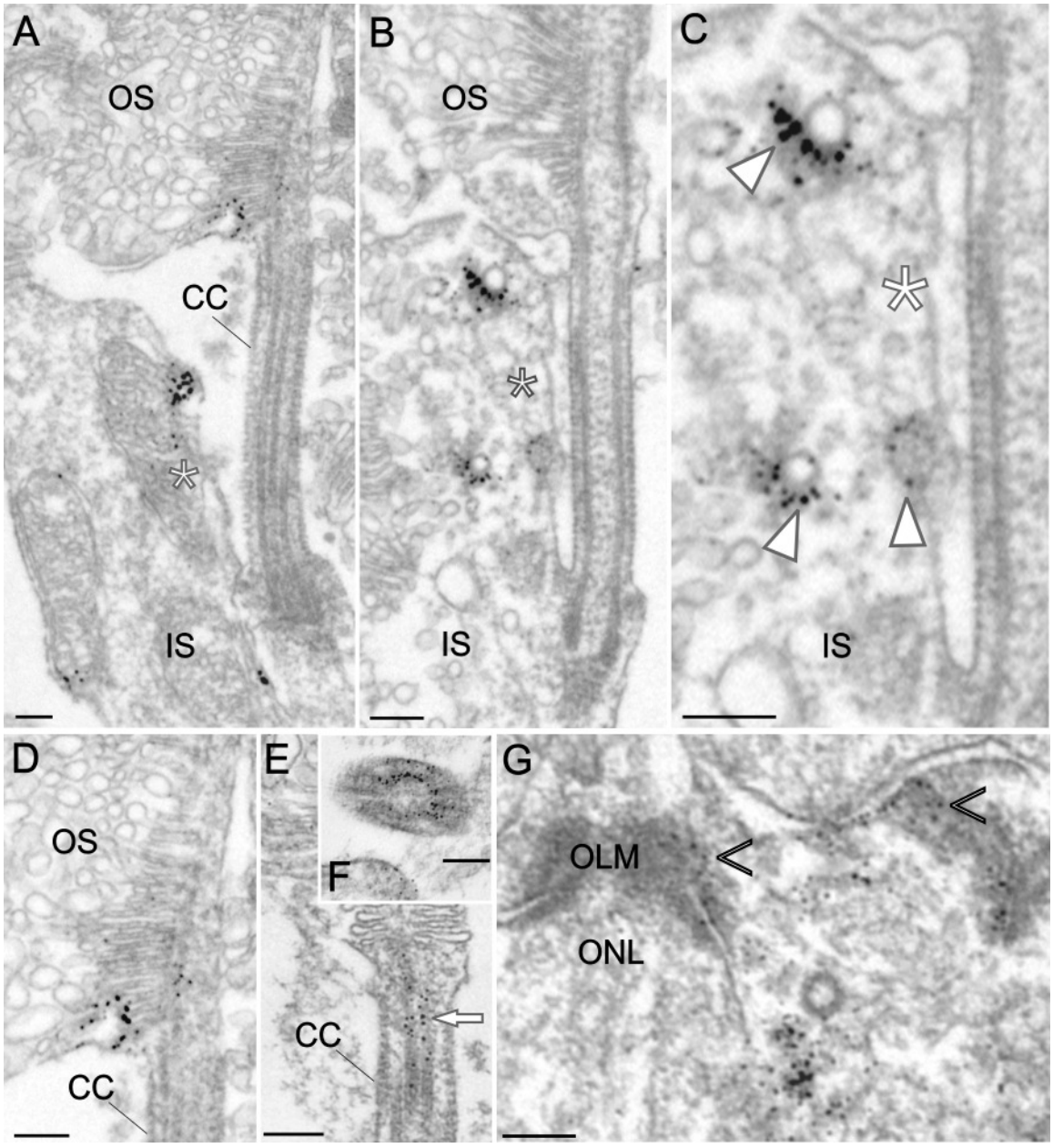

Abb. 6. Subzelluläre Lokalisation von MAGI-2. (**A-G**) Immunelektronenmikroskopische Aufnahmen der MAGI-2 Markierung in Longitudinalschnitten (**A-E, G**) und Querschnitten (**F**) in Photorezeptorzellen von Mausretina. (**A**) MAGI-2 Lokalisation im basalen Außensegment (OS) und an der Membran des apikalen Innensegments (IS, Stern). (**B,C**) Anti-MAGI-2 Antikörper detektieren MAGI-2 an Transportvesikeln an der Membran des apikalen IS (Pfeilköpfe). (**D**) Der vergrößerte Teilausschnitt aus (**C**) stellt die Lokalisation von MAGI-2 im basalen Bereich des OS heraus. (**E, F**) MAGI-2 wird in Longitudinal- und Querschnitten im Verbindungscilium (CC) von Photorezeptorzellen detektiert (Pfeil). (**G**) MAGI-2 lokalisiert in Zell-Zelladhäsionsbereichen der *Membrana limitans externa* (OLM, offene Pfeilköpfe). ONL = äußere nukleäre Schicht. Größenbalken: A-G: 0,2 µm.

Als weiterer Modellorganismus zur Analyse der subzellulären Lokalisation von MAGI-2 wurde *Xenopus laevis* herangezogen. Charakteristisch für *Xenopus laevis* ist eine Struktur, die apikal im Innensegment lokalisiert ist und das Verbindungscilium basal umschließt. Es handelt sich dabei um den so genannten „periciliary ridge complex". Diese Struktur ist als homolog zum apikalen Innensegment der Maus anzusehen (Liu *et al.*, 2007; Dissertation Publikation II) und bildet den Bereich aus, mit dem Transportvesikel aus dem Innensegment fusionieren. Anti-MAGI-2 Antikörper detektieren MAGI-2 im Innensegment, am Basalkörperkomplex, an Transportvesikeln im „periciliary ridge complex" sowie im Verbindungscilium und im ciliären Axonem (Abb. 7.).

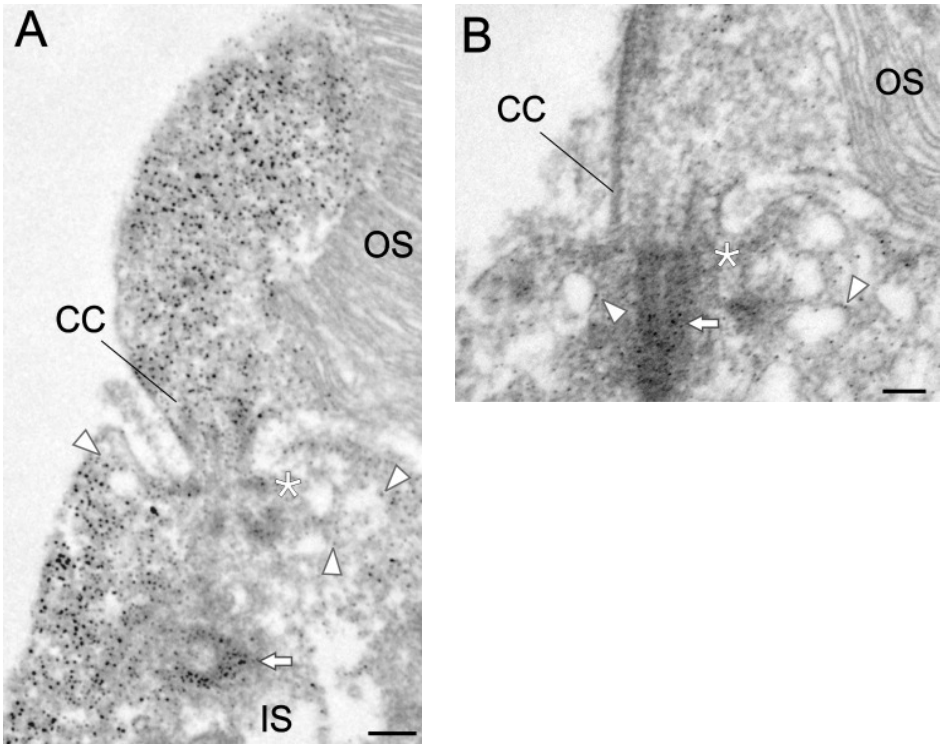

Abb. 7. Subzelluläre Lokalisation von MAGI-2 in Photorezeptorzellen von *Xenopus laevis*. (**A,B**) Anti-MAGI-2 Antikörper markieren im Innensegment (IS), am Basalkörperkomplex (Pfeil), an Transportvesikeln (Pfeilköpfe), im so genannten „periciliary ridge complex" (Stern), im Verbindungscilium (CC) sowie im ciliären Axonem (**A**). OS = Außensegment. Größenbalken: A: 0,2 µm, B: 0,1 µm.

3.1.3. Identifikation weiterer Bindepartner von SANS

Neben dem Hefe-2-Hybrid „Screen" mit der SAM („Sterile Alpha Motif") Domäne und PDZ-Bindemotiv wurde auch die zentrale Domäne (CEN) von SANS zu einem späteren Zeitpunkt in den Hefe-2-Hybrid Analysen zur Identifikation neuer Interaktionspartner verwendet. Die neu ermittelten Interaktionspartner der zentralen Domäne von SANS sind in Tabelle 4 aufgeführt.

Protein	#	Funktion	Expression	Lokalisation	Referenzen
Myomegalin	15	rekrutiert Komponenten cAMP-abhängiger Signalwege	Testis, Herz, Skelettmus-kulatur	Golgi Apparat, Centrosomen, Sarkomer	Verde *et al.*, 2001 Tasken *et al.*, 2001
Alsin (Amyotrophe lateral Sclerose2)	10	Transport, Signaltransduktion Endosomendynamik, Makropinocytose	Gehirn, Leber	Membran, Cytosol, Vesikeln, Endosomen	Otomo *et al.*, 2003 Topp *et al.*, 2004 Hadano *et al.*, 2007 Kunita *et al.*, 2007
MCC (mutated in colorectal cancer)	3	Tumorsuppressor	Gehirn, Muskel	n.b.	Hoshino *et al.*, 1991 Kinzler *et al.*, 1991
AKAP9 (A-kinase anchor protein 9)	3	Komplexorganisation am Centrosom und Golgi-Apparat, Transport, Signaltransduktion	Gehirn, Pankreas, Muskel,	perinukleär, Centrosomen, Golgi-Apparat	Kim *et al.*, 2007 Gillingham, Munro, 2000 Shanks *et al.*, 2002 Keryer *et al.*, 2003
CEP290 (centrosomal protein 290kDa)	2	Ciliärer Transport, Regulation von Transkriptionsfaktoren	Gehirn, Retina, Niere	Centrosomen, Cilien, Zellnuklei	Chang *et al.*, 2006 Valente *et al.*, 2006 Sayer *et al.*, 2006
"likely ortholog of kinesin light chain 2"	2	n.b.	n.b.	n.b.	n.b.
Dynaktin-1	2	Dynein-vermittelter Vesikeltransport, Positionierung des Zellkerns in Photorezeptorzellen	Gehirn, Retina	Nukleus	Holzbaur, Tokito, 1996 Tsujikawa *et al.*, 2007
Periphilin 1	1	Differenzierung von Epithelien	Keratinozyten	Nukleus	Kurita *et al.*, 2004 Kazerounian,Aho, 2003
abLIM 2 (Aktin-binding LIM Protein 2)	1	Linker zwischen Aktin-cytoskelett und intra-zellulären Signalwegen	Gehirn, Retina, Herzmuskel	IS, OPL, Z-Scheiben der gestreiften Muskulatur	Klimov *et al.*, 2005 Roof *et al.*, 1997
MEGF10 (multiple EGF-like-domains 10)	1	Endocytose	Gehirn	n.b.	Suzuki und Nakayama, 2007 Hamon *et al.*, 2006;
CARD 10 (Caspase recruitment domain protein10)	1	Organisation von Signalkomplexen an Plasmamembranen	Herz, Niere, Leber	n.b.	Wang *et al.*, 2001
CDR2 (cerebellar degeneration-related protein 2)	1	Regulation der c-Myc Aktivität	Gehirn, Niere	Cytoplasma	Okano *et al.*, 1999
KIS (kinase interacting with stathmin)	1	Serin / Threonin Kinase, Zellmigration, Zellzyklusprogression	Gehirn, Herz, Muskel, Leber, Niere	nukleär	Alam *et al.*, 1996 Maucuer *et al.*, 1995 Maucuer *et al.*, 1997 Crook *et al.*, 2007
costal2	1	Signaltransduktion	Imaginalscheiben	Cytoplasma, Mikrotubuli	Sisson *et al.*, 1997 Nybakken *et al.*, 2002 Tay *et al.*, 2005
triple functional domain (PTPRF interacting) (TRIO)	1	Cytoskelettregulation, Zellzyklus, Apoptose, Vesikel "trafficking", Zell-Zelladhäsion, neuronale Entwicklung	ubiquitär	extra- und intazellulär	Adamowicz *et al.*, 2006 Portales-Casamar *et al.*, 2006
Desmuslin	1	Intermediärfilamentprotein	Herz, Skelett-muskulatur, Gehirn	Z-Discs	Mizuno *et al.*, 2001 Titeux *et al.*, 2001
USH2A Isoform b	1	Transmembranprotein	Retina, Cochlea, Herz, Gehirn, Niere, Lunge	Bruch´sche Membran, CC, OPL	van Wijk *et al.*, 2004 Reiners *et al.*, 2005b* Reiners *et al.*, 2006*

Tabelle 4. Übersicht der mittels Hefe-2-Hybrid Analysen identifizierten Interaktionspartner der zentralen Domäne (CEN) von SANS. CC = Verbindungscilium, IS = Innensegment, OPL = äußere plexiforme Schicht, n.b. = nicht beschrieben, # = Häufigkeit der im Hefe-2-Hybrid „Screen" identifizierten Interaktionspartner.

4. Zusammenfassende Diskussion

Die vorliegende Dissertation hatte die Charakterisierung der zellbiologischen und molekularen Funktion des USH1G-Proteins SANS („Scaffold protein containing Ankyrin repeats and SAM domain“) in der Retina zum Ziel. Zur Aufklärung der Funktion eines Proteins ist das Wissen um Interaktionspartner von großem Wert. Durch bereits identifizierte Eigenschaften der Bindepartner können Rückschlüsse auf die Funktion des zu untersuchenden Proteins innerhalb eines Komplexes bzw. innerhalb der Zelle gezogen werden. Die Untersuchung des Zusammenspiels unterschiedlicher Proteine im zellulären Kontext ist für das Verständnis der Ursache einer Krankheit von besonderem Interesse. Aufgrund dessen waren die Identifikation und Validierung neuer Interaktionspartner zur funktionellen Charakterisierung von SANS weitere wichtige Zielsetzungen der vorliegenden Arbeit.

Die in den beiden zentralen Hauptpublikationen Overlack *et al.*, 2007 und Maerker *et al.*, 2007 dargestellten Ergebnisse sollen zusammen mit bisher unveröffentlichten Resultaten im Folgenden diskutiert werden.

4.1. Erweiterung der Netzwerkkomponenten des USH-Interaktoms

Die Darstellung der Interaktionen der USH-Proteine in Abbildung 8 soll verdeutlichen wie vielseitig die Beteiligungen der USH-Proteine an unterschiedlichen zellulären Prozessen sind. Neben der Heterogenität der USH-Proteine selbst, deren Proteinklassen von molekularen Motoren, Gerüstproteinen über Transmembranproteinen bis hin zu Zell-Zelladhäsionproteinen reichen, deuten die direkten Interaktionspartner der USH-Proteine auf weitere zelluläre Funktionen des USH-Interaktoms hin (Abb. 8.). MAGUK („Membrane-Associated Guanylate Kinase“)-Proteine wie das direkt mit Whirlin interagierende MPP1 („Membrane Palmitoylated Protein 1“) spielen eine Rolle in der Ausbildung der Zellpolarität von Photorezeptorzellen (Gosens *et al.*, 2007*). Darüber hinaus sind MAGUK-Proteine wie PSD-95, β-Catenin und MAGI-2 („Membrane-Associated Guanylate Kinase Inverted-2“) in die Organisation von Synapsen involviert (Koulen *et al.*, 1998; Dimitratos *et al.*, 1999; Hirao *et al.*, 2000; Nishimura *et al.*, 2002). Für die Interaktionspartner Harmonin und DOCK4 wird eine Beteiligung an der Regulation der Aktincytoskelettformation diskutiert (Yan *et al.*, 2006). Direkte Assoziationen des USH-Interaktoms zu Aktinfilamenten sind über die Motorproteine Myosin XVa und VIIa gegeben (Belyantseva *et al.*, 2005; Delprat *et al.*, 2005; Hasson *et al.*, 1995; Michalski *et al.*, 2007). Besonders prägnant ist die Verbindung des USH-Interaktoms

zum Mikrotubulicytoskelett und Mikrotubuli-assoziierten Transportvorgängen. Diese Assoziationen werden über SANS und dessen neu identifizierte Interaktionspartner MAGI-2, Dynaktin-1, Alsin, CEP290 („Centrosomal Protein 290kDa“), AKAP9 („A-Kinase Anchor Protein 9“) und Myomegalin vermittelt (Gill *et al.*, 1991; Lin *et al.*, 1998; Wood *et al.*, 1998; Hadano *et al.*, 2001; Verde *et al.*, 2001; Sayer *et al.*, 2006; Tab. 4.). Aufgrund der Akkumulation Mikrotubuli-assoziierter Bindepartner von SANS innerhalb des USH-Interaktoms, soll der Schwerpunkt der vorliegenden Diskussion auf die mögliche Funktion dieser Proteine in Photorezeptorzellen gerichtet werden.

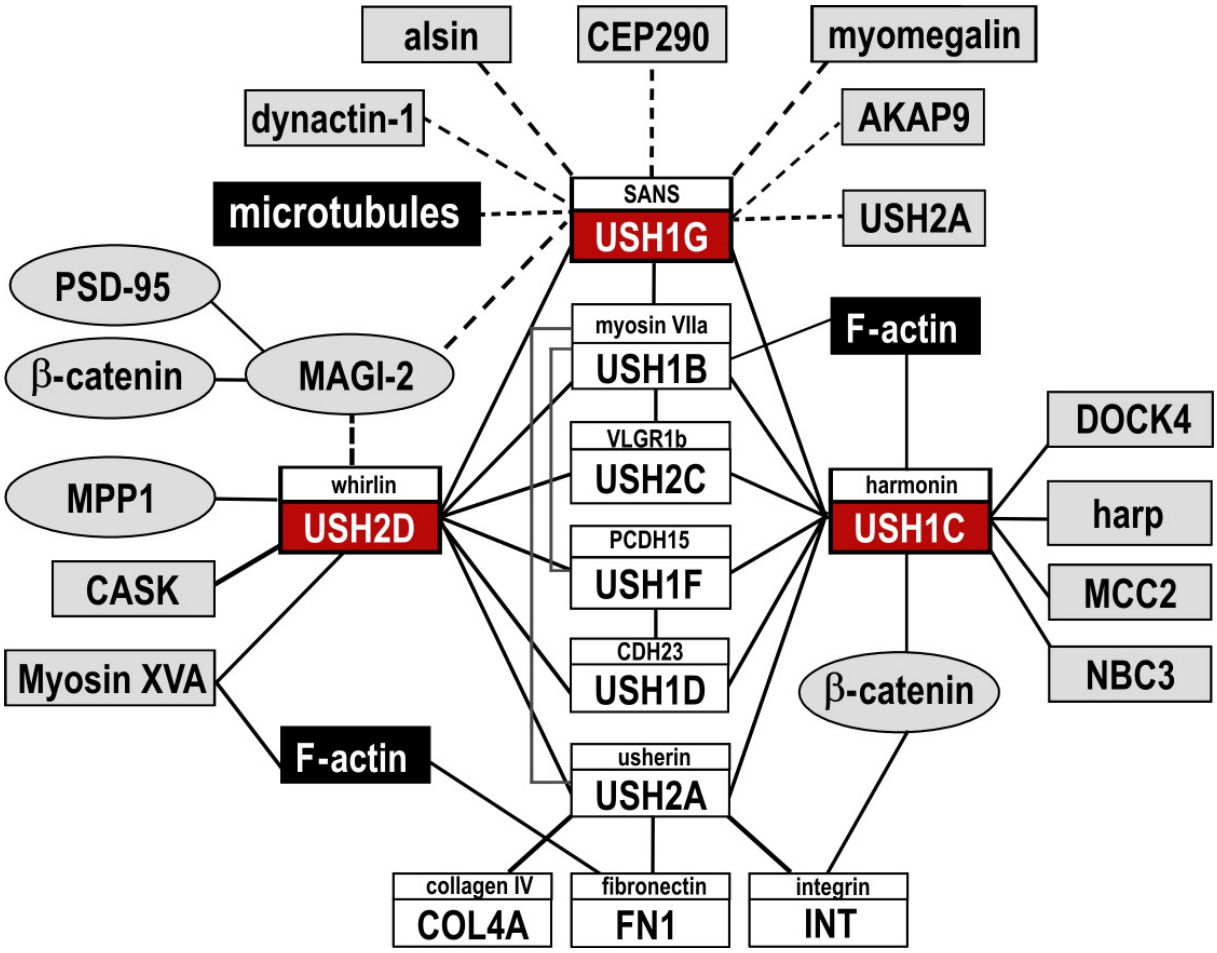

Abb. 8. Das USH-Interaktom. Das Kastenschema ist auf die Darstellung der Interaktionspartner von USH-Proteinen beschränkt. Die bestätigten Wechselwirkungen sind mit durchgehender Linie, die potentiellen Interaktionen mit gestrichelter Linie dargestellt. Die Gerüstproteine Whirlin (USH2D), SANS (USH1G) und Harmonin (USH1C) sind rot, die Cytoskelettelemente F-Aktin und Mikrotubuli schwarz unterlegt. Alle MAGUK-(„Membrane Associated Guanylate Kinase“) Proteine sind rund umrandet (modifiziert nach Kremer *et al.*, 2006*; Referenzen: Hirao *et al.*, 2000; Nishimura *et al.*, 2002; Kazmierczak *et al.*, 2007; Michalski *et al.*, 2007; Dissertation Publikation II).

4.2. Die Partizipation des USH-Interaktoms am Transport und der Fusion von Cargovesikeln

Das MAGUK-Protein MAGI-2 gehört zu den Proteinen, die im Rahmen der vorliegenden Arbeit als weitere Bindepartner von SANS identifiziert werden konnten (Hirao *et al.*, 1998; Tab. 3.; Abb. 8.). Bisherige Resultate der vorliegenden Arbeit konnten die Kolokalisation von MAGI-2 mit SANS und allen USH2-Proteinen auf subzellulärem Niveau visualisieren (Abb. 5.; Abb. 6.; Dissertation Publikation II). Diese Kolokalisationen sind die Voraussetzung für eine potentielle Interaktion von MAGI-2 zu weiteren USH-Interaktomkomponenten neben SANS. Durch bereits publizierte Daten ist bekannt, dass MAGUK-Proteine in der Lage sind, mit den C-Termini von Transmembranproteinen zu interagieren (Fanning *et al.*, 1998; Dimitratos *et al.*, 1999). Demnach wäre neben der Verankerung der USH2-Transmembranproteine USH2A Isoform b und VLGR1b an ciliären-periciliären Membranen über Whirlin auch eine Assoziation über MAGI-2 denkbar (Abb. 9.; Dissertation Publikation II). Auf eine weitere Integration von MAGI-2 in das USH-Interaktom über Whirlin deutet die Kolokalisation beider Proteine hin (Abb. 5.). Die Wechselwirkung von MAGUK-Proteinen mit Whirlin konnte bereits für MPP1 gezeigt werden (Mburu *et al.*, 2006; Gosens *et al.*, 2007*; Abb. 8.). Darüber hinaus war es im Rahmen der vorliegenden Arbeit möglich, neben der direkten Interaktion von MAGI-2 mit SANS, die Assoziation von MAGI-2 mit Transportvesikeln in verschiedenen Modellorganismen erstmalig zu visualisieren (Abb. 6. B, C; Abb. 7. A,B). Hinweise auf die Mitwirkung von MAGUK-Proteinen an synaptischen Transportprozessen existieren bereits (Dimitratos *et al.*, 1999; El-Husseini *et al.*, 2000; Schnell *et al.*, 2002; Cai *et al.*, 2006). Diese neu gewonnenen Daten verifizieren die Resultate der Publikationen I und II, die SANS eine essentielle Rolle im Transport von Cargovesikeln zuordnen. Zusätzliche wichtige Befunde konnten weitere neu identifizierte Interaktionspartner von SANS, Dynaktin-1 und AKAP9, liefern (Tab. 4.). Dynaktin-1 ($p150^{Glued}$) ist eine Untereinheit des Dynaktinkomplexes, der mit dem Mikrotubuli-assoziierten Motorprotein Dynein in Verbindung steht. AKAP9 ist ein centrosomales Protein das wie auch SANS in der Lage ist mit $p150^{Glued}$ zu interagieren (Kim *et al.*, 2007; Abb. 8.; Abb. 9.). Demnach ist es naheliegend, dass Dynaktin-1 zusammen mit SANS, AKAP9 und weiteren Proteinen an Mikrotubuli-vermittelten Transportvorgängen in Photorezeptorzellen beteiligt ist. Als potentielle Komponenten dieser Prozesse kommen auch weitere neue Bindepartner von SANS, CEP290 und Myomegalin, in Frage. CEP290 ist an Centrosomen und im Verbindungscilium von Photorezeptorzellen lokalisiert und spielt eine Rolle in Mikrotubuli-abhängigen ciliären

Transportvorgängen (Chang *et al.*, 2006; Sayer *et al.*, 2006). Myomegalin ist wie SANS mit Mikrotubuli assoziiert und zudem in vesikuläre Transportvorgänge involviert (Pierre *et al.*, 1992). Folglich validieren die neu identifizierten Interaktionspartner von SANS die Ergebnisse der Publikationen I und II und bestätigen SANS als wesentliche Komponente in Mikrotubuli-vermittelten Transportvorgängen.

SANS könnte nach aktuellen Befunden zufolge über Dynaktin-1 am Transport von Cargovesikeln in Richtung des sich verkürzenden Mikrotubulus-Ende (minus-Ende) zur Membran des apikalen Innensegments in Photorezeptorzellen beteiligt sein. An der periciliären Membran könnte durch direkte Interaktion mit weiteren Proteinen eine Übergabe, Positionierung und die Fusion von Transportvesikeln stattfinden (Dissertation Publikation II; Abb. 9.). Denkbar ist, dass weitere identifizierte Bindepartner von SANS, wie das Protein Alsin, direkt in diese Prozesse involviert sind. Für Alsin konnte bereits die Interaktion zur GTPase rac1, die eine Rolle bei der Vesikelfusion im „periciliary ridge complex“ spielt sowie dessen Assoziation mit Endosomen und Membranstrukturen dokumentiert werden (Hadano *et al.*, 2001; Otomo *et al.*, 2003; Topp *et al.*, 2004; Deretic, 2006; Hadano *et al.*, 2007). Als weiterer aussichtsreicher Kandidat für Vesikelfusionsprozesse kommt MAGI-2 in Frage, da die Assoziation von MAGUK-Proteinen mit Tyrosinkinase Substraten bereits beschrieben wurde (Anderson, 1996). Zu letzterer Proteinfamilie gehören die Moleküle Ezrin und Moesin, die eine essentielle Rolle bei der Regulation der Fusion von Transportvesikeln an der Plasmamembran von Photorezeptoren spielen (Deretic *et al.*, 2004; Deretic, 2006). Aus diesen Resultaten lässt sich schlussfolgern, dass die Interaktionspartner von SANS, MAGI-2 und Alsin, zusammen mit weiteren Proteinen die Positionierung und Fusion von Transportvesikeln mit der Membran des apikalen Innensegments in Photorezeptorzellen vermitteln könnten.

Neben der Rolle von MAGUK-Proteinen bei der Vesikelfusion an der Membran des apikalen Innensegments wäre auch eine Beteiligung an der Fusion synaptischer Vesikel denkbar. Eine direkte Interaktion des MAGUK-Proteins CASK („Calcium/calmodulin-dependent Serine protein Kinase“) mit Neurexin, einem Protein das bei der Anlagerung von Vesikeln an die Plasmamembran von Axonen eine Rolle spielt, konnte bereits gezeigt werden (Hata *et al.*, 1996). Vermutlich bildet CASK zusammen mit Mint1, Veli und weiteren Proteinen einen Komplex zwischen Plasmamembran und synaptischen Vesikeln aus, der die Exocytose von synaptischen Vesikeln vermittelt (Butz *et al.*, 1998; Hsueh, 2006). Diese

Resultate lassen die potentielle Mitwirkung des MAGUK-Proteins und USH-Interaktomkomponente MAGI-2 an der Exocytose von synaptischen Vesikeln zu.

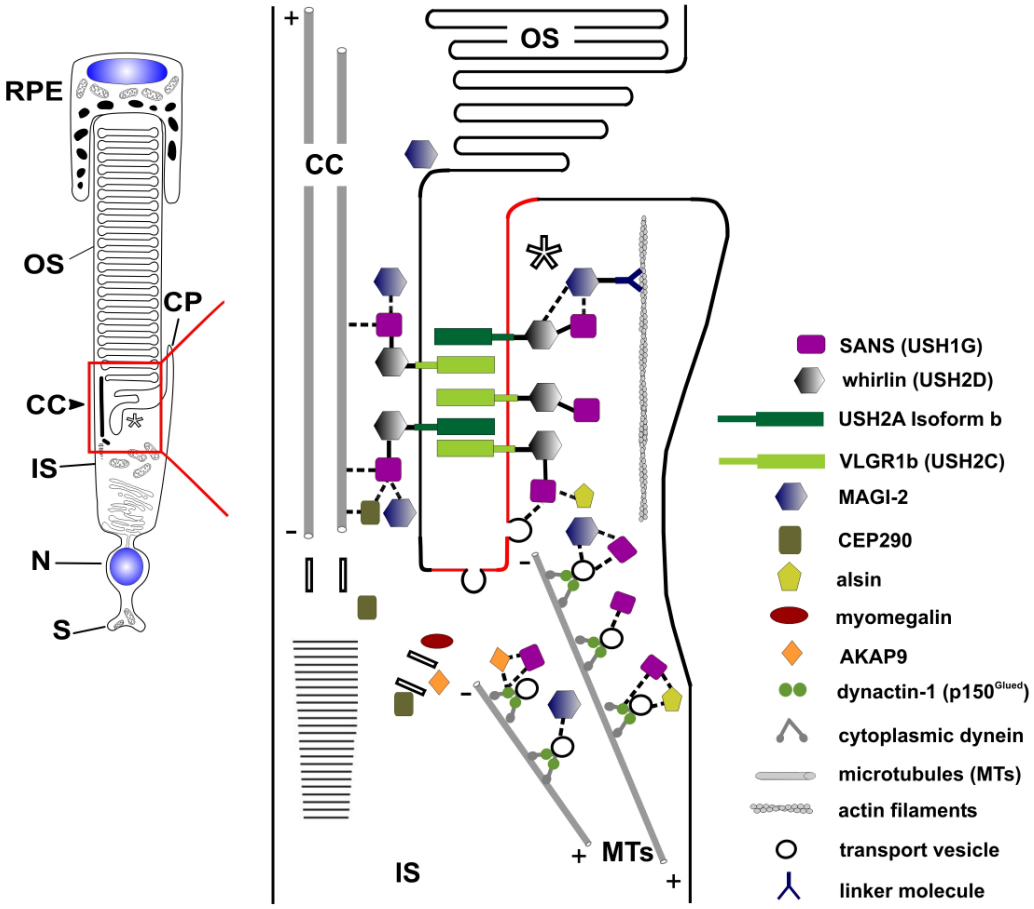

Abb. 9. Schema der Organisation des ciliären-periciliären USH-Proteinnetzwerkes in Photorezeptorzellen. Durch die direkte Interaktion der Gerüstproteine SANS (USH1G) und Whirlin (USH2D) werden die Transmembranproteine USH2A Isoform b und VLGR1b (USH2C) an der Membran des Verbindungsciliums (CC) und benachbarten Membran des apikalen Innensegments (IS) positioniert. Das apikale IS (Stern) ist eine Struktur, die das CC basal und kragenförmig umschließt. Die Ektodomänen der beiden USH2-Transmembranproteine sind in der Lage, den extrazellulären Spalt zu überbrücken und durch Interaktion mit Whirlin die Aufrechterhaltung der periciliären Membran (rot) zu gewährleisten. Cytoplasmatisches Dynein organisiert den Transport von Vesikeln entlang Mikrotubuli (MTs) zur Membran des apikalen IS (rot). An dieser definierten Membran können Transportvesikel anlagern und mit der Plasmamembran fusionieren. Die Beteiligung des USH1G-Proteins SANS und dessen potentiellen Interaktionspartnern MAGI-2, Dynaktin-1 ($p150^{Glued}$), AKAP9 („A-Kinase Anchor Protein 9"), CEP290 („Centrosomal Protein 290kDa") und Alsin an Mikrotubuli-assoziiertem Transport von Cargovesikeln ist angedeutet. Bestätigte Interaktionen sind mit durchgehender Linie, potentielle Interaktionen mit gestrichelter Linie dargestellt. RPE = Retinales Pigmentepithel, OS = Außensegment, CP = „calycal process", N = Photorezeptorzellkern, S = Photorezeptorzellsynapse.

Abgesehen von einer Rolle bei der Vesikelfusion mit der periciliären Plasmamembran könnte SANS auch an den sich daran anschließenden Prozessen, dem ciliären Proteintransport, beteiligt sein. Derzeit werden zwei unterschiedliche ciliäre Transportmechanismen diskutiert.

Einerseits könnte das Aktin-assoziierte Motorprotein Myosin VIIa den Transport durch das Verbindungscilium vermitteln (Liu *et al.*, 1999; Wolfrum und Schmitt, 2000; Williams, 2002). SANS würde somit als Bindeglied zwischen Mikrotubuli- und Aktin-assoziiertem Transport agieren und könnte durch direkte Interaktion mit Myosin VIIa eine regulatorische Funktion erfüllen (Adato *et al.*, 2005a). Andererseits könnte SANS neben der Translokation von Transportvesikeln vom Mikrotubuli- zum Aktin-vermittelten ciliären Transport, auch in einen weiteren diskutierten ciliären Transportmechanismus - den intraflagellaren Transport (IFT) entlang Mikrotubuli - involviert sein (Marzalek et al., 2000; Rosenbaum und Witman, 2002). Die Voraussetzung für eine Partizipation von SANS an intraflagellaren Transport-mechanismen ist gegeben, da SANS sowie intraflagellare Transportpartikel am Basalkörperkomplex und innerhalb des Verbindungsciliums von Photorezeptorzellen lokalisiert werden konnten (Pazour *et al.*, 2000; Dissertation Publikation I, II). Aufgrund der direkten Assoziation von SANS zum Dynein-Dynaktinkomplex ist augenblicklich eine Mitwirkung von SANS am retrograden Dynein-vermittelten Transport wahrscheinlicher.

Zusammenfassend lässt sich sagen, dass die im Rahmen der vorliegenden Arbeit identifizierten neuen Interaktionspartner von SANS, insbesondere MAGI-2, Dynaktin-1, Alsin und AKAP9, eine Beteiligung von SANS an der Fusion von Transportvesikeln zulassen sowie die essentielle Mitwirkung von SANS an Mikrotubuli-assoziierten Transportvorgängen validieren. Dies zeigt deutlich, dass SANS eine generelle zellbiologische Funktion innerhalb von Photorezeptorzellen zukommen könnte, die nicht auf die Netzwerkorganisation von USH-Proteinen beschränkt ist.

4.3. Ausblick auf weitere Forschungsvorhaben

Im Rahmen der vorliegenden Arbeit konnten wertvolle Erkenntnisse zur zellulären Funktion des USH1G-Proteins SANS gewonnen werden. Insbesondere die Identifikation neuer Interaktionspartner konnte zur funktionellen Charakterisierung von SANS in Photorezeptorzellen beitragen. Dennoch sind weiterführende Experimente zur Validierung der potentiellen Interaktionspartner von SANS wie Dynaktin-1, Alsin, AKAP9, CEP290 und Myomegalin unabdingbar. Hierzu zählen Kolokalisationsstudien in der Zellkultur und der Retina sowie Kolokalisationsanalysen auf subzellulärem Niveau mittels hochauflösender Fluoreszenz- und Elektronenmikroskopie. Darüber hinaus sind klassische Interaktionsassays

wie GST (Glutathion-S-Transferase) pull-downs und Koimmunpräzipitationen aus Retinaextrakt notwendig, um die gefundenen Interaktionen zu verifizieren.

Des Weiteren wäre es sinnvoll, die Funktion von USH-Proteinnetzwerken an Photorezeptorzellsynapsen näher zu analysieren. Zu diesem Zwecke könnten Immunfluoreszenzanalysen mit synaptischen Markerproteinen sowie subzelluläre Lokalisationsstudien der USH-Interaktomkomponenten durchgeführt werden

Darüber hinaus sind verschiedene experimentelle Ansätze für die weitere funktionelle Charakterisierung von SANS denkbar. Zum Einen wäre die Analyse einer Überexpression von SANS nach subretinaler Injektion von großem Wert. Es müsste geklärt werden, welchen Einfluss überexprimiertes SANS-Protein auf die Lokalisation und Funktion weiterer Genprodukte hätte. Zum Anderen wäre es von Bedeutung weiterführende Untersuchungen mit SANS „knock-out" Mäusen durchzuführen, da erst in defizienten Tieren das volle Ausmaß eines defekten Proteins zum Tragen kommt. Als weitere aussichtsreiche experimentelle Alternative sind RNAi (RNA-„interference")-Analysen anzusehen, die eine „knock-down" Situation kreieren und es ermöglichen, die damit verbundenen Auswirkungen zu untersuchen. Erst kürzlich wurde eine Methode etabliert, die den „knock-down" eines intrinsisch exprimierten Proteins mittels sh („short hairpin")-RNA sowie die Expression eines sh-resistenten Proteins durch die Transfektion ein und desselben Konstruktes ermöglicht (Chuang et al., 2007). Durch solche „Rescue"-Experimente kann der ursprüngliche Zustand in Photorezeptorzellen wiederhergestellt und das zu untersuchende Protein einer bestimmten zellulären Funktion zugeordnet werden.

Zusammenfassend lässt sich sagen, dass die Ergebnisse der vorliegenden Dissertation eine richtungsweisende Grundlage zur weiteren funktionellen Analyse von USH-Interaktomproteinen schaffen konnte.

5. Zusammenfassung

Das Usher Syndrom (USH) führt beim Menschen zur häufigsten Form erblicher Taub-Blindheit und ist genetisch heterogen. Im Rahmen der vorliegenden Dissertation wurde die Expression und subzelluläre Lokalisation des USH1G-Proteins SANS („Scaffold protein containing Ankyrin repeats and SAM domain“) in der Retina verschiedener Modell-organismen untersucht. Da das Gerüstprotein Harmonin (USH1C) bereits als Organisator von USH-Proteinnetzwerken beschrieben wurde, eine ciliäre Lokalisation aber ausgeschlossen werden konnte, wurde die Rolle von SANS als Organisationsmolekül eines ciliären USH-Proteinnetzwerkes in Abwesenheit von Harmonin analysiert. Ein weiterer wichtiger Fokus lag auf der Identifikation neuer Interaktionspartner, zur funktionellen Charakterisierung von SANS.

Im Rahmen der vorliegenden Arbeit konnte die direkte Interaktion der „Scaffold“-Proteine SANS und Whirlin (USH2D) mit Hilfe verschiedener Methoden identifiziert werden. Darüber hinaus war es mittels elektronenmikroskopischer Analysen möglich, die subzelluläre Kolokalisation der USH-Proteine SANS, USH2A Isoform b (USH2A), VLGR1b („Very Large G-protein coupled Receptor 1b“, USH2C) und Whirlin an den Membranen des Verbindungsciliums und des apikalen Innensegments zu visualisieren. Aufgrund dieser Kolokalisation sowie der direkten Interaktion von Whirlin mit SANS, USH2A Isoform b und VLGR1b kann von einer Harmonin-unabhängigen Netzwerkorganisation dieser vier USH-Proteine im Verbindungscilium von Photorezeptorzellen ausgegangen werden. Innerhalb dieses Proteinnetzwerkes sind die USH-Transmembranproteine USH2A Isoform b und VLGR1b durch die direkte Interaktion mit Whirlin in ciliären-periciliären Membranen verankert und projizieren mit ihren langen extrazellulären Domänen in den Spalt zwischen Verbindungscilium und apikalem Innensegment. Ferner konnten die Ektodomänen von VLGR1b als essentielle Komponente von filamentösen Strukturen zwischen Verbindungscilium und apikalem Innensegment bestätigt werden. Darüber hinaus war es möglich, durch vergleichende elektronenmikroskopische Analysen unterschiedlicher Modellorganismen das ciliäre-periciliäre USH-Proteinnetzwerk am so genannten „periciliary ridge complex“ zu visualisieren. In Amphibien ist der „periciliary ridge complex“ als definierte Membranstruktur für die Anlagerung und Fusion von Transportvesikeln beschrieben. Die vorliegenden Resultate weisen darauf hin, dass die Membranen des Verbindungsciliums und apikalen Innensegments der Maus homolog zum „periciliary ridge

complex“ des Frosches sind. Die Funktion des ciliären-periciliären USH-Proteinnetzwerkes könnte demnach in der Aufrechterhaltung benachbarter Membranstrukturen sowie der Beteiligung der Positionierung und Fusion von Transportvesikeln liegen. Im Weiteren konnte das MAGUK-Protein MAGI-2 als Interaktionspartner von SANS identifiziert und subzellulär an Transportvesikeln visualisiert werden. Darüber hinaus was es möglich, eine direkte Wechselwirkung zwischen SANS und Dynaktin-1 ($p150^{Glued}$), einer Untereinheit des an Mikrotubuli-vermittelten Transportvorgängen beteiligten Dynaktinkomplexes, aufzuzeigen.

Zusammenfassend lässt sich sagen, dass die Daten der vorliegenden Arbeit die Resultate der Publikationen I und II verifizieren und die Partizipation von SANS an Mikrotubuli-assoziiertem Vesikeltransport bestätigen. Somit spielt das USH1G-Protein SANS eine essentielle Rolle in Photorezeptorzellen, die über eine USH-assoziierte Netzwerkorganisation hinausgeht.

6. Literaturverzeichnis

Aartsen WM, Kantardzhieva A, Klooster J, van Rossum AG, van de Pavert SA, Versteeg I, Cardozo BN, Tonagel F, Beck SC, Tanimoto N, Seeliger MW, Wijnholds J (2006) Mpp4 recruits Psd95 and Veli3 towards the photoreceptor synapse. Hum Mol Genet 15:1291-1302

Adamowicz M, Radlwimmer B, Rieker RJ, Mertens D, Schwarzbach M, Schraml P, Benner A, Lichter P, Mechtersheimer G, Joos S (2006) Frequent amplifications and abundant expression of TRIO, NKD2, and IRX2 in soft tissue sarcomas. Genes Chromosomes Cancer 45:829-838

Adato A, Lefevre G, Delprat B, Michel V, Michalski N, Chardenoux S, Weil D, El Amraoui A, Petit C (2005b) Usherin, the defective protein in Usher syndrome type IIA, is likely to be a component of interstereocilia ankle links in the inner ear sensory cells. Hum Mol Genet 14:3921-3932

Adato A, Michel V, Kikkawa Y, Reiners J, Alagramam KN, Weil D, Yonekawa H, Wolfrum U, El Amraoui A, Petit C (2005a) Interactions in the network of Usher syndrome type 1 proteins. Hum Mol Genet 14:347-356

Adato A, Vreugde S, Joensuu T, Avidan N, Hamalainen R, Belenkiy O, Olender T, Bonne-Tamir B, Ben Asher E, Espinos C, Millan JM, Lehesjoki AE, Flannery JG, Avraham KB, Pietrokovski S, Sankila EM, Beckmann JS, Lancet D (2002) USH3A transcripts encode clarin-1, a four-transmembrane-domain protein with a possible role in sensory synapses. Eur J Hum Genet 10:339-350

Ahmed ZM, Riazuddin S, Bernstein SL, Ahmed Z, Khan S, Griffith AJ, Morell RJ, Friedman TB, Riazuddin S, Wilcox ER (2001) Mutations of the protocadherin gene *PCDH15* cause usher syndrome type 1F. Am J Hum Genet 69:25-34

Ahmed ZM, Riazuddin S, Riazuddin S, Wilcox ER (2003) The molecular genetics of Usher syndrome. Clin Genet 63:431-444

Alagramam KN, Murcia CL, Kwon HY, Pawlowski KS, Wright CG, Woychik RP (2001a) The mouse Ames waltzer hearing-loss mutant is caused by mutation of *Pcdh15*, a novel protocadherin gene. Nat Genet 27:99-102

Alagramam KN, Yuan HJ, Kuehn MH, Murcia CL, Wayne S, Srisailpathy CRS, Lowry RB, Knaus R, Van Laer L, Bernier FP, Schwartz S, Lee C, Morton CC, Mullins RF, Ramesh A, Van Camp G, Hagemen GS, Woychik RP, Smith RJH (2001b) Mutations in the novel protocadherin *PCDH15* cause Usher syndrome type 1F. Hum Mol Genet 10:1709-1718

Alam MR, Caldwell BD, Johnson RC, Darlington DN, Mains RE, Eipper BA (1996) Novel proteins that interact with the COOH-terminal cytosolic routing determinants of an integral membrane peptide-processing enzyme. J Biol Chem 271:28636-28640

Ali MY, Krementsova EB, Kennedy GG, Mahaffy R, Pollard TD, Trybus KM, Warshaw DM (2007) Myosin Va maneuvers through actin intersections and diffuses along microtubules. Proc Natl Acad Sci U S A 104:4332-4336

Anderson JM (1996) Cell signalling: MAGUK magic. Curr Biol 6:382-384

Arts HH, Doherty D, van Beersum SE, Parisi MA, Letteboer SJ, Gorden NT, Peters TA, Maerker T, Voesenek K, Kartono A, Ozyurek H, Farin FM, Kroes HY, Wolfrum U, Brunner HG, Cremers FP, Glass IA, Knoers NV, Roepman R (2007) Mutations in the gene encoding the basal body protein RPGRIP1L, a nephrocystin-4 interactor, cause Joubert syndrome. Nat Genet 39: 882-888

Astuto LM, Weston MD, Carney CA, Hoover DM, Cremers CW, Wagenaar M, Moller C, Smith RJ, Pieke-Dahl S, Greenberg J, Ramesar R, Jacobson SG, Ayuso C, Heckenlively JR, Tamayo M, Gorin MB, Reardon W, Kimberling WJ (2000) Genetic heterogeneity of Usher syndrome: analysis of 151 families with Usher type I. Am J Hum Genet 67:1569-1574

Belyantseva IA, Boger ET, Naz S, Frolenkov GI, Sellers JR, Ahmed ZM, Griffith AJ, Friedman TB (2005) Myosin-XVa is required for tip localization of whirlin and differential elongation of hair-cell stereocilia. Nat Cell Biol 7:148-156

Beningo KA, Lillie SH, Brown SS (2000) The yeast kinesin-related protein Smy1p exerts its effects on the class V myosin Myo2p via a physical interaction. Molecular Biology Of The Cell 11:691-702

Bhattacharya G, Miller C, Kimberling WJ, Jablonski MM, Cosgrove D (2002) Localization and expression of usherin: a novel basement membrane protein defective in people with Usher's syndrome type IIa. Hearing Res 163:1-11

Bilder D (2003) PDZ domain polarity complexes. Curr Biol 13:R661-R662

Bitner-Glindzicz M, Lindley KJ, Rutland P, Blaydon D, Smith VV, Milla PJ, Hussain K, Furth-Lavi J, Cosgrove KE, Shepherd RM, Barnes PD, O'Brien RA, Farndon PA, Sowden J, Liu X-Z, Scanlan MJ, Malcolm S, Dunne MJ, Aynsley-Green A, Glaser B (2000) A recessive contiguous gene deletion causing infantile hyperinsulinism, enteropathy and deafness identifies the Usher type 1C gene. Nature Genet 26:56-60

Boeda B, El-Amraoui A, Bahloul A, Goodyear R, Daviet L, Blanchard S, Perfettini I, Fath KR, Shorte S, Reiners J, Houdusse A, Legrain P, Wolfrum U, Richardson G, Petit C (2002) Myosin VIIa, harmonin and cadherin 23, three Usher 1 gene products that cooperate to shape the sensory hair cell bundle. EMBO J 21:6689-6699

Bok D, Galbraith G, Lopez I, Woodruff M, Nusinowitz S, BeltrandelRio H, Huang W, Zhao S, Geske R, Montgomery C, Van S, I, Friddle C, Platt K, Sparks MJ, Pushkin A, Abuladze N, Ishiyama A, Dukkipati R, Liu W, Kurtz I (2003) Blindness and auditory impairment caused by loss of the sodium bicarbonate cotransporter NBC3. Nat Genet 34:313-319

Bolz H, von BB, Ramirez A, Bryda EC, Kutsche K, Nothwang HG, Seeliger M, del C-S, Vila MC, Molina OP, Gal A, Kubisch C (2001) Mutation of CDH23, encoding a new member of the cadherin gene family, causes Usher syndrome type 1D. Nat Genet 27:108-112

Bork JM, Peters LM, Riazuddin S, Bernstein SL, Ahmed ZM, Ness SL, Polomeno R, Ramesh A, Schloss M, Srikumari CRS, Wayne S, Bellman S, Desmukh D, Ahmed Z, Khan SN, Der Kaloustian VM, Li XC, Lalwani A, Riazuddin S, Bitner-Glindzicz M, Nance WE, Liu X-Z, Wistow G, Smith RJH, Griffith AJ, Wilcox ER, Friedman TB, Morell RJ (2001) Usher syndrome 1D and nonsyndromic autosomal recessive deafness DFNB12 are caused by allelic mutations of the novel cadherin-like gene *CDH23*. Am J Hum Genet 68:26-37

Brown SS (1999) Cooperation between microtubule- and actin-based motor proteins. Annu Rev Cell Dev Biol 15:63-80

Burgess DL (2001) Listen carefully: positional cloning of an audiogenic seizure mutation may yield Frings benefits. Neuron 31:507-508

Butz S, Okamoto M, Sudhof TC (1998) A tripartite protein complex with the potential to couple synaptic vesicle exocytosis to cell adhesion in brain. Cell 94:773-782

Cai C, Li H, Rivera C, Keinanen K (2006) Interaction between SAP97 and PSD-95, two Maguk proteins involved in synaptic trafficking of AMPA receptors. J Biol Chem 281:4267-4273

Cao TT, Chang W, Masters SE, Mooseker MS (2004) Myosin-Va binds to and mechanochemically couples microtubules to actin filaments. Mol Biol Cell 15:151-161

Caruana G (2002) Genetic studies define MAGUK proteins as regulators of epithelial cell polarity. Int J Dev Biol 46:511-518

Chaib H, Kaplan J, Gerber S, Vincent C, Ayadi H, Slim R, Munnich A, Weissenbach J, Petit C (1997) A newly identified locus for usher syndrome type I, USH1E, maps to chromosome 21q21. Hum Mol Genet 6:27-31

Chang B, Khanna H, Hawes N, Jimeno D, He S, Lillo C, Parapuram SK, Cheng H, Scott A, Hurd RE, Sayer JA, Otto EA, Attanasio M, O'Toole JF, Jin G, Shou C, Hildebrandt F, Williams DS, Heckenlively JR, Swaroop A (2006) In-frame deletion in a novel centrosomal/ciliary protein CEP290/NPHP6 perturbs its interaction with RPGR and results in early-onset retinal degeneration in the rd16 mouse. Hum Mol Genet 15:1847-1857

Chuang JZ, Zhao Y, Sung CH (2007) SARA-regulated vesicular targeting underlies formation of the light-sensing organelle in mammalian rods. Cell 130:535-547

Cole DG, Diener DR, Himelblau AL, Beech PL, Fuster JC, Rosenbaum JL (1998) Chlamydomonas kinesin-II-dependent intraflagellar transport (IFT): IFT particles contain proteins required for ciliary assembly in Caenorhabditis elegans sensory neurons. J Cell Biol 141:993-1008

Crook MF, Olive M, Xue HH, Langenickel TH, Boehm M, Leonard WJ, Nabel EG (2007) GA-binding protein regulates KIS gene expression, cell migration, and cell cycle progression. FASEB J

Davenport JR, Watts AJ, Roper VC, Croyle MJ, van GT, Wyss JM, Nagy TR, Kesterson RA, Yoder BK (2007) Disruption of intraflagellar transport in adult mice leads to obesity and slow-onset cystic kidney disease. Curr Biol 17:1586-1594

Davenport SL, Omenn GS (1977) The heterogeneity of Usher Syndrome. Vth Int Conf Birth Defects Montreal:nn

Delprat B, Michel V, Goodyear R, Yamasaki Y, Michalski N, El Amraoui A, Perfettini I, Legrain P, Richardson G, Hardelin JP, Petit C (2005) Myosin XVa and whirlin, two deafness gene products required for hair bundle growth, are located at the stereocilia tips and interact directly. Hum Mol Genet 14:401-410

Deng F, Price MG, Davis CF, Mori M, Burgess DL (2006) Stargazin and other transmembrane AMPA receptor regulating proteins interact with synaptic scaffolding protein MAGI-2 in brain. J Neurosci 26:7875-7884

Deretic D (2006) A role for rhodopsin in a signal transduction cascade that regulates membrane trafficking and photoreceptor polarity. Vision Res 46:4427-4433

Deretic D, Traverso V, Parkins N, Jackson F, Rodriguez de Turco EB, Ransom N (2004) Phosphoinositides, ezrin/moesin, and rac1 regulate fusion of rhodopsin transport carriers in retinal photoreceptors. Mol Biol Cell 15:359-370

Dimitratos SD, Woods DF, Stathakis DG, Bryant PJ (1999) Signaling pathways are focused at specialized regions of the plasma membrane by scaffolding proteins of the MAGUK family. Bioessays 21:912-921

Dryja TP, Adams SM, Grimsby JL, McGee TL, Hong DH, Li T, Andreasson S, Berson EL (2001) Null RPGRIP1 alleles in patients with Leber congenital amaurosis. Am J Hum Genet 68: 1295-1298

Ebermann I, Scholl HP, Charbel IP, Becirovic E, Lamprecht J, Jurklies B, Millan JM, Aller E, Mitter D, Bolz H (2007) A novel gene for Usher syndrome type 2: mutations in the long isoform of whirlin are associated with retinitis pigmentosa and sensorineural hearing loss. HUM GENET 121:203-211

El-Husseini AE, Craven SE, Chetkovich DM, Firestein BL, Schnell E, Aoki C, Bredt DS (2000) Dual palmitoylation of PSD-95 mediates its vesiculotubular sorting, postsynaptic targeting, and ion channel clustering. J Cell Biol 148:159-172

Eudy JD, Yao SF, Weston MD, Maedmonds M, Talmadge CB, Cheng JJ, Kimberling WJ, Sumegi J (1998) Isolation of a gene encoding a novel member of the nuclear receptor superfamily from the critical region of usher syndrome type IIa at 1q41. Genomics 50:382-384

Fanning AS, Jameson BJ, Jesaitis LA, Anderson JM (1998) The tight junction protein ZO-1 establishes a link between the transmembrane protein occludin and the actin cytoskeleton. J Biol Chem 273:29745-29753

Garner CC, Nash J, Huganir RL (2000) PDZ domains in synapse assembly and signalling. Trends Cell Biol 10:274-280

Gill SR, Schroer TA, Szilak I, Steuer ER, Sheetz MP, Cleveland DW (1991) Dynactin, a Conserved, Ubiquitously Expressed Component of an Activator of Vesicle Motility Mediated by Cytoplasmic Dynein. J Cell Biol 115:1639-1650

Gillingham AK, Munro S (2000) The PACT domain, a conserved centrosomal targeting motif in the coiled-coil proteins AKAP450 and pericentrin. EMBO Rep 1:524-529

Gosens I, van WE, Kersten FF, Krieger E, van der ZB, Marker T, Letteboer SJ, Dusseljee S, Peters T, Spierenburg HA, Punte IM, Wolfrum U, Cremers FP, Kremer H, Roepman R (2007) MPP1 links the Usher protein network and the Crumbs protein complex in the retina. Hum Mol Genet 16:1993-2003

Hadano S, Hand CK, Osuga H, Yanagisawa Y, Otomo A, Devon RS, Miyamoto N, Showguchi-Miyata J, Okada Y, Singaraja R, Figlewicz DA, Kwiatkowski T, Hosler BA, Sagie T, Skaug J, Nasir J, Brown RH, Jr., Scherer SW, Rouleau GA, Hayden MR, Ikeda JE (2001) A gene encoding a putative GTPase regulator is mutated in familial amyotrophic lateral sclerosis 2. Nat Genet 29:166-173

Hadano S, Kunita R, Otomo A, Suzuki-Utsunomiya K, Ikeda JE (2007) Molecular and cellular function of ALS2/alsin: implication of membrane dynamics in neuronal development and degeneration. Neurochem Int 51:74-84

Hamon Y, Trompier D, Ma Z, Venegas V, Pophillat M, Mignotte V, Zhou Z, Chimini G (2006) Cooperation between engulfment receptors: the case of ABCA1 and MEGF10. PLoS ONE 1:e120

Hasson T, Heintzelman MB, Santos-Sacchi J, Corey DP, Mooseker MS (1995) Expression in cochlea and retina of myosin VIIa, the gene product defective in Usher syndrome type 1B. Proc Natl Acad Sci USA 92:9815-9819

Hata Y, Butz S, Sudhof TC (1996) CASK: a novel dlg/PSD95 homolog with an N-terminal calmodulin-dependent protein kinase domain identified by interaction with neurexins. J Neurosci 16:2488-2494

Hirao K, Hata Y, Ide N, Takeuchi M, Irie M, Yao I, Deguchi M, Toyoda A, Sudhof TC, Takai Y (1998) A novel multiple PDZ-domain-containing molecule interacting with *N*-Methyl-D-aspartate receptors and neuronal cell adhesion proteins. J Biol Chem 273:21105-21110

Hirao K, Hata Y, Yao I, Deguchi M, Kawabe H, Mizoguchi A, Takai Y (2000) Three isoforms of synaptic scaffolding molecule and their characterization. Multimerization between the isoforms and their interaction with N-methyl-D-aspartate receptors and SAP90/PSD-95-associated protein. J Biol Chem 275:2966-2972

Holzbaur EL, Tokito MK (1996) Localization of the DCTN1 gene encoding p150Glued to human chromosome 2p13 by fluorescence in situ hybridization. Genomics 31:398-399

Hoshino Y, Horikawa I, Oshimura M, Yuasa Y (1991) Normal human chromosome 5, on which a familial adenomatous polyposis gene is located, has tumor suppressive activity. Biochem Biophys Res Commun 174:298-304

Hsueh YP (2006) The role of the MAGUK protein CASK in neural development and synaptic function. Curr Med Chem 13:1915-1927

Huang JD, Brady ST, Richards BW, Stenolen D, Resau JH, Copeland NG, Jenkins NA (1999) Direct interaction of microtubule- and actin-based transport motors. Nature 397:267-270

Izaddoost S, Nam SC, Bhat MA, Bellen HJ, Choi KW (2002) Drosophila Crumbs is a positional cue in photoreceptor adherens junctions and rhabdomeres. Nature 416: 178-183

Joensuu T, Hamalainen R, Yuan B, Johnson C, Tegelberg S, Gasparini P, Zelante L, Pirvola U, Pakarinen L, Lehesjoki AE, de la CA, Sankila EM (2001) Mutations in a novel gene with transmembrane domains underlie Usher syndrome type 3. Am J Hum Genet 69:673-684

Katoh M, Katoh M (2004) Identification and characterization of PDZRN3 and PDZRN4 genes in silico. Int J Mol Med 13:607-613

Kazerounian S, Aho S (2003) Characterization of periphilin, a widespread, highly insoluble nuclear protein and potential constituent of the keratinocyte cornified envelope. J Biol Chem 278:36707-36717

Kazmierczak P, Sakaguchi H, Tokita J, Wilson-Kubalek EM, Milligan RA, Muller U, Kachar B (2007) Cadherin 23 and protocadherin 15 interact to form tip-link filaments in sensory hair cells. Nature 449:87-91

Keryer G, Di FB, Celati C, Lechtreck KF, Mogensen M, Delouvee A, Lavia P, Bornens M, Tassin AM (2003) Part of Ran is associated with AKAP450 at the centrosome: involvement in microtubule-organizing activity. Mol Biol Cell 14:4260-4271

Kikkawa Y, Shitara H, Wakana S, Kohara Y, Takada T, Okamoto M, Taya C, Kamiya K, Yoshikawa Y, Tokano H, Kitamura K, Shimizu K, Wakabayashi Y, Shiroishi T, Kominami R, Yonekawa H (2003) Mutations in a new scaffold protein Sans cause deafness in Jackson shaker mice. Hum Mol Genet 12:453-461

Kim E, Naisbitt S, Hsueh YP, Rao A, Rothschild A, Craig AM, Sheng M (1997) GKAP, a novel synaptic protein that interacts with the guanylate kinase-like domain of the PSD-95/SAP90 family of channel clustering molecules. J Cell Biol 136:669-678

Kim HS, Takahashi M, Matsuo K, Ono Y (2007) Recruitment of CG-NAP to the Golgi apparatus through interaction with dynein-dynactin complex. Genes Cells 12:421-434

Kinzler KW, Nilbert MC, Vogelstein B, Bryan TM, Levy DB, Smith KJ, Preisinger AC, Hamilton SR, Hedge P, Markham A, . (1991) Identification of a gene located at chromosome 5q21 that is mutated in colorectal cancers. Science 251:1366-1370

Klimov E, Rud'ko O, Rakhmanaliev E, Sulimova G (2005) Genomic organisation and tissue specific expression of ABLIM2 gene in human, mouse and rat. Biochim Biophys Acta 1730:1-9

Kneussel M, Loebrich S (2007) Trafficking and synaptic anchoring of ionotropic inhibitory neurotransmitter receptors. Biol Cell 99:297-309

Kozminski KG, Beech PL, Rosenbaum JL (1995) The Chlamydomonas kinesin-like protein FLA10 is involved in motility associated with the flagellar membrane. J Cell Biol 131:1517-1527

Kremer H, van Wijk E, Märker T, Wolfrum U, Roepman R (2006) Usher syndrome: molecular links of pathogenesis, proteins and pathways. Hum Mol Genet in press:nn

Kunita R, Otomo A, Mizumura H, Suzuki-Utsunomiya K, Hadano S, Ikeda JE (2007) The Rab5 activator ALS2/alsin acts as a novel Rac1 effector through Rac1-activated endocytosis. J Biol Chem 282:16599-16611

Kurita M, Suzuki H, Masai H, Mizumoto K, Ogata E, Nishimoto I, Aiso S, Matsuoka M (2004) Overexpression of CR/periphilin downregulates Cdc7 expression and induces S-phase arrest. Biochem Biophys Res Commun 324:554-561

Leonoudakis D, Conti LR, Anderson S, Radeke CM, McGuire LM, Adams ME, Froehner SC, Yates JR, III, Vandenberg CA (2004) Protein trafficking and anchoring complexes revealed by proteomic analysis of inward rectifier potassium channel (Kir2.x)-associated proteins. J Biol Chem 279:22331-22346

Lin JW, Wyszynski M, Madhavan R, Sealock R, Kim JU, Sheng M (1998) Yotiao, a novel protein of neuromuscular junction and brain that interacts with specific splice variants of NMDA receptor subunit NR1. J Neurosci 18:2017-2027

Liu X, Bulgakov OV, Darrow KN, Pawlyk B, Adamian M, Liberman MC, Li T (2007) Usherin is required for maintenance of retinal photoreceptors and normal development of cochlear hair cells. Proc Natl Acad Sci U S A 104:4413-4418

Liu X, Udovichenko IP, Brown S.D., Steel KP, Williams DS (1999) Myosin VIIa participates in opsin transport through the photoreceptor cilium. J Neurosci 19:6267-6274

Liu XR, Vansant G, Udovichenko IP, Wolfrum U, Williams DS (1997) Myosin VIIa, the product of the Usher 1B syndrome gene, is concentrated in the connecting cilia of photoreceptor cells. Cell Motil Cytoskeleton 37:240-252

Marszalek JR, Liu X, Roberts EA, Chui D, Marth JD, Williams DS, Goldstein LS (2000) Genetic evidence for selective transport of opsin and arrestin by kinesin-II in mammalian photoreceptors. Cell 102:175-187

Maucuer A, Camonis JH, Sobel A (1995) Stathmin interaction with a putative kinase and coiled-coil-forming protein domains. Proc Natl Acad Sci U S A 92:3100-3104

Maucuer A, Ozon S, Manceau V, Gavet O, Lawler S, Curmi P, Sobel A (1997) KIS is a protein kinase with an RNA recognition motif. J Biol Chem 272:23151-23156

Mburu P, Kikkawa Y, Townsend S, Romero R, Yonekawa H, Brown SD (2006) Whirlin complexes with p55 at the stereocilia tip during hair cell development. Proc Natl Acad Sci U S A 103:10973-10978

Mburu P, Mustapha M, Varela A, Weil D, El Amraoui A, Holme RH, Rump A, Hardisty RE, Blanchard S, Coimbra RS, Perfettini I, Parkinson N, Mallon AM, Glenister P, Rogers MJ, Paige AJ, Moir L, Clay J, Rosenthal A, Liu XZ, Blanco G, Steel KP, Petit C, Brown SD (2003) Defects in whirlin, a PDZ domain molecule involved in stereocilia elongation, cause deafness in the whirler mouse and families with DFNB31. Nat Genet 34:421-428

Michalski N, Michel V, Bahloul A, Lefevre G, Barral J, Yagi H, Chardenoux S, Weil D, Martin P, Hardelin JP, Sato M, Petit C (2007) Molecular characterization of the ankle-link complex in cochlear hair cells and its role in the hair bundle functioning. J Neurosci 27:6478-6488

Mizuno Y, Thompson TG, Guyon JR, Lidov HG, Brosius M, Imamura M, Ozawa E, Watkins SC, Kunkel LM (2001) Desmuslin, an intermediate filament protein that interacts with alpha -dystrobrevin and desmin. Proc Natl Acad Sci U S A 98:6156-6161

Nishimura W, Yao I, Iida J, Tanaka N, Hata Y (2002) Interaction of synaptic scaffolding molecule and Beta -catenin. J Neurosci 22:757-765

Nybakken KE, Turck CW, Robbins DJ, Bishop JM (2002) Hedgehog-stimulated phosphorylation of the kinesin-related protein Costal2 is mediated by the serine/threonine kinase fused. J Biol Chem 277:24638-24647

Okano HJ, Park WY, Corradi JP, Darnell RB (1999) The cytoplasmic Purkinje onconeural antigen cdr2 down-regulates c-Myc function: implications for neuronal and tumor cell survival. Genes Dev 13:2087-2097

Otomo A, Hadano S, Okada T, Mizumura H, Kunita R, Nishijima H, Showguchi-Miyata J, Yanagisawa Y, Kohiki E, Suga E, Yasuda M, Osuga H, Nishimoto T, Narumiya S, Ikeda JE (2003) ALS2, a novel guanine nucleotide exchange factor for the small GTPase Rab5, is implicated in endosomal dynamics. Hum Mol Genet 12:1671-1687

Papermaster DS (2002) The birth and death of photoreceptors: the Friedenwald Lecture. Invest Ophthalmol Vis Sci 43:1300-1309

Pazour GJ, Dickert BL, Vucica Y, Seeley ES, Rosenbaum JL, Witman GB, Cole DG (2000) *Chlamydomonas IFT88* and its mouse homologue, polycystic kidney disease *Tg737*, are required for assembly of cilia and flagella. J Cell Biol 151(3):709-718

Pazour GJ, Dickert BL, Witman GB (1999) The DHC1b (DHC2) isoform of cytoplasmic dynein is required for flagellar assembly. J Cell Biol 144:473-481

Pellikka M, Tanentzapf G, Pinto M, Smith C, McGlade CJ, Ready DF, Tepass U (2002) Crumbs, the Drosophila homologue of human CRB1/RP12, is essential for photoreceptor morphogenesis. Nature 416: 143-149

Petit C (2001) Usher syndrome: from genetics to pathogenesis. Annu Rev Genomics Hum Genet 2:271-297

Portales-Casamar E, Briancon-Marjollet A, Fromont S, Triboulet R, Debant A (2006) Identification of novel neuronal isoforms of the Rho-GEF Trio. Biol Cell 98:183-193

Porter ME, Bower R, Knott JA, Byrd P, Dentler W (1999) Cytoplasmic dynein heavy chain 1b is required for flagellar assembly in Chlamydomonas. Mol Biol Cell 10:693-712

Reiners J, Marker T, Jurgens K, Reidel B, Wolfrum U (2005) Photoreceptor expression of the Usher syndrome type 1 protein protocadherin 15 (USH1F) and its interaction with the scaffold protein harmonin (USH1C). Mol Vis 11:347-355

Reiners J, Nagel-Wolfrum K, Jurgens K, Marker T, Wolfrum U (2006) Molecular basis of human Usher syndrome: deciphering the meshes of the Usher protein network provides insights into the pathomechanisms of the Usher disease. EXP EYE RES 83:97-119

Reiners J, Reidel B, El-Amraoui A, Boeda B, Huber I, Petit C, Wolfrum U (2003) Differential distribution of harmonin isoforms and their possible role in Usher-1 protein complexes in mammalian photoreceptor cells. Invest Ophthalmol Visual Sci 44:5006-5015

Reiners J, van Wijk E, Marker T, Zimmermann U, Jurgens K, te BH, Overlack N, Roepman R, Knipper M, Kremer H, Wolfrum U (2005) Scaffold protein harmonin (USH1C) provides molecular links between Usher syndrome type 1 and type 2. Hum Mol Genet 14:3933-3943

Roepman R, Schick D, Ferreira PA (2000) Isolation of retinal proteins that interact with retinitis pigmentosa GTPase regulator by interaction trap screen in yeast. Methods Enzymol 316:688-704

Roepman R, and Wolfrum U (2007) Protein networks and complexes in photoreceptor cilia. Chapter 10 in: E. Bertrand, & M. Faupel (Eds.) *Subcellular Proteomics From Cell Deconstruction to System Reconstruction* Vol. 43. (pp 209-235). New York: Springer.

Roh MH, Margolis B (2003) Composition and function of PDZ protein complexes during cell polarization. Am J Physiol Renal Physiol 285:F377-F387

Roof DJ, Hayes A, Adamian M, Chishti AH, Li T (1997) Molecular characterization of abLIM, a novel actin-binding and double zinc finger protein. J Cell Biol 138:575-588

Rosenbaum JL, Cole DG, Diener DR (1999) Intraflagellar transport: The eyes have it. J Cell Biol 144(3):385-388

Rosenbaum JL, Witman GB (2002) Intraflagellar transport. Nat Rev Mol Cell Biol 3:813-825

Satoh K, Yanai H, Senda T, Kohu K, Nakamura T, Okumura N, Matsumine A, Kobayashi S, Toyoshima K, Akiyama T (1997) DAP-1, a novel protein that interacts with the guanylate kinase-like domains of hDLG and PSD-95. Genes Cells 2:415-424

Sayer JA, Otto EA, O'Toole JF, Nurnberg G, Kennedy MA, Becker C, Hennies HC, Helou J, Attanasio M, Fausett BV, Utsch B, Khanna H, Liu Y, Drummond I, Kawakami I, Kusakabe T, Tsuda M, Ma L, Lee H, Larson RG, Allen SJ, Wilkinson CJ, Nigg EA, Shou C, Lillo C, Williams DS, Hoppe B, Kemper MJ, Neuhaus T, Parisi MA, Glass IA, Petry M, Kispert A, Gloy J, Ganner A, Walz G, Zhu X, Goldman D, Nurnberg P, Swaroop A, Leroux MR, Hildebrandt F (2006) The centrosomal protein nephrocystin-6 is mutated in Joubert syndrome and activates transcription factor ATF4. Nat Genet 38:674-681

Schnell E, Sizemore M, Karimzadegan S, Chen L, Bredt DS, Nicoll RA (2002) Direct interactions between PSD-95 and stargazin control synaptic AMPA receptor number. Proc Natl Acad Sci U S A 99:13902-13907

Shanks RA, Larocca MC, Berryman M, Edwards JC, Urushidani T, Navarre J, Goldenring JR (2002) AKAP350 at the Golgi apparatus. II. Association of AKAP350 with a novel chloride intracellular channel (CLIC) family member. J Biol Chem 277:40973-40980

Shoji H, Tsuchida K, Kishi H, Yamakawa N, Matsuzaki T, Liu Z, Nakamura T, Sugino H (2000) Identification and characterization of a PDZ protein that interacts with activin type II receptors. J Biol Chem 275:5485-5492

Siemens J, Kazmierczak P, Reynolds A, Sticker M, Littlewood Evans A, Müller U (2002) The Usher syndrome proteins cadherin 23 and harmonin form a complex by means of PDZ-domain interactions. Proc Natl Acad Sci USA 99:14946-14951

Sisson JC, Ho KS, Suyama K, Scott MP (1997) Costal2, a novel kinesin-related protein in the Hedgehog signaling pathway. Cell 90:235-245

Sung CH, Tai AW (2000) Rhodopsin trafficking and its role in retinal dystrophies. Int Rev Cytol 195:215-267

Suzuki E, Nakayama M (2007) MEGF10 is a mammalian ortholog of CED-1 that interacts with clathrin assembly protein complex 2 medium chain and induces large vacuole formation. Exp Cell Res 313:3729-3742

Tabb JS, Molyneaux BJ, Cohen DL, Kuznetsov SA, Langford GM (1998) Transport of ER vesicles on actin filaments in neurons by myosin V. J Cell Sci 111 (Pt 21):3221-3234

Tai AW, Chuang JZ, Bode C, Wolfrum U, Sung CH (1999) Rhodopsin´s carboxy-terminal cytoplasmic tail acts as a membrane receptor for cytoplasmic dynein by binding to the dynein light chain Tctex-1. Cell 97:877-887

Takeuchi M, Hata Y, Hirao K, Toyoda A, Irie M, Takai Y (1997) SAPAPs. A family of PSD-95/SAP90-associated proteins localized at postsynaptic density. J Biol Chem 272:11943-11951

Tasken KA, Collas P, Kemmner WA, Witczak O, Conti M, Tasken K (2001) Phosphodiesterase 4D and protein kinase a type II constitute a signaling unit in the centrosomal area. J Biol Chem 276:21999-22002

Tay SY, Ingham PW, Roy S (2005) A homologue of the Drosophila kinesin-like protein Costal2 regulates Hedgehog signal transduction in the vertebrate embryo. Development 132:625-634

Titeux M, Brocheriou V, Xue Z, Gao J, Pellissier JF, Guicheney P, Paulin D, Li Z (2001) Human synemin gene generates splice variants encoding two distinct intermediate filament proteins. Eur J Biochem 268:6435-6449

Topp JD, Gray NW, Gerard RD, Horazdovsky BF (2004) Alsin is a Rab5 and Rac1 guanine nucleotide exchange factor. J Biol Chem 279:24612-24623

Tsujikawa M, Omori Y, Biyanwila J, Malicki J (2007) Mechanism of positioning the cell nucleus in vertebrate photoreceptors. Proc Natl Acad Sci U S A 104:14819-14824

Tuxworth RI, Titus MA (2000) Unconventional myosins: anchors in the membrane traffic relay. Traffic 1:11-18

Valente EM, Silhavy JL, Brancati F, Barrano G, Krishnaswami SR, Castori M, Lancaster MA, Boltshauser E, Boccone L, Al-Gazali L, Fazzi E, Signorini S, Louie CM, Bellacchio E, Bertini E, Dallapiccola B, Gleeson JG (2006) Mutations in CEP290, which encodes a centrosomal protein, cause pleiotropic forms of Joubert syndrome. Nat Genet 38:623-625

van Wijk E, Pennings RJ, te BH, Claassen A, Yntema HG, Hoefsloot LH, Cremers FP, Cremers CW, Kremer H (2004) Identification of 51 novel exons of the Usher syndrome type 2A (USH2A) gene that encode multiple conserved functional domains and that are mutated in patients with Usher syndrome type II. Am J Hum Genet 74:738-744

van Wijk E, van der Zwaag B, Peters T, Zimmermann U, te BH, Kersten FF, Marker T, Aller E, Hoefsloot LH, Cremers CW, Cremers FP, Wolfrum U, Knipper M, Roepman R, Kremer H (2006) The DFNB31 gene product whirlin connects to the Usher protein network in the cochlea and retina by direct association with USH2A and VLGR1. Hum Mol Genet 15:751-765

Verde I, Pahlke G, Salanova M, Zhang G, Wang S, Coletti D, Onuffer J, Jin SL, Conti M (2001) Myomegalin is a novel protein of the golgi/centrosome that interacts with a cyclic nucleotide phosphodiesterase. J Biol Chem 276:11189-11198

Verpy E, Leibovici M, Zwaenepoel I, Liu X-Z, Gal A, Salem N, Mansour A, Blanchard S, Kobayashi I, Keats BJB, Slim R, Petit C (2000) A defect in harmonin, a PDZ domain-containing protein expressed in the inner ear sensory hair cells, underlies Usher syndrome type 1C. Nature Genet 26:51-55

Wang L, Guo Y, Huang WJ, Ke X, Poyet JL, Manji GA, Merriam S, Glucksmann MA, DiStefano PS, Alnemri ES, Bertin J (2001) Card10 is a novel caspase recruitment domain/membrane-associated guanylate kinase family member that interacts with BCL10 and activates NF-kappa B. J Biol Chem 276:21405-21409

Weil D, Blanchard S, Kaplan J, Guilford P, Gibson F, Walsh J, Mburu P, Varela A, Levilliers J, Weston MD, Kelley PM, Kimberling WJ, Wagenaar M, Levi-Acobas F, Larget-Piet D, Munnich A, Steel KP, Brown SDM, Petit C (1995) Defective myosin VIIA gene responsible for Usher syndrome type 1B. Nature 374(6517):60-61

Weil D, El-Amraoui A, Masmoudi S, Mustapha M, Kikkawa Y, Lainé S, Delmaghani S, Adato A, Nadifi S, Ben Zina Z, Hamel C, Gal A, Ayadi H, Yonekawa H, Petit C (2003) Usher syndrome type I G (USH1G) is caused by mutations in the gene encoding SANS, a protein that associates with the USH1C protein, harmonin. Hum Mol Genet 12:463-471

Weston MD, Luijendijk MW, Humphrey KD, Moller C, Kimberling WJ (2004) Mutations in the VLGR1 gene implicate G-protein signaling in the pathogenesis of Usher syndrome type II. Am J Hum Genet 74:357-366

Williams DS (2002) Transport to the photoreceptor outer segment by myosin VIIa and kinesin II. Vision Res 42:455-462

Wolfrum U, Schmitt A (2000) Rhodopsin transport in the membrane of the connecting cilium of mammalian photoreceptor cells. Cell Motil Cytoskeleton 46:95-107

Wood JD, Yuan J, Margolis RL, Colomer V, Duan K, Kushi J, Kaminsky Z, Kleiderlein JJ, Sharp AH, Ross CA (1998) Atrophin-1, the DRPLA gene product, interacts with two families of WW domain-containing proteins. Mol Cell Neurosci 11:149-160

Woods DF, Bryant PJ (1991) The discs-large tumor suppressor gene of Drosophila encodes a guanylate kinase homolog localized at septate junctions. Cell 66:451-464

Yagi H, Takamura Y, Yoneda T, Konno D, Akagi Y, Yoshida K, Sato M (2005) Vlgr1 knockout mice show audiogenic seizure susceptibility. J Neurochem 92:191-202

Yan D, Li F, Hall ML, Sage C, Hu WH, Giallourakis C, Upadhyay G, Ouyang XM, Du LL, Bethea JR, Chen ZY, Yajnik V, Liu XZ (2006) An isoform of GTPase regulator DOCK4 localizes to the stereocilia in the inner ear and binds to harmonin (USH1C). J Mol Biol 357:755-764

7. Anhang

A. Zuordnung der geleisteten Beträge zu den einzelnen Publikationen

An dieser Stelle möchte ich erläutern, welche Beiträge zu den einzelnen in der Dissertation durch einen Stern (*) hervorgehobenen Arbeiten geleistet werden konnten. Zunächst werde ich auf die beiden Hauptpublikationen Overlack *et al.*, 2007 (I) und Maerker *et al.*, 2007 (II) eingehen. In Overlack *et al.*, 2007 sind Nora Overlack und ich gleichberechtigte Erstautoren. Mein Beitrag zu dieser Arbeit war die Herstellung und Charakterisierung spezifischer Antikörper gegen das USH1G-Protein SANS, die für alle immunhistochemischen und molekularbiologischen Experimente verwendet wurden (Abb. 2.-8.). Besonders hervorzuheben ist die von mir erarbeitete und visualisierte (sub-) zelluläre Lokalisation von SANS in der Retina (Abb. 2.; Abb. 4.). Darüber hinaus wurde die Expression von SANS in Zellkulturzellen von mir untersucht (Abb. 8.). Die Analyse der Gewebe- und Zellextrakte sowie die Daten zur entwicklungsabhängigen Expression von SANS wurden im Rahmen der Diplomarbeit von Nora Overlack gewonnen, die von mir begleitet wurde. Die Daten der biochemischen Fraktionierungen und Tangentialschnitte wurden mit technischer Unterstützung von Frau Ulrike Maas und Herrn Dr. Martin Latz gewonnen und dokumentiert (Abb. 5.).

In der zweiten Publikation (Maerker *et al.*, 2007) wurden Experimente gemeinsam mit unseren Kooperationspartnern Hannie Kremer, Ronald Roepman, Ferry Kersten und Erwin van Wijk (Medical Centre Radboud University, Nijmegen) durchgeführt. Aus diesen gemeinsamen Versuchen resultieren die in Abbildung 1 dargestellten Ergebnisse (Abb. 1. B, D). Ferry Kersten hat eigenständig die Resultate der GST pull-down Analyse erarbeitet (Abb. 1. C). Die Ergebnisse der Koimmunpräzipitation von SANS konnten in Eigenarbeit geleistet werden (Abb. 1. E). Darüber hinaus sind die Resultate der subzellulären Lokalisation von SANS, Whirlin, USH2A Isoform b und VLGR1b in der Maus und in *Xenopus* selbständig erarbeitet worden (Abb. 2.; Abb. 3.; Abb. 4.; Abb. 6.; Abb. 7.). Die in Abbildung 5 von mir analysierten *Vlgr1/del7TM* Retinae wurden uns freundlicherweise von unseren Kooperationspartnern Frau JoAnn McGee und Herrn Edward J. Walsh (Developmental Auditory Physiology Laboratory, Boys Town National Research Hospital, Omaha) zur Verfügung gestellt (Abb. 5. G-J). Die Assoziation von SANS mit Mikrotubuli konnte durch Tobias Goldmann und Nora Overlack identifiziert werden (Abb. 8.). Die Schemata sowie die

ergänzenden Daten (Abb. 9.; „supplementary material“ Abb. 1.; Abb. 2; Abb. 3.) sind in Eigenarbeit entstanden.

Neben den beiden Hauptpublikationen Overlack *et al.*, 2007 und Maerker *et al.*, 2007 konnten weitere Beiträge zu Veröffentlichungen unserer Arbeitsgruppe sowie gemeinsamer Publikationen mit unseren Kooperationspartnern geleistet werden. Durch die Mitwirkung an der Herstellung und Charakterisierung spezifischer Antikörper gegen Protocadherin 15 (USH1F) konnten Immunfluoreszenzdaten zur Lokalisation von Protocadherin 15 in der Retina sowie biochemische Resultate in die Veröffentlichung Reiners *et al.*, 2005a* einfließen (Abb. 3.; Abb. 4.). Darauf folgte die erste gemeinsame Publikation mit unseren holländischen Kollegen zur Analyse des Gerüstproteins Harmonin als Bindeglied zwischen USH1- und USH2-Proteinen (Reiners *et al.*, 2005b*). Zu dieser Arbeit konnten GST pull-down Analysen beigetragen werden sowie spezifische Antikörper zur Verfügung gestellt werden, die eine subzelluläre Lokalisation der USH-Proteine in Retina und Cochlea ermöglichten (Abb. 2. B, D; Abb. 4. C, E; Abb. 5. D-F, I, J). In einer weiteren Publikation unserer holländischen Kooperationspartner konnte die direkte Interaktion des „Scaffold“-Proteins Whirlin mit USH2A Isoform b und VLGR1b gezeigt werden (van Wijk *et al.*, 2006*). Ein wesentlicher Bestandteil dieser Arbeit stellten Immunfluoreszenzanalysen im Innenohr und in der Retina dar, die mittels der in der vorliegenden Arbeit generierten, charakterisierten und zur Verfügung gestellten spezifischen Antikörper gegen VLGR1b erst möglich waren (Abb. 6. L, M; Abb. 7. F, G, I, L). Des Weiteren konnte eine Beteiligung an einem Übersichtsartikel über USH-Proteinnetzwerke in sensorischen Zellen erwirkt werden (Reiners *et al.*, 2006*). Von Jan Reiners und mir durchgeführte vergleichende Immunfluoreszenzanalysen in Mausretina mit bis dato allen bekannten USH-Proteinen konnten die zentrale Rolle von Harmonin als Organisator eines USH-Proteinnetzwerkes in der Synapsenregion von Photorezeptorzellen bestätigen (Reiners *et al.*, 2006*; Abb. 6.). In einem weiteren Übersichtsartikel verdeutlichen Kremer und Kollegen die essentielle Rolle eines durch Harmonin organisierten USH-Proteinnetzwerkes im Synapsenbereich von sowohl Photorezeptorzellen als auch Haarsinneszellen (Kremer *et al.*, 2006*). Erstmals konnten im Rahmen der vorliegenden Dissertation erarbeitete elektronenmikroskopische Daten zur Lokalisation von USH2A Isoform b und Whirlin einfließen (Kremer *et al.*, 2006*; Abb. 4.).

Als weitere Forschungsbeteiligung wäre der Beitrag zur Aufklärung der Interaktion von Whirlin mit dem MAGUK-Protein MPP1 („Membrane Palmitoylated Protein 1“) zu nennen (Gosens *et al.*, 2007*). MPP1 ist zusammen mit weiteren MAGUK-Proteinen (MPP3-

5) an der *Membrana limitans externa* in der Retina lokalisiert und dort am Aufbau des so genannten Crumbs Komplexes beteiligt (Gosens *et al.*, 2007*). Der durch die Proteine MPP5 und Crumbs organisierte Proteinkomplex ist in die Entstehung und Aufrechterhaltung der Zellpolarität der Photorezeptorzelle involviert und somit für die korrekte Formation von Photorezeptorzellen unabdingbar (Izaddoost *et al.*, 2002; Pellikka *et al.*, 2002; Gosens *et al.*, 2007*). Mittels elektronenmikroskopischer Analysen der vorliegenden Arbeit wurde zur Validierung der Interaktion von Whirlin mit MPP1 beigetragen und Whirlin als molekulares Bindeglied zwischen USH-Proteinkomplexen und dem Crumbs Netzwerk an der *Membrana limitans externa* bestätigt (Gosens *et al.*, 2007*; Abb. 5. D1-E2).

Darüber hinaus konnten von mir erarbeitete Daten zur subzellulären Lokalisation von RPGRIP1L in Photorzeptorzellen der Maus in eine weitere Veröffentlichung einfließen (Arts *et al.*, 2007*; Abb. 4. A-L). RPGRIP1L ist homolog zu RPGRIP1 („Retinitis Pigmentosa GTPase Regulator Interacting Protein 1“) und wurde als ciliäres Protein, welches bei Defekten zu Leber congenital amaurosis (LCA) führen kann, beschrieben (Roepman *et al.*, 2000; Dryja *et al.*, 2001). Die von uns gewonnenen Resultate haben zusammen mit weiteren aussagekräftigen Ergebnissen RPGRIP1L als Kandidaten für das Joubert Syndrom bestätigt und verdeutlicht, dass das Verbindungscilium und der Basalkörperkomplex eine essentielle Rolle in der Pathophysiologie des Joubert Syndromes spielen.

B. Abkürzungen

Im Folgenden sind die im Text häufig verwendeten Abkürzungen nochmals alphabetisch aufgelistet. Zusätzlich wurden in diese Liste allgemein gebräuchliche Abkürzungen von Einheiten und Chemikalien aufgenommen, die nicht im Text definiert wurden.

AKAP9	A-kinase anchor protein 9
BAPTA	1,2-bis(o- aminophenoxy)ethane-N,N,N',N'-tetraacetic acid
CASK	Calcium/calmodulin-dependent Serine protein Kinase
CC	Verbindungscilium von Photorzeptorzellen
CC1	Coiled-Coil-Domäne 1
CDH23	Cadherin 23 (USH1D)
cDNA	komplementäre DNA (complementary DNA)
CEN	zentrale Domäne des USH1G-Proteins SANS
CEP290	Centrosomal Protein 290kDa
CP	Calycal Process
DAPI	4,6-Diamidino-2-Phenylindol; blau fluoreszierende Zellkernfärbung
DIC	Differenzieller Interferenzkontrast
DMSO	Dimethylsulfoxid
DNA	Desoxyribonukleinsäure
EC	Ectodomäne; Ca2+-Bindedomäne in Cadherinen und VLGR1b
ECM	extrazelluläres Matrixprotein
GST	Glutathion-S-Transferase
IFT	intraflagellarer Transport
IPL	Innere plexiforme Schicht
IS	Innensegment der Photorezeptorzelle
kDa	Kilodalton
MAGI-2	Membrane-Associated Guanylate Kinase Inverted-2
MAGUK	Membrane-Associated Guanylate Kinase
MPP1	Membrane Palmitoylated Protein 1
MT	Mikrotubuli
NBC3	Natrium Bicarbonate Cotransporter-3
OLM	*Membrana limitans externa*
ONL	Äußere Körnerschicht

OPL	Äußere plexiforme Schicht
OS	Außensegment
PBM	PDZ Binding Motif
PCDH15	Protocadherin 15 (USH1F)
PDZ	Postsynaptic density 95, Discs large, Zonula occludens-1
PRC	periciliary ridge complex
PSD-95	Postsynaptic densitiy 95
RP	Retinitis pigmentosa; Degeneration der Photorezeptorzellen
RPE	Retinales Pigmentepithel
SAM	Sterile alpha motif
SANS	Scaffold protein containing Ankyrin repeats and SAM domain (USH1G)
USH	Usher Syndrom
USH1,2, 3	Usher Syndrom Typ 1, 2 oder 3
USH1B	Usher Syndrom Subtyp 1B - MyosinVIIa
USH1C	Usher Syndrom Subtyp 1C - Harmonin
USH1D	Usher Syndrom Subtyp 1D - Cadherin 23
USH1E	Usher Syndrom Subtyp 1E - Gen nicht bekannt; ev. JAM2
USH1F	Usher Syndrom Subtyp 1F - Protocadherin 15
USH1G	Usher Syndrom Subtyp 1G - SANS
USH2A	Usher Syndrom Subtyp 2A – Usherin, USH2A Isoform b
USH2B	Usher Syndrom Subtyp 2B - vermutlich NBC3
USH2C	Usher Syndrom Subtyp 2C - VLGR1b
USH3A	Usher Syndrom Subtyp 3A - Clarin-1
VLGR1b	Isoform b von Very Large G-protein coupled Receptor-1 (USH2C)
wt	Im Labor etablierte Wildtyp-Maus *Mus musculus* C57 BL/6J

Eidesstattliche Erklärung

Hiermit erkläre ich an Eides statt, dass ich meine Dissertation selbstständig und nur unter Verwendung der angegebenen Hilfsmittel angefertigt habe. Ich habe keinen anderen Promotionsversuch unternommen.

Mainz, den 2007

.....

Tina Märker